SPATIAL VARIABILITY IN CEMENT-TREATED MARINE CLAY – A FIELD DATA STUDY

JIANG YIJIE

NATIONAL UNIVERSITY OF SINGAPORE

2015

SPATIAL VARIABILITY IN CEMENT-TREATED MARINE CLAY – A FIELD DATA STUDY

JIANG YIJIE
(B. Eng. (Hons.), NUS)

A THESIS SUBMITTED

FOR THE DEGREE OF MASTER OF ENGINEERING
DEPARTMENT OF CIVIL & ENVIRONMENTAL ENGINEERING
NATIONAL UNIVERSITY OF SINGAPORE

2015

Declaration

I hereby declare that this thesis is my original work and it has been written by me in its entirety. I have duly acknowledged all the sources of information which have been used in the thesis.

This thesis has also not been submitted for any degree in any university previously.

JIANG Yijie

11 November 2015

Acknowledgements

I would like to extend my ultimate gratitude to many people who have assisted me in various ways during my final year project.

Firstly, I would like to express grateful acknowledgement to my supervisor, Professor LEE Fook Hou for his invaluable guidance and constant supervision. His encouragement and advice have inspired me to diligence in my final year project.

In addition, I would like to extend my gratitude to Dr LIU Yong for his assistance and patient counsels. Working with him has been very pleasant and rewarding, and I have definitely learnt many things beyond academic matters.

Grateful acknowledgement is expressed to Professor MENG Qiang and Doctor Ong Ghim Ping Raymond for their academic instruction. The knowledge taught in their class CE6002 enhanced my understanding of statistics and probability.

I would like to express many thanks to Dr Sandeep Narayan Kundu (Department of Geography, Faculty of Art and Social Science of National University of Singapore) for his generous sharing on spatial variability analysis.

Last but not least, many thanks to all the research fellows in office E1-8-23, NUS for their cheerful accompany and prompt supports. In particular, I am thankful to Ms Akanksha TYAGI for her instructions on ABAQUS, Mr ZHANG Lei for his patient assistance.

The financial support from French-NUS Double Degree Program of National University of Singapore is gratefully acknowledged.

Table of Contents

Summary

The spatial variability of cement-treated clay is a common concern in geotechnical engineering. This study focuses on the spatial variability of soil resulting from deep cement mixing (DCM).

Firstly, by back-analysis of the field data from Marina One and Marina Bay Financial Centre (MBFC) in Singapore, it shows that various in-situ water content and dispersed curing duration from DCM to testing are two possible causes of variability.

Secondly, based on generalized hyperbolic relationship (Xiao *et al.*, 2014) a two-parameter model was established to predict the probability density function (PDF), mean, variance and auto-correlation structure of 28-day equivalent unconfined compressive strength (UCS) in cement-treated soil. The precision of prediction was examined by comparing predicted results with measured one.

Finally, in order to characterize soil properties with small amount of data, the reliability of three proposed robust criteria was examined by Mont-Carlo simulation and Bootstrapping method. Recommendation was made based on stability and consistency of results.

List of Figures

List of Tables

List of Symbols

q_u Unconfined Compressive Strength (UCS), unit: Mpa

w water content in in-situ soil, defined as the mass ratio of water and soil in natural soil

c cement slurry concentration, defined as the mass ratio of cement slurry to total mass of soil column

$A_w = \frac{C}{S}$ ratio of cement and soil by mass in soil column

$\frac{W}{C}$ ratio of total water and cement by mass in soil column

q_0 a value defined in Eq. 2.2, unit: Mpa

$\mathbf{q}_\infty$ the limit of q_0, unit: Mpa

α the initial rate of increase in q0 with time, unit: Mpa/day

r a fitted index by Eqs. 2.6

z depth in vertical direction. Downward is positive value

x axis in horizontal direction

y axis in horizontal direction, perpendicular to x-axis

COV coefficient of variation, defined as the ratio of standard deviation over mean value.

σ **(*S*)** standard deviation

μ mean

τ distance lag, separated distance between two data points

SOF($\boldsymbol{\theta}$) Scale of Fluctuation

a the water-cement ratio in cement slurry

r strength ratio depending on mixing ingredient; defined in Eqs.5.3

1. Introduction

1.1. Background

Soft marine clay is a typical soft clay underlain many coastal cities in the world. In Singapore, Singapore marine clay occurs over an area covering almost one quarter of Singapore Island, which is found in river valleys, river mouths and along the coast. Singapore Marine clay is kaolinite-rich clay, of which two divisions are recognized, namely upper marine clay (2A) and lower marine clay (2B). Since marine clay's natural strength is generally low, soil improvement is generally required to increase the strength of soil when infrastructure is required to be constructed over soft marine clay. One common method of soil improvement is cement treatment. Two main methods of cement treatment are widely used in many ground improvement projects, namely deep-cement mixing (DCM) and jet-grouting techniques. **Figure 1.1** illustrates a typical construction sequence of soil column improved by wet-deep-mixing. By injecting cement slurry into a cut cavity underground, in-situ soil can be mixed with cement and water, to form a cement-treated soil column.

The strength of deep-cement mixed columns usually possesses significant spatial variabilities (Honjo, 1982, Babasaki *et al.*, 1997, Larsson *et al.*, 2005, Lee *et al.*, 2006, Lee *et al.*, 2008, Chen *et al.*, 2011, Lee *et al.*, 2013), which is noticed to be about twice as high as variability of strength in natural soil (Bruce *et al.* 2013). Many factors are attributable to the non-uniformity in improved soil, including in-situ soil condition, non-uniform mixing process and differences in curing time between installation and testing.

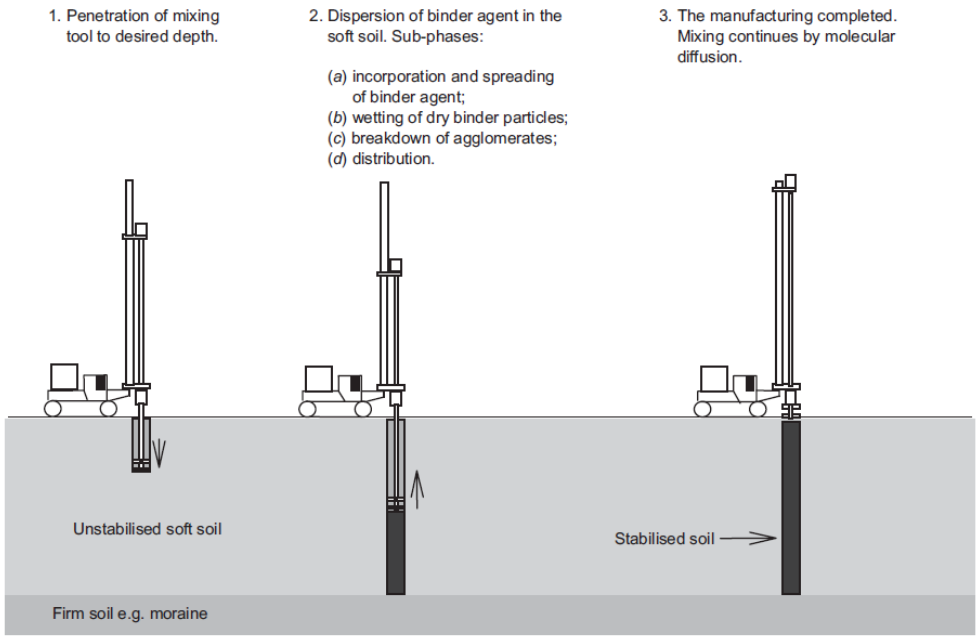

Figure 1. 1 A typical construction sequence of lime-cement columns for dry deep mixing (after Larsson *et al.*, 2005).

1.2. Consideration of Variability in Cement-Treated Soil in Current Engineering Practice

Minimum Amount of Core-Samples

The most common method of quality control in cement-treatment is by core strength measurement. In this method, core samples shall be taken from site after installation for strength assessment. Owing to the large variability of strength in cement-treated clay, a large number of core-samples are normally required for strength testing. For example, BS EN 12716-2001(B/526, 2011) states that:

"(9.4.2.3) Where *relevant, the compressive strength of jet grouted structure should be assessed by testing* ***four samples taken from the structure for each 1000 m^3 of its volume****, if not otherwise specified by the design*."

The Land Transport Authority of Singapore's standard on quality control of Jet grouting and deep cement mixing (LTA, 2010) also states that *"...**A minimum of 3 samples shall be taken from top and middle and bottom** of each core for strength and stiffness testing."*

Curing Time's Impact

The curing time between installation and testing has a significant influence on the strength of the cement-soil mix (e.g. Xiao et al. 2014). This effect is also captured by BS EN 12716-2001 (B/526, 2011) which states that *"(*9.4.*2.5) **The tendency of the strength and modulus to increase with time** is strongly dependent on the soil type, with longer development for higher fine content"*. However, BS EN 12716-2001 (B/526, 2011) does not offer any specific suggestion on a recommended curing time or methods to account for time-strength effect. As will be seen in the case study for the Marina One project considered herein, more than thousand core samples were tested, with curing times ranging from a few weeks to several months. All of the measured core strengths were reduced by 10% to a "28-day equivalent strengths" in strength testing report. Since the strength is clearly not out by a constant amount, this method appears to have no scientific basis whatsoever and is merely intended to yield a more conservative strength value.

Criteria on Strength Assessment

The method of inferring a representative strength for the entire treated soil mass is also similarly uncertain. The sample-minima criterion is favoured by BS-EN 12716:2001 (B/526, 2011) for strength-assessment in cement–treated soil:

*"(7.3.4) The **required statistical minimum strength** of mass should be established at the design stage, taking into consideration the variability of the soil conditions".*

Similarly, LTA (2010) also sets up a minimum targeted value for jet grouting and deep cement mixing activities:

"(Jet grouting) If either of the strength or stiffness test fails to ***achieve its target value****, two additional samples in the same core shall be tested for strength and stiffness at no additional cost to the Authority. In the event that either of the additional samples fails to conform with the requirement, the Jet Grouting work is deemed to have failed."*

"(Deep cement mixing) A minimum of four samples shall be tested for strength and stiffness, and the results shall ***comply with the minimum requirements specified in the design****."*

The maximum and minimum values are extremely sensitive to the outliers (Garth, 2008). Similarly, Wikipedia (2015) noted "*The sample maximum and minimum are the least robust statistics: they are maximally sensitive to outliers*". This is likely to be particularly so in cement-treated soil, which has very high spatial variability.

In summary, considering the high variability of strength in cement-treated clay, many issues shall be considered in current engineering practice. Firstly, effect of curing duration to soil strength should be, but has not yet been well quantified. Secondly, a statistically sound basis for the number of samples to be collected is still unavailable. Finally, current approach of sample-minima criterion can hardly represent the real soil strength with presence of high variation in treated soil.

Objective and Outline of this Study

The object of this study is to examine the spatial variation in strength in cement-treated marine clay improved using deep mixing by means of field data from two sites. As will be discussed in the subsequent chapters, the contribution of this work lies in the following aspects:

(a) A method of normalizing strength to account for the effect of curing time;

(b) An alternative method of inferring a representative strength, based on the mean and standard deviation and a comparison of its sensitivity with the sample minima approach;

(c) Some statistically derived guidelines on the sample size needed for statistical robustness;

(d) A method of estimating the spatial variation of strength in the field considering the spatial variation in cement slurry concentration and in-situ variation in water content of the soil.

Chapter 2 will review the previous and related studies on the variability in properties of cement-treated soil. Chapter 3 will provide a detailed description of site before and after cement-improvement. Chapter 4 will discussed the influence of curing time and water content on strength in cement treated soil. Chapter 5 will focus on strength prediction by generalized hyperbolic relationships (Xiao *et al.*, 2014). In Chapter 6, robustness of three criteria in soil property characterization will be examined and compared by site data. Finally, summaries and conclusions will be presented in Chapter 7.

2. Literature Review

2.1. Factors Affecting Strength of Soil-Cement Mix

2.1.1. Variation in Mix Ratio

It is well-known that the strength of cement-admixed soil depends intimately on the mix ratio (e.g. Gallavresi, 1992; Xiao *et al.*, 2014; Lee et al., 1997). For instance, Gallavresi (1992) proposed a relationship between unconfined compressive strength (UCS) of cement-treated cohesive soil and mixing ratio of water (*W*) and cement (*C*). It can be formulated by the following equation:

$$q_u = \frac{q_0}{(\frac{W}{C})^n} \tag{2.1}$$

Where q_0 and n are parameters fitted by experimental results.

Lee *et al.* (1997) extended Gallavresi's relationship to include impact of water content on final UCS (see **Figure 2.1**). His experimental results emphasized that the not only injected water in cement slurry, but the variability of water portion in in-situ soil may also contribute to variation of final UCS.

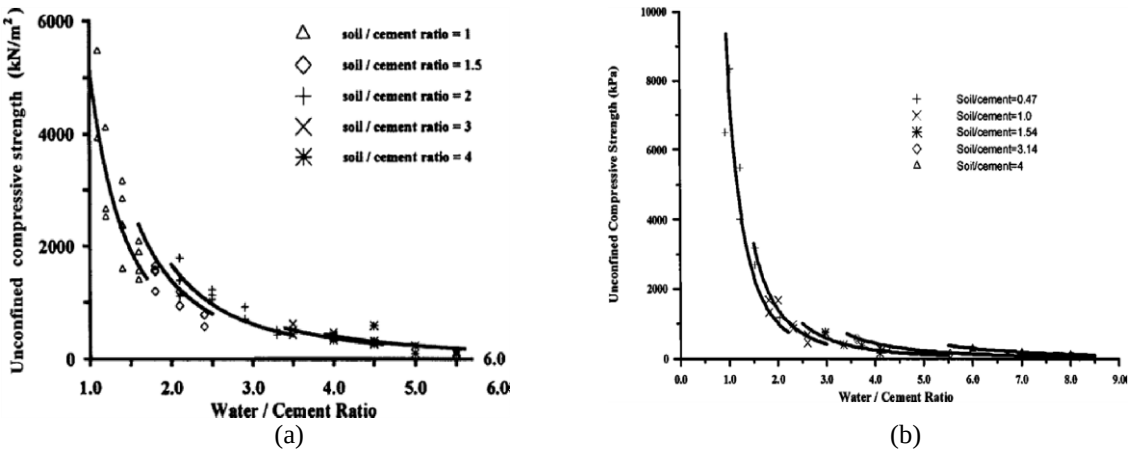

(a) (b)

Figure 2. 1 28-Day strength of cement treated clay prepared from (a) dried pulverized clay and (b) slurry clay (after Lee et al, 1997)

After that, based on Gallavresi (1992)'s proposal and observations from field data, Lee *et al.* (2005) proposed a model to predict unconfined compressive strength, q_u of cement-treated clay:

$$q_u = \mathrm{q}_0 \frac{exp(\mathrm{m}*\frac{S}{C})}{(\frac{W}{C})^n} \tag{2.2}$$

in which q_0 is a constant and m and n are indices; $\frac{S}{C}$ and $\frac{W}{C}$ are soil-cement ratio, water-cement ratio in cemented soil column, respectively. In his study, the plasticity index of in-situ clay was about 59%, hence following parameters are proposed to fit experimental results: q_0=4000 kPa for 7-days, and 6000 kPa for 28 days, m = 0.62 and n = 3. However, by same equation, Xiao *et al.* (2014)'s testing results were better fitted by q_0=13,000 kPa and 20,000 kPa for UCS of cement-treated Singapore marine clay with curing time of 7 days and 28 days, respectively. He selected m and n equal to 0.28 and 2.93, respectively. Xiao *et al.* (2014) concluded that differences between two sets of fitting parameters proposed by Lee *et al.* (2005) and him were due to the disparity in plasticity index of clay in two sites.

Many papers focus on the non-uniformity of binder concentration within one soil column, which may lead to the non-uniformity in strength (e.g. Larsson *et al.*, 2005; Lee *et al.*, 2008; Lee *et al.*, 2006). For example, Larsson (2001) conducted experimental study on cement slurry concentration in lime-cement columns with dry deep-cement mixing technics. He observed that cement slurry distribution pattern varies radially within one soil column: cement slurry concentration gradually declines from column centre to the edge of column. He concluded that the mixing quality is affected by the process of integrating the cement slurry by an air jet.

2.1.2. Curing Time from Installation to Core Sample Testing

It is well-established that cement-treated soil gains strength along with curing time (Bruce *et al.*, 2013; Mitchell, 1976; Xiao *et al.*, 2014; Al-Tabbaa *et al.*, 2003). For instance, Lu (2014) observed that the strength-development in cement-mixed soil can be sub-divided into two phases: the rapid strength gain in early age and the slower strength gain in long term approaching the strength plateau.

Al-Tabbaa *et al.* (2003) traced the long-term time-related development of q_u in deep-cement-mixed contaminated soil in a site of UK. In their study, it was observed that soil strength increased continuously for up to 2.3 years; in addition, little sign of deterioration was observed at 4.5 years after treatment (**Figure 2.2**). However, the duration in **Figure 2.2** is too long to be useful for estimating unconfined compressive strength of deep-mixed soil. For the latter, the typical curing period is between 14 days and 150 days.

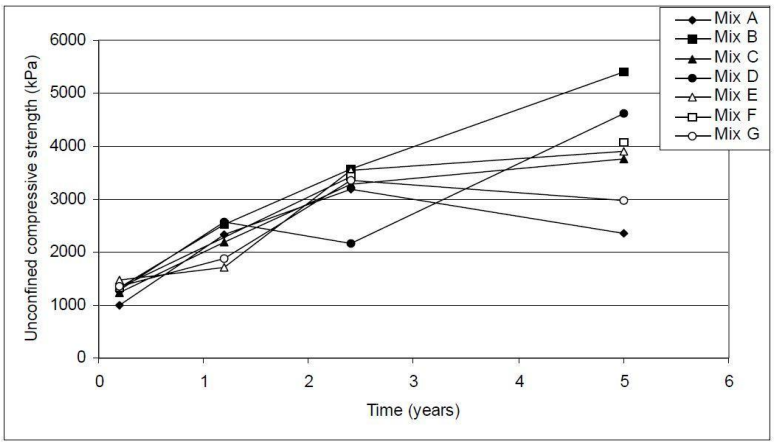

Figure 2.2 Time-related development of the unconfined compressive strength in long-term (after Al-Tabbaa *et al.*, 2003).

Several mathematical models were proposed to articulate the correlation between strength and curing time in cement-treated soil, including logarithmic relationships, reversed-linear relationships and even more complex composite forms.

Mitchell (1976) defined a relationship between Unconfined Compressive Strength (UCS) q_u and the curing time t in a logarithmic form:

$$q_u(t) = q_u(\mathrm{t}_0) + kln\,(\frac{t}{\mathrm{t}_0}) \tag{2.3}$$

He proposed that k=480C for sand, and 70C for silt and clay; C refers to cement content by weight; t_0 is equal to 28 days.

The logarithmic form was recommended in Design Manual by Federal Highway Administration of USA (Bruce *et al.*, 2013), in which the normalized strength, f_c is given by

$$f_c = 0.187ln\,(t)\ + 0.375 \tag{2.4}$$

Where: f_c = Ratio of UCS at time t to the UCS at 28 days;

t = Curing times in day.

Verastegui Flores and Di Emidio (2011) compared effects of different cement type on hardening pattern up to 60 days. Two admixed cement slurry material are Portland ordinary cement and blast furnace slag cement. They highlighted that, shortly after cement mixing, samples treated with Portland cement showed the greatest strength-gain; whereas that for samples treated with blaster-furnace-slag cement increased more gradually. When strengths are normalized by 28-day-strength, the strength-gain curves of soil treated by two types of cements follow same logarithmic trend (see **Figure 2.3**). They proposed this logarithmic hardening trend as a guide for strength gain over time. However, the logarithmic relationship implies that, as time increases to infinity, so does the strength. This is evidently counter-intuitive. As such, the logarithmic relationship is likely to be unsuitable for predicting very long period strength gain.

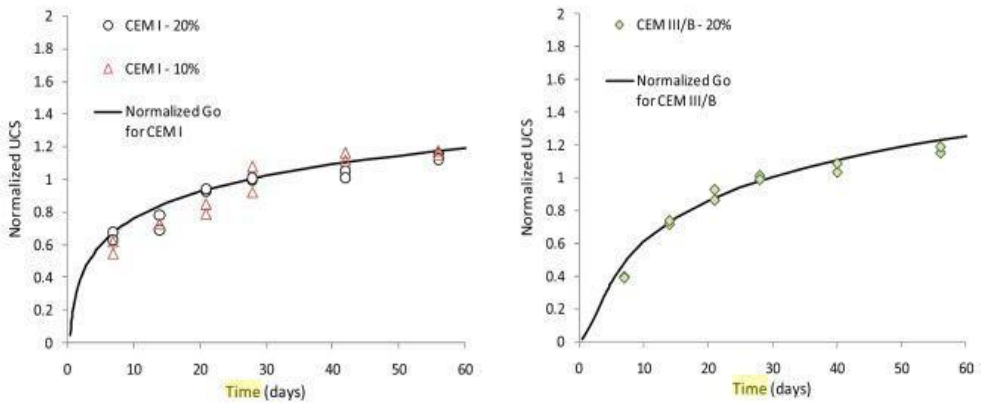

(a) Portland Cement (b) Furnace Blast Cement

Figure 2.3 Normalized UCS versus curing time for (a) Sample treated with Portland cement and (b) Sample treated with blast furnace slag cement (after Verastegui Flores *et al.*, 2011)

Lim and Zollinger (2003) proposed a hyperbolic relationship between the UCS and curing time, of the form

$$q_u(t) = q_u(28)\frac{t}{\mathrm{a+b}t} \tag{2.5}$$

Where $q_u(t)$ = compressive strength at time t,

$q_u(28)$ = reference 28−day compressive strength, and

a, b are experimental coefficients. For cement-treated aggregate based material, Lim and Zollinger (2003) proposed that *a* = 2.5 and *b* = 0.9.

One of the limitations of the standard hyperbolic form is that it implies that the rate of strength gain with time during early hardening is almost constant. This is not necessarily so. To overcome this limitation, Xiao *et al*. (2014) proposed a generalized hyperbolic relationship of the form

$$q_0 = \mathrm{q}_\infty\{1 - \frac{1}{1+(\frac{\alpha t}{\mathrm{q}_\infty})^{\mathrm{r}}}\} \tag{2.6}$$

Where q_∞ is the limit of q_0 in long term, α is the initial rate of increase in q_0 with time, and r is a fitted index. Xiao et al. (2014) chose q_∞ =39,000 kPa, α = 2000 kPa/day and r = 0.9 to fit the testing results in his experiments (see **Figure 2.4**).

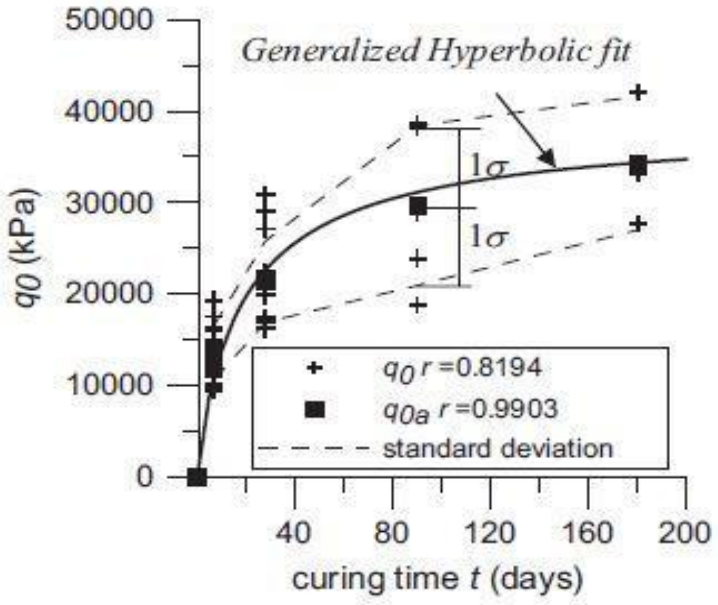

Figure 2. 4 Parameter q_0 in Eq. 2.6 versus curing time for cement–treated marine clay samples after different curing periods with no curing stress (after Xiao *et al.*, 2014)

Furthermore, by combining Eqs. 2.2 & 2.6, they proposed a general relationship between strength, mix ratio and curing time,

$$q_u = q_\infty\{1 - \frac{1}{1+(\frac{\alpha t}{q_\infty})^r}\}\{\frac{exp(m(\frac{1}{A_w}))}{(\frac{W}{C})^n}\} \tag{2.7}$$

Where $A_w = \frac{C}{S}$. Unlike other proposed models (for example, Eqs.2.2, 2.4 & 2.5) which only consider influence of curing time or mixing ingredients on final strength, Eq.2.7 suggests that the improved soil strength depends on three main factors: in-situ water content, binding concentration and curing time. It implies that the high variability of UCS is mainly attributable to the variation of water-soil ratio, variation of cement-soil ratio and variation of curing time.

2.2. Study on Spatial Variability of Properties of Cement-Treated Clay

The spatial variation of strength in cement-treated soil is well-documented. For instance, in Singapore, Lee (1997) found that COV of unconfined compressive strength (UCS) in jet-grouted marine clay from the Geylang River project and the Singapore River Reconstruction project are 0.3 and 0.52, respectively. Lee also found that histogram of UCS is left-shifted (See **Figure 2.5**). Kawasaki *et al.* (1984) reported that the coefficient of variation (COV) of shear strength of improved soil was observed to be between 0.25 and 0.35 in several projects at Tokyo. Namikawa and Koseki (2013) found that COV of UCS in deep-cement-mixed soil columns ranges from 0.269 to 0.4 in lower clay layer, which is slightly higher than COV in upper sandy layer (**Figure 2.6)** in coastal areas of Japan. Honjo (1982) summarised the statistical analysis of UCS in soil improved by deep-cement-mixing in various locations of Japan, and reported coefficients of variation (COV) between 0.21 and 0.36 in cohesive soil layers, with a higher range of 0.32 - 0.4 in sandy layers. Kasama *et al.* (2012) also reported UCS of cement treated soil in Japan, with mean value of UCS ranging from 100 to 7500 kPa and COV of 0.14-0.99. Based on 10 deep-mixing projects in the USA, Bruce *et al.* (2013) reported COV of un-drained shear strength ranging from 0.34 to 0.79, with a mean value of 0.56 Mpa. Recent reports on coefficient of variation of cement-treated soil are summarized in chronological order in **Table 2.1**.

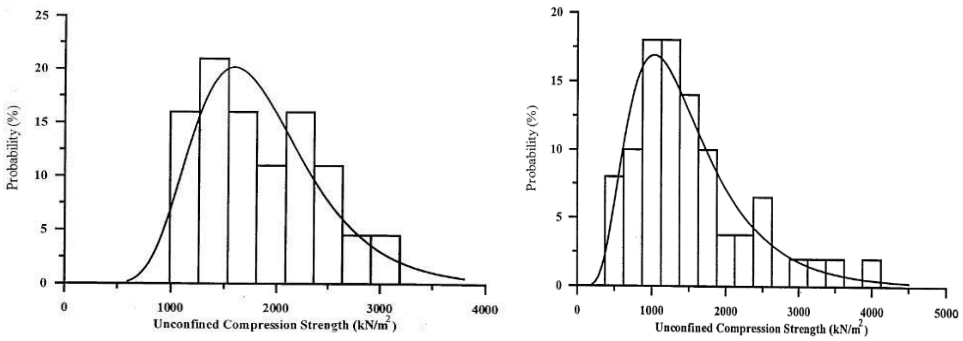

(a) (b)

Figure 2. 5 Histogram of core sample strength in DSM soil of (a) Geylang River Project. (b) Singapore River Contact 1 and 2. (after Lee, 1999)

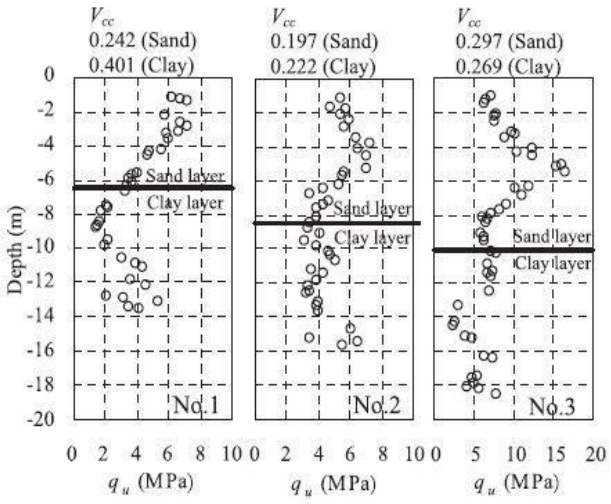

Figure 2. 6 Profile of unconfined compressive strength of core samples. $\boldsymbol{V_{cc}}$ is the coefficient of variation. (after Namikawa and Koseki, 2013)

Table 2. 1 A summary of coefficient of variation of strength in cement-treated soil in recent reports.

References	**Properties**	**COV**	**Soil types**	**Location**
Honjo, 1982	UCS	0.21-0.36 0.32-0.4	Cohesive soil Sandy soil	YokohamaPort, Tokyo Bay, Koto-ku Ariake, Chiba Port, Japan
Kawasaki *et al.*, 1984	Shear strength	0.25, 0.35	Clay	Tokyo
Lee, 1997	UCS	0.3,0.52	Marine clay	Singapore
Kasama *et al.*, 2012	UCS	0.14-0.99	N.A.	Various construction projects in Japan
Namikawa and Koseki, 2013	UCS	0.2-0.3 0.2-0.4	Sand Clay	Coast area, Japan
Bruce *et al.*, 2013	Un-drained shear strength	0.34-0.79, 0.56 in mean	N.A.	From 10 deep mixing projects in the Unites Status

In recent years, many researchers have made efforts to determine the factors resulting in the high spatial variability in cement-treated soil. Namikawa and Koseki (2013) summarized main factors influencing spatial correlation of strength in core samples as follows: non-uniform distribution of cement content, variation in in-situ soil properties and construction conditions. In the Federal Highway Administration Design Manual (Bruce *et al.*, 2013), 17 key factors resulting in the variability of treated ground (**Table 2.2**) were classified into three categories: site and project characteristics, factors that may be controlled by project specifications, and factors that may be controlled by the deep-mixing contractors.

Table 2. 2 Summary of factors which may affect strength of mixing soil. (after Bruce *et al.*, 2013)

Category	Factors
Characteristics of binder	• Type of binder(s) • Quality • Mixing water and additives
Characteristics and conditions of soil (especially important for clays)	• Physical, chemical, and mineralogical properties of soil • Organic content • pH of pore water • Water content
Mixing conditions	• Amount of binder • Mixing efficiency • Timing of mixing/remixing
Curing conditions	• Temperature • Curing time • Humidity • Wetting and drying, freezing and thawing, etc.
Loading conditions	• Loading rate • Confining pressure • Stress path (e.g., compression, tension, and simple shear)

2.2.1. Mixing Process

The statistical characteristics of the spatial variation of cement-treated soil have also been found to be related to operational parameters during installation. Using Lee *et al.*'s (2006, 2008) data, Chen *et al.* (2014) fitted an empirical relationship between blade rotation speed and UCS within cement-treated columns. The test data was found to lie within three bands, depending upon the cement slurry density (See **Figure 2.7**).

In a study on dry lime-mixed columns assessed by penetrometer test, Larsson (2005a, 2005b) observed a significant influence of blade rotation number in mixing process on the reduction of coefficient of variation (**Figure 2.8**) in strength. However, he reported that the parameters of mixing process, with respect to the blade rotation number, may only influence the spatial correlation within a short distance of few centimetres.

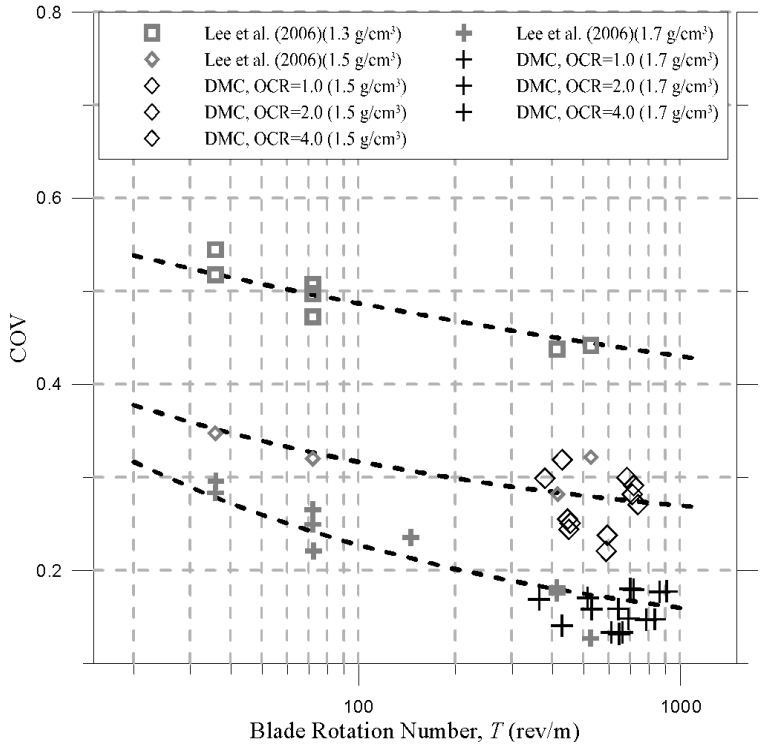

Figure 2. 7 Curve for coefficient of variation with blade rotation number with data from Lee (*et al.* 2008) (after Chen *et al.*, 2014)

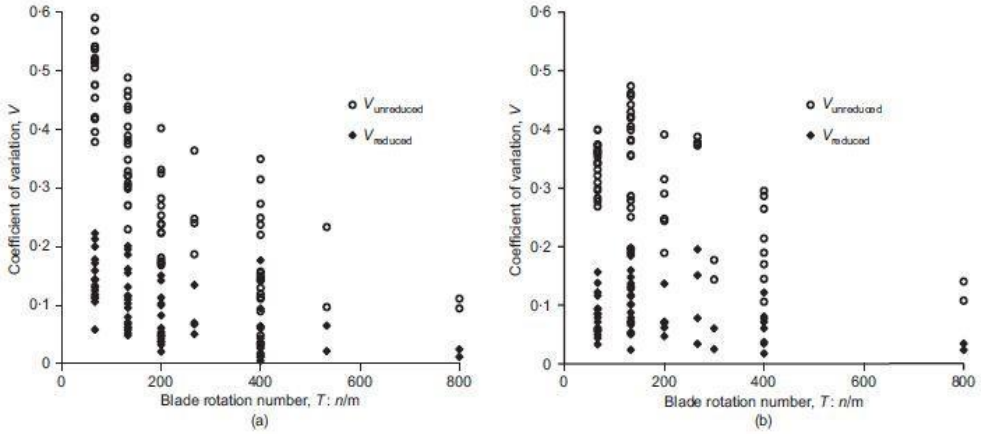

Figure 2. 8 The reduction effect on coefficient of variation from (a) Strangnas; (b) Haby (after Larsson, 2005a)

2.2.2. Other Uncontrollable Factors

Besides inherent variability of soil structure, inconsistency in mixing process, uncertainty in geotechnical monitoring are inevitable error sources in data process. Al-Naqshabandy (2011) postulated and classified uncontrollable error sources leading to the high variability in cement-treated soil, such as random testing error, statistical error of mean, bias in measurement procedure (**Figure 2.9**). He proposed that the variation in improved soil properties shall be the sum of variations caused by each factors listed. In addition, Liu *et al.* (2015) highlighted that positioning errors and off-verticality of mixing shaft in operation can also give rise to the variability in improved soil properties.

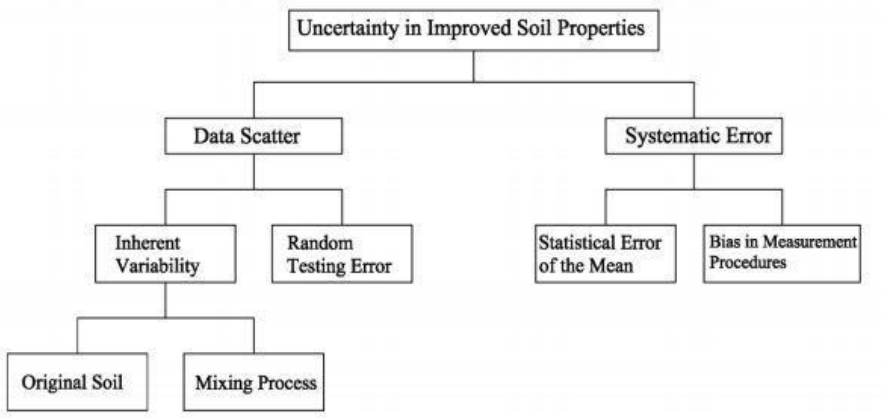

Figure 2. 9 Summary of sources leading to uncertainty in cement-improved soil properties (after Al-Naqshabandy, 2011).

2.2.3. Effect of Variation in Soil Property on Design Strength

In deterministic design, the properties of a given soil type are assumed to be homogeneous. In contrast, a stochastic medium possesses significant spatial variation in soil properties and this can affect mass performance. For instance, compared to homogeneous soil model, variation in soil strength changes the failure load and mechanism, thereby modifying the design strength. One aspect of this is reduction in bearing capacity (e.g. Kasama *et al.*, 2012; Fenton, 2003; Popescu *et al.*, 2005). Using random numerical simulation, Popescu *et al.*

(2005) demonstrated that the spatial variability of soil's shear strength results in reduction of bearing capacity, compared to corresponding homogeneous soil case. He also found that Coefficient of Variation (COV) and Probability Density Function (PDF) of shear strength has the greatest effect on the reduction in bearing capacity. Similarly, Kasama *et al.* (2012) pointed out that, for a random soil field with coefficient of variation in shear strength in a range from 40% to 80%, the expected mean bearing capacity is approximately 50%-80% of that of a deterministic soil.

2.3. Summary of Knowledge Gaps and Issues

Knowledge gaps currently exist in three main aspects of the characterisation and consideration of spatial variation in cement-treated ground:

2.3.1. Consideration of Curing Time Effect in Core Strength Interpretation

Based on experimental results, many researchers (Mitchell, 1976; Lim and Zollinger, 2003; Xiao *et al.*, 2014) have proposed several relationships to describe the correlation between curing time and strength of cement-treated soil. However, few, if any, of these relationships have been verified with a large amount of field data, and none has been proposed for being used in core strength assessment. In this study, this issue has been examined based on over 1000 core strength measurements from two sites. By doing so, the applicability of proposed time-strength relationships to field data can be critically examined.

2.3.2. Influence of Site Condition to the Strength of improved soil

In-situ soil state and condition often varies from one location to another, even before improvement. This may influence the resulting strength of the mix. Several studies (Gallavresi, 1992; Lee *et al.*, 2005; Larsson, 2001) reported that different mix ratio (i.e. soil-cement-water mass proportions) can result in disparity of strength of cement-mixed soil from a deterministic point of view. During cement-mixing, in-situ water can be introduced in mixing slurry along with in-situ soil. Variation in in-situ water content may be one of major sources leading to high variability in strength of cement-treated soil. Although experimental reports can derive correlation between in-situ water content and strength of cement-treated soil, it is hard and rare to find feedback from site works. In addition, in current engineering practice, the design value for water-cement-soil ratio is usually assumed to be fixed. Thus, there is a necessity to investigate the influence of in-situ soil condition to the strength of improved soil. This issue is examined in this study.

2.3.3. Sample Size and Soil Property Estimation in a Random Medium

In many engineering situations, it is time-consuming and expensive to collect hundreds of core strength measurements. Especially in the small projects, there is often a question on reliability of measured soil properties if the sample size is small. Amundaray (1994) showed that the coefficient of variation and mean of unconfined compression test data are unstable for sample size less than 30. Based on result shown in **Figure 2.10**, he suggested that 30 probably is a good indicator of representative sample population in soil property determination.

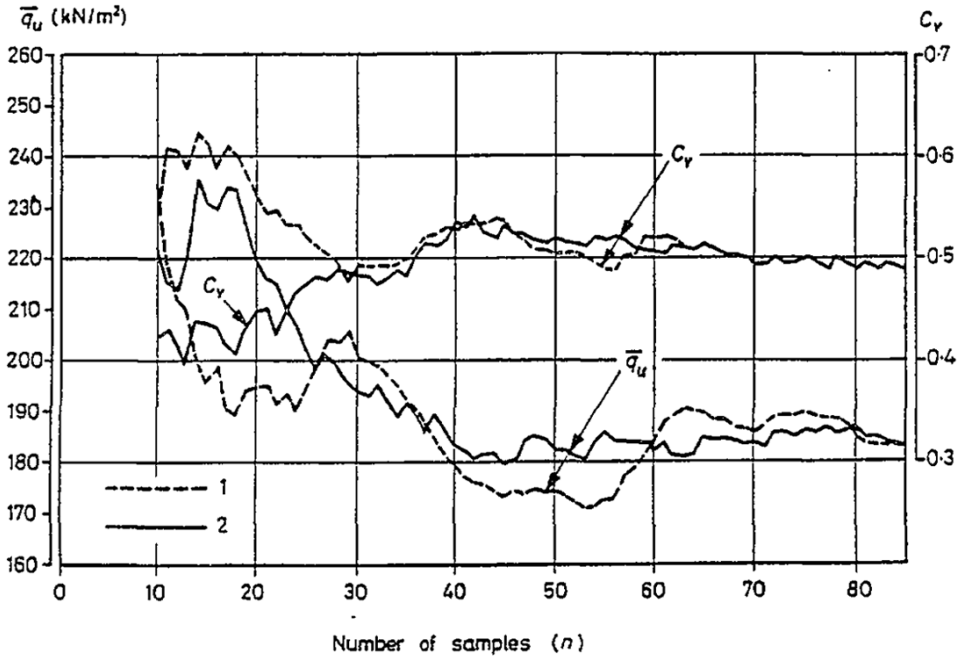

Figure 2. 10 Mean $\bar{q}_u$ and coefficient of variation C_v of unconfined compression strength of the soil versus the number of samples. 1-samples in the original sequence; 2-samples in random sequence (after Amundaray, 1994)

Instead of minimum sample size, sample density is required in current practical method of estimation via minimum soil strength proposed by LTA (2010) and BS-EN 12716:2001 (B/526, 2011). However, these criteria appear to be based more on sizes of the sites rather than statistical reliability. For instance, LTA (2010) requires that "*"...A minimum of 3 samples shall be taken from top and middle and bottom of each core for strength and stiffness testing"*. This implicitly assumes that the top-to-bottom variation is a low-order function which can be adequately defined by just three points. It is also at-odds with Larsson's (2005) finding that the scale of fluctuation of the strength variation of lime-treated soil can be short, of the order of a few centimetres. Where the scale of fluctuation is so short, interpolation between 3 points may not adequately address the variation. Moreover, small sample size will quite often result from small sites. Hence, there is a necessity to find robust criteria which can offer reliable statistical evaluation of soil properties even if only a small amount of measured data is available.

2.4. Scope of Study

This study examines the above issues using field data from two cement-improvement projects in Singapore, namely, Marina One project and Marina Bay Financial Centre (MBFC) project. Based on available information from two projects, the scope of study is to address the following unknowns and issues related to the spatial variability of cement-treated clay:

2.4.1. Influence of curing time between installation and core testing on the measured strength

In the Marina One and MBFC sites, soil samples had experienced various durations of curing from installation of soil columns to strength testing, which vary from few weeks up to hundred days. In order to assess the influence of curing time on strength of cement-treated soil, accuracy of several time-strength relationships will be examined with data samples from two projects. Once the time impact is identified, strength of cement-treated soil can be normalized to its equivalent strength corresponding a 28-day curing time, in such a way that the ultimate strength can also be predicted.

2.4.2. Effect of in-situ moisture content on the measured strength of cement-treated soil

In the MBFC and Marina One sites, the in-situ moisture content both laterally and vertically varies (i.e. with depth). During cement mixing process, the in-situ soil and water were mixed with cement slurry within the mixing column. For a constant slurry portion, more water will be present in the cement-treated soil if natural soil possesses higher in-situ moisture content. Experimental studies (Lee *et al.*, 1997) found that more water in mixing may result in low strength of cement-treated soil. In this study, the impact of in-situ

moisture content on strength of cement-treated soil will be evaluated with field data from MBFC project and Marina One project. If water-strength correlation can be observed in site data, the variation in in-situ water content shall not be negligible during soil-improvement works. That is to say, the variability of strength in cement-treated soil may depend on the distribution of in-situ moisture content in site.

2.4.3. Robustness of criteria for characteristic soil strength in small sample size

There are over 1000 core strength measurements from Marina One project. By the standard of cement-soil mixing works, this can be considered as a large sample to represent the real strength distribution in cement-treated soil. In contrast, in many small projects, only limited amount of sample data are available, and estimation of soil strength might be unreliable. In order to reduce the errors in strength interpretation from small datasets, robust criteria of characteristic soil strength are proposed. Based on measured soil strength from Marina One project, random data of different sizes varying from 20 to 1000 will be generated. Robust criteria will be applied on randomly generated data, and their reliability and consistency will examined in different sample size.

If a robust criterion performs consistently regardless of sample size, it can be considered as a reliable practice to characterize soil strength, especially in small sample size. One potential application is to reduce the required amount of testing samples by LTA (2010) to a relatively small amount, in such a way that budgets for soil improvement can be lowered.

3. Site Description

Marine clay of the Kallang Formation underlies almost one quarter of Singapore Island, and is mainly found in river valleys, estuaries and coastal area. It is the major constituent of the Kallang Formation, mainly consisting of recent deposits of marine, alluvial, littoral and estuarine origins (Tan, 1983). In areas where the marine clay deposit is thick, it is usually present in two layers, namely upper marine clay (2A) and lower marine clay (2B). These two kaolinite-rich clay layers are usually separated by a stiffer intermediate layer, which is widely believed to be the desiccated crust of the lower marine clay.

The upper marine clay is often classified as an inorganic clay with high liquid limit and plastic index (Lee *et al.*, 2005). In general, the upper marine clay is classified as soft even very soft clay, whereas the lower marine clay can reach medium stiff at desiccated top (Tan, 1983).

In this study, upper and lower marine clay were considered as two different clays due to their significantly different in-situ water contents. Generally, upper marine clay possesses a much higher liquid limit and plastic limit than lower marine clay. That is to say, the range of in-situ water content in upper marine clay is higher than the one in lower water content. **Table 3.1** and **Figure 3.1** show some published data on the Atterberg Limits of Singapore marine clay.

As can been seen in **Figure 3.1**, even within the small Singapore Island, the Atterberg Limits and Water content of the marine clay vary from one location to another. Recommended Atterberg Limits can be approximated as follows: Plastic Limits of upper and lower marine clays are usually lower than 45% and 30%, respectively; whereas Liquid Limits of upper and lower marine clays are usually higher than 80% and 60%, respectively. Water content of upper marine clay is reported usually between 60% and 90%; while in lower marine clay layer, water content falls between 40% and 60%.

Table 3. 1 Summary of Atterberg Limits of Singapore Marine Clay in recent papers L = Liquid Limit; WC = Water Content; PL = Plastic Limit

References	**Atterberg Limits**	**Marine Clay Types**		**Location**
		Upper	**Lower**	
Lu, 2014	LL (%)	85 - 92	-	N.A.
	PL (%)	25 - 46	-	
Arulrajah and Bo, 2008	WC (%)	70 - 80	40 - 60	Changi Airport
	LL (%)	80 - 95	65 - 90	
	PL (%)	20 - 28	20 - 30	
Chong, 2002	LL (%)	-	63 - 80	site of the proposed Singapore National Arts Centre
	PL (%)	-	22 - 24	
Chin, 2006	WC (%)	72	-	from 4 to 5m depth below seabed, at a dredge site offshore of Pulau Tekong
	LL (%)	90	-	
	PL (%)	40	-	
Tan, 1983	WC (%)	60 - 110	47 - 70	N.A.
	LL (%)	75 - 115	63 - 80	
	PL (%)	50 - 77	39 - 55	
Yong and Karunaratne, 1990	WC (%)	60 - 90	50 - 70	N.A.
	LL (%)	80 - 120	60 - 90	
	PI (%)	50 - 80	40 - 50	
Tanaka *et al.*, 2001	WC (%)	50 - 60		14-28m, Land reclaimed about 1975
	LL (%)	65 - 80		
	PL (%)	40 - 60		
Xiao *et al.*, 2014	WC (%)	70		4-5m below seabed off Singapore's north eastern coast
	LL (%)	88		
	PL (%)	38		

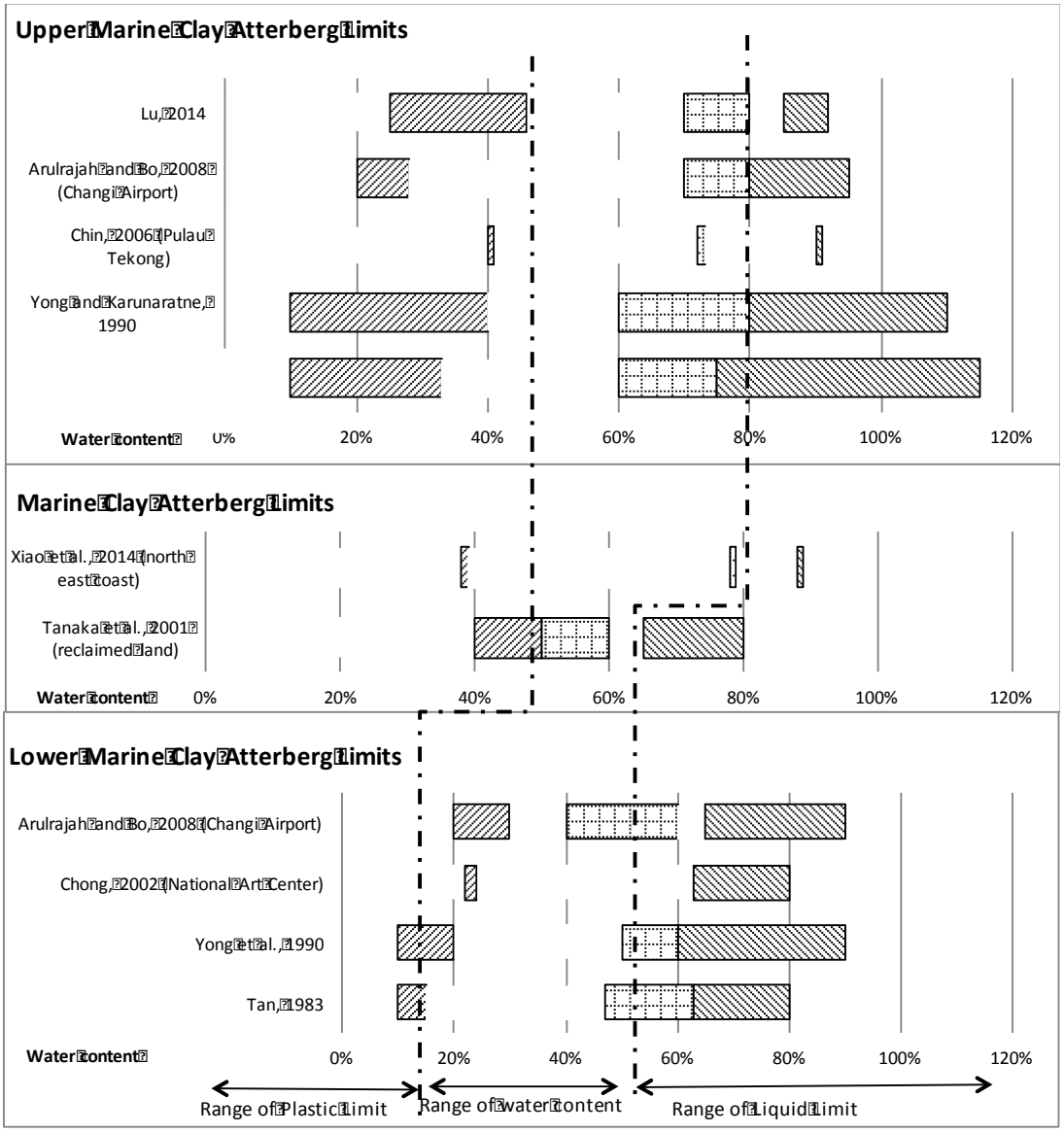

Figure 3. 1 Summary of Atterberg Limits of Singapore Marine Clay in recent papers

3.1. MBFC site

The Marina Bay Financial Centre (MBFC) is sited on land reclaimed from the sea in the 1970's in the Marina South district of Singapore (see **Figure 3.2**). As part of the MBFC construction, the soft marine clay underlying the sand-fill was improved using deep-cement-mixed column from 8 m to 20 m in depth.

Before soil improvement, site investigation was carried out over whole area, with borehole layout as shown in **Figure 3.3**. **Figure 3.4** shows a typical in-situ soil profile. In general, the upper marine clay layer reaches up to 30 meter in depth. Hence, only the upper marine clay was treated by deep-cement mixing. **Figure 3.3** enclosed the cement-treated area in bolded line. **Table 3.2**, from Chen (2014), summarized operational parameters of deep cement mixing process.

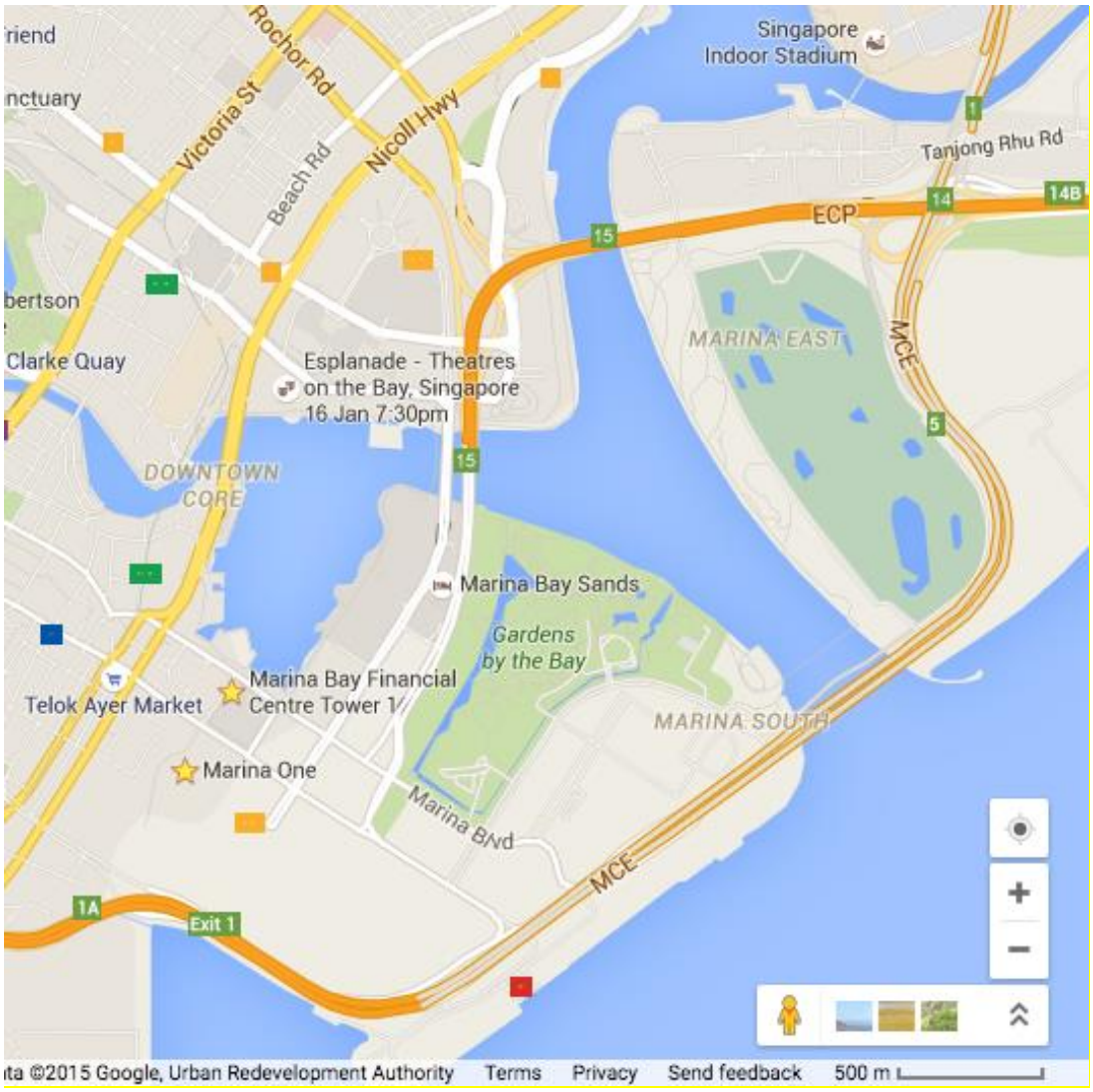

Figure 3. 2 Location of MBFC site and Marina One site (Source: Google Maps)

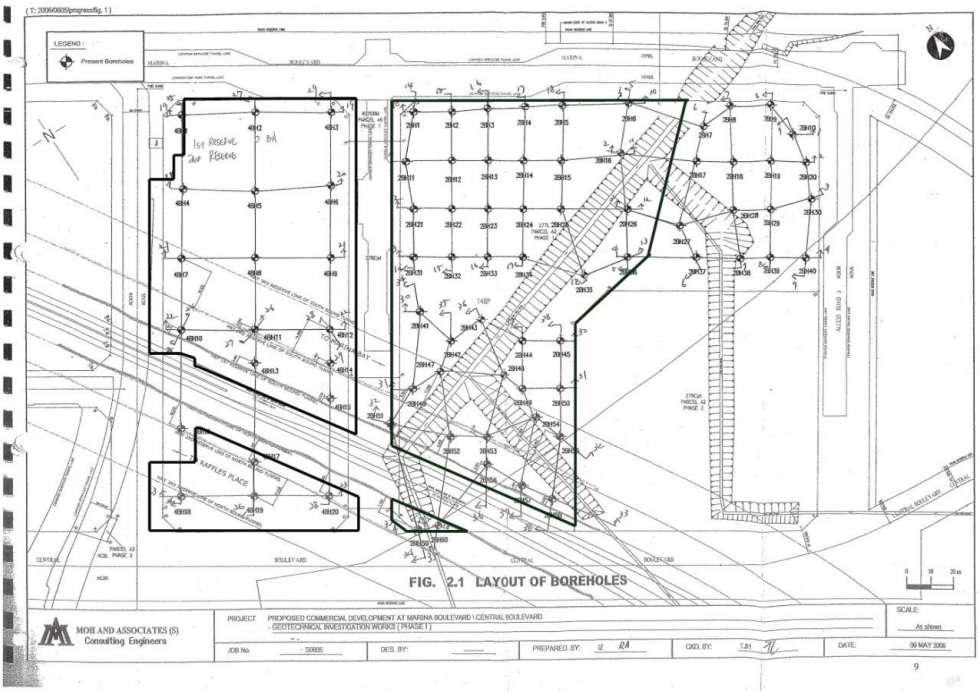

Figure 3. 3 Site Investigation lab map in MBFC site; DMC test panel layout enclosed in bold black line.

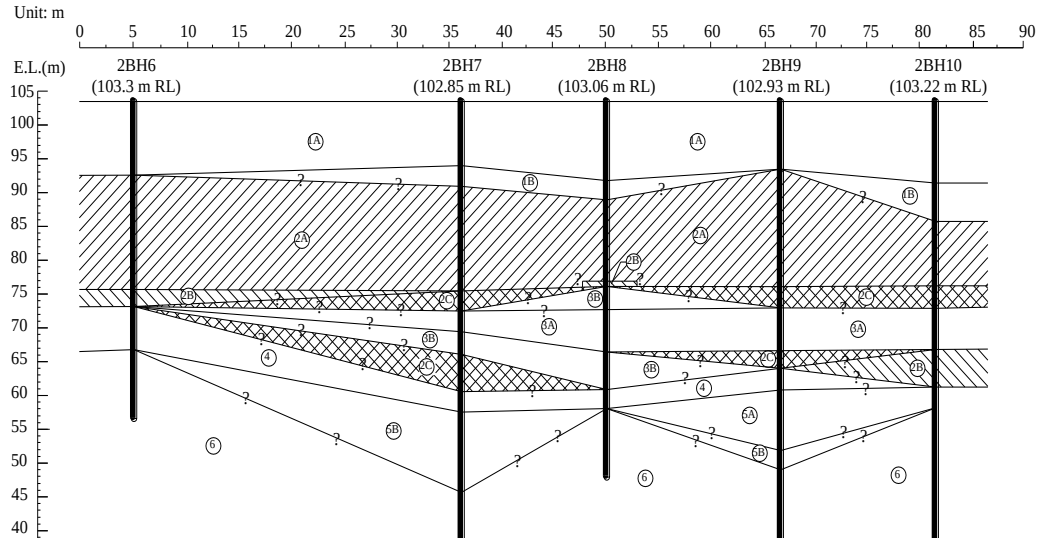

Figure 3. 4 Typical in-situ soil profiles before ground improvement in MBFC site. (2A: Upper marine clay; 2B: Lower Marine Clay; 2C: Silty Clay; 3A:F1 Kallang Formation; 3B: F2 Kallang Formation; 4: Old Alluvium(D); 5A: Old Alluvium(C); 5B: Old Alluvium (B); 6: Old Alluvium (A)).

Table 3. 2 Deep mixing parameters for Marina Bay Financial Centre (after Chen, 2014)

Parameters	Design values
Strength and Stiffness Requirements	
Minimum unconfined compressive strength at 28 days (kPa)	800
Minimum Young's Modulus at 28 days (Mpa)	150
Operating Parameters	
Water cement ratio (w/c) for cement grout, a	0.9
Unit weight of cement γ_b (g/cm^3)	3.2
Area covered by one deep mixing column A_c (m^2)	0.785
Number of columns simultaneously installed, n	4
Discharge rate of cement grout for 4-shaft Q (L/min)	480
Total discharge time per m length of column t_b (min)	2.54
Jack-in speed/withdrawal speed v_s (m/min)	0.394/0.394
Number of blades	4
Rotational speed of blade, v_r (rpm)	27.5

Figure 3.5 shows a three-dimensional scatter plot of in-situ water content in cement-treated layer. As shown in **Figure 3.5**, significant variation exists in in-situ water content not only in vertical direction, but in horizontal direction as well. In general, distribution of in-situ water content in MBFC increases along depth. In some measured points, in-situ water content reaches as high as 70%-80% at the deeper parts of the soil layer.

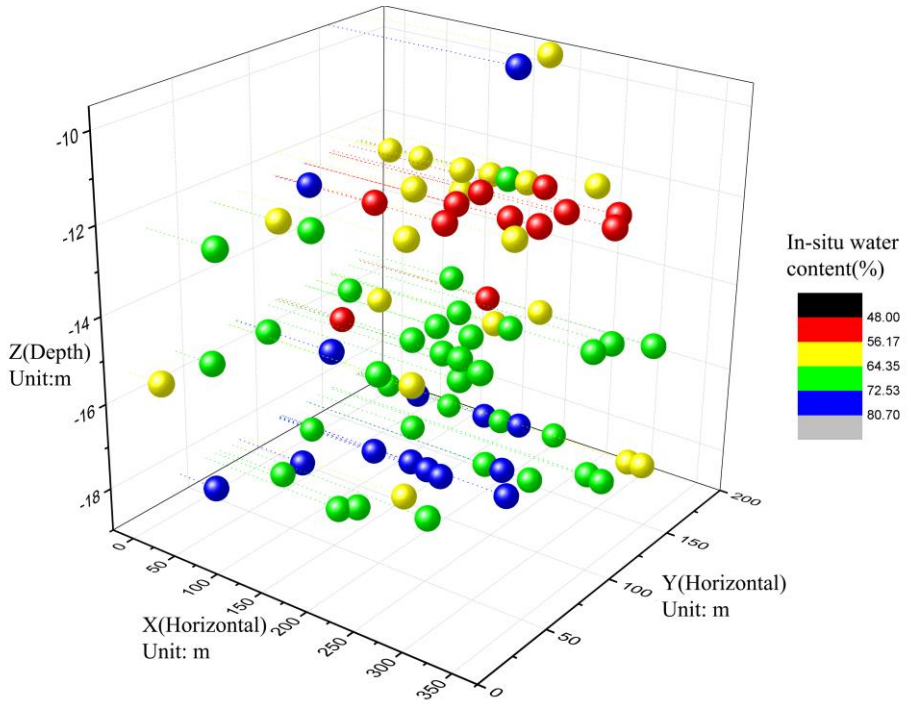

Figure 3. 5 3-dimensional scatter plot of in-situ water content in MBFC (Number of data: 78)

The strength of improved soil was assessed by UCS testing of core samples following BS 1377: PART7:1999. The curing times of the samples vary from 28 days to 180 days. As can be seen in **Table 3.2**, the requirement on the minimum targeted value of 28-day UCS and 28-day Young's modulus were 800 kPa and 150 Mpa, respectively. **Table 3.3** summarized the variation in curing times from installation to testing in MBFC project.

The histogram of unconfined compressive strength in cement-admixed soil in MBFC is shown in **Figure 3.6**. As can be seen, the histogram of UCS is strongly left-skewed with few outliers in upper-tail. The coefficient of variation (COV) of UCS in cement-treated soil is approximately 0.416, which is higher than the COV reported by Honjo (1982), Kawasaki *et al.* (1984) and Namikawa and Koseki (2013), but is within the range of COV reported by Lee (1997) and Bruce *et al.* (2013).

Table 3. 3 Summary of curing durations from soil column installation to core sampling tests in MBFC site

	28 – 50 days	**50 – 100 days**	**100 – 150 days**	**>150 days**
Percentage	0.4%	88%	4%	8%
Sample size	1	204	9	18
Total sample size	232			

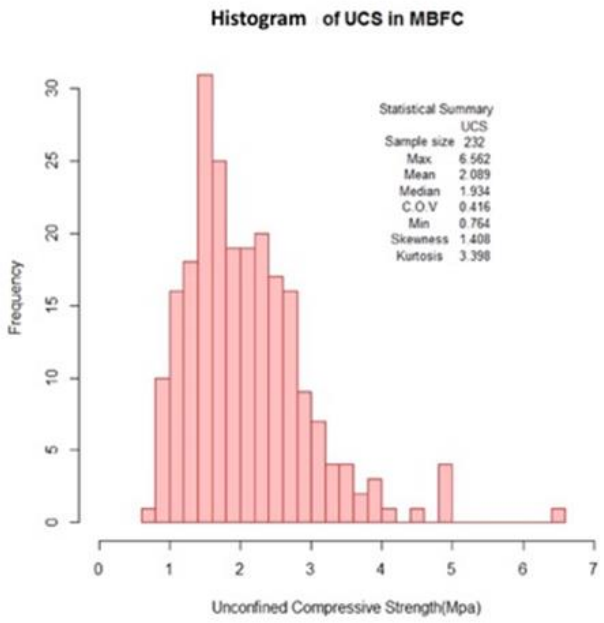

Figure 3. 6 Histogram of UCS of cement-treated marine clay in MBFC

3.2. Marina One

The Marina One site is adjacent to the MBFC site. Its in-situ soil profile is similar to that of the MBFC site. The ground improvement zone is consisted of four equal-sized areas around a tower block (see **Figure 3.7**), overlying a soft clay zone from 15m to 25m in depth. As **Figure 3.8** shows, two types of soil layers were recognized in cement-treated zone, namely upper marine clay layer (2A) and the lower marine clay layer (2B) below. A stiff clay layer separates upper and lower marine clay layers. This clay layer is considered as a part of lower marine clay layer in site investigation report.

Figure 3.9 shows a three-dimensional scatter plot of in-situ water content in cement-treated layer. The in-situ water content in Marina One site shows a two-layer structure, decreasing gradually from 60% to 30% as depth increases.

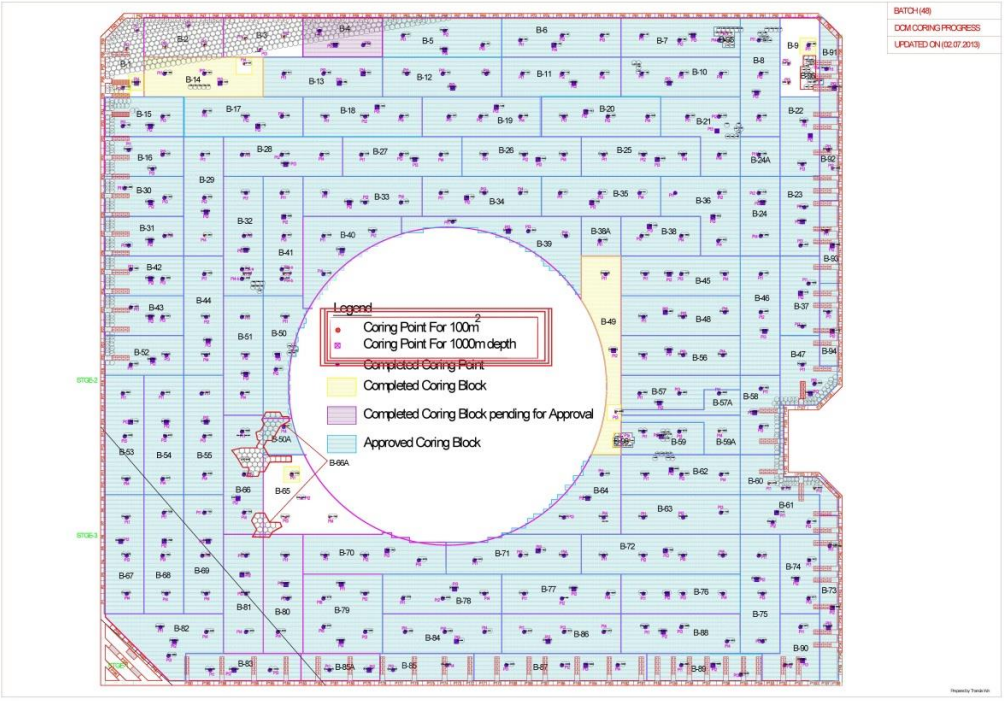

Figure 3. 7 Deep-cement-mixing testing borehole layout in Marina One project.

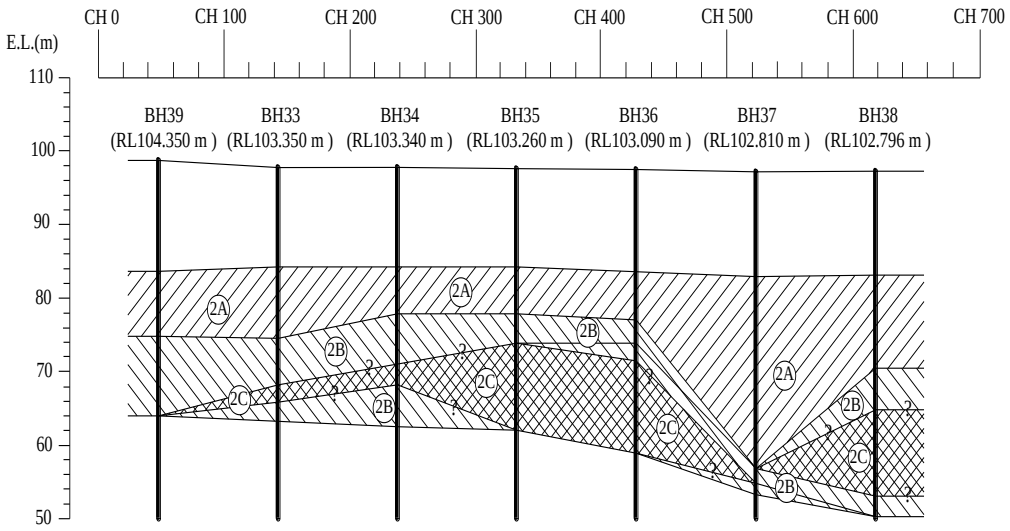

Figure 3. 8 A typical soil profile in Marina One site before ground improvement (2A: Upper marine clay; 2B: Lower Marine Clay; 2C: Silty Clay).

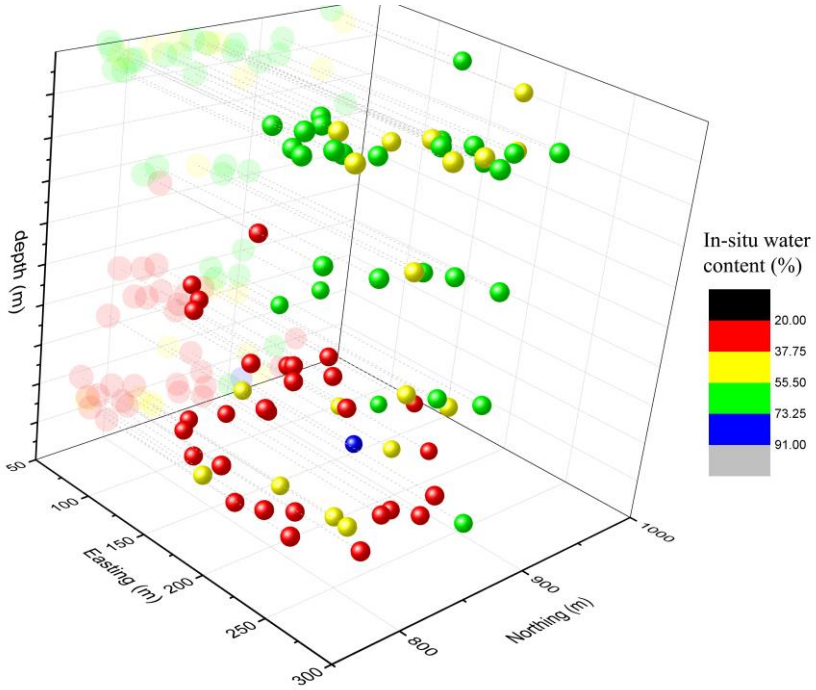

Figure 3. 9 A 3-dimensional scatter plot of in-situ water content in Marina One site. (Number of data: 72)

The deep soil mixing (DSM) technics has been applied in marine clay of depth from 10 m to 25 m in approximation, by injecting slurry of Portland Blast Furnace Cement (PBFC) with a cement-water ratio of 1:1, to achieve an in-situ cement content of 180 kg/m^3 in cemented soil columns. Compared to Ordinary Portland Cement (OPC), PBFC-mixed soil possesses lower strength-gain rate, but its ultimate long term strength may be higher (Lafarge, 2014). Other designed operational parameters are listed in **Table 3.4**, and the DSM jack-in-withdrawal cycle is illustrated in **Figure 3.10**.

After DSM works, core samples were tested for Unconfined Compressive Strength following BS 1377: PART7:1999. A typical lab report has been shown in **Figure 3.11**. Curing times of core samples from cement mixing to strength testing vary from few days to few months. A summary of curing times is shown in **Table 3.5**.

Table 3. 4 Designed operational parameters of DSM works in Marina One project

No		1	2
Cement Content	**Thickness**	9	20
	kg/m3	180	180
	Litre	5343	11878
	Ton	4.02	894
Descending	**Thickness**	16	6
	Time(min)	16	6
	Speed (m/min)	1	1
Injection	**Time(min)**	20.9	46.5
	Speed (m/min)	0.43	0.43
	Flow	255	255
Toe	**Time(min)**	4	4
Mixing	**Time(min)**	18	40
	Speed (m/min)	0.5	0.5
Ascending	**Time(min)**	16	6
	Speed (m/min)	1	1
Total Time		74.9	102.5

Description	**Parameter**
Diameter of DSM	1300x2 shafts
Area of 2-shaft DSM	2.484m2
Grout flow	354319283+-10%
speed	Normal+-10%
Ratio	1.405+-0.03
Water cement ratio	1:01

Table 3. 5 Summary of curing durations from soil column installation to core sampling tests in Marina One site

	<28 days	28 – 50 days	50 – 100 days	>100 days
Percentage	17%	58%	18%	7%
Sample size	198	665	208	78
Total sample size	1149			

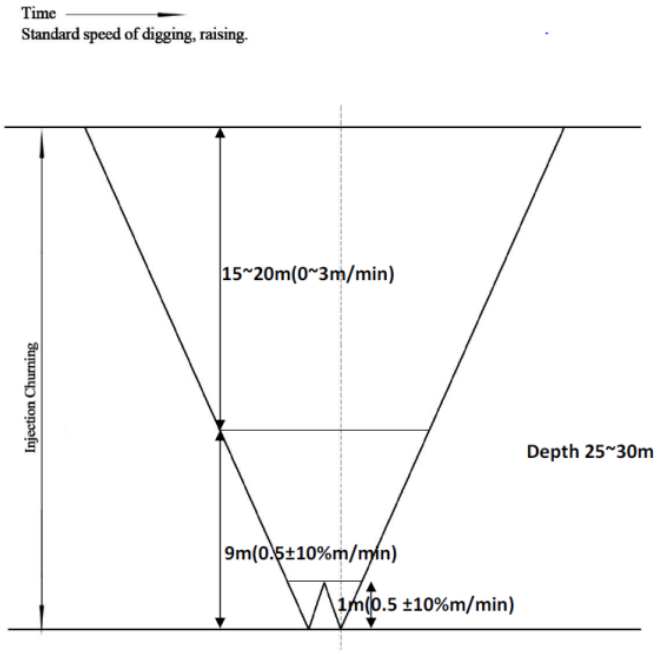

Figure 3. 10 A schematic DSM jack-in-withdrawal Cycle in Marina One

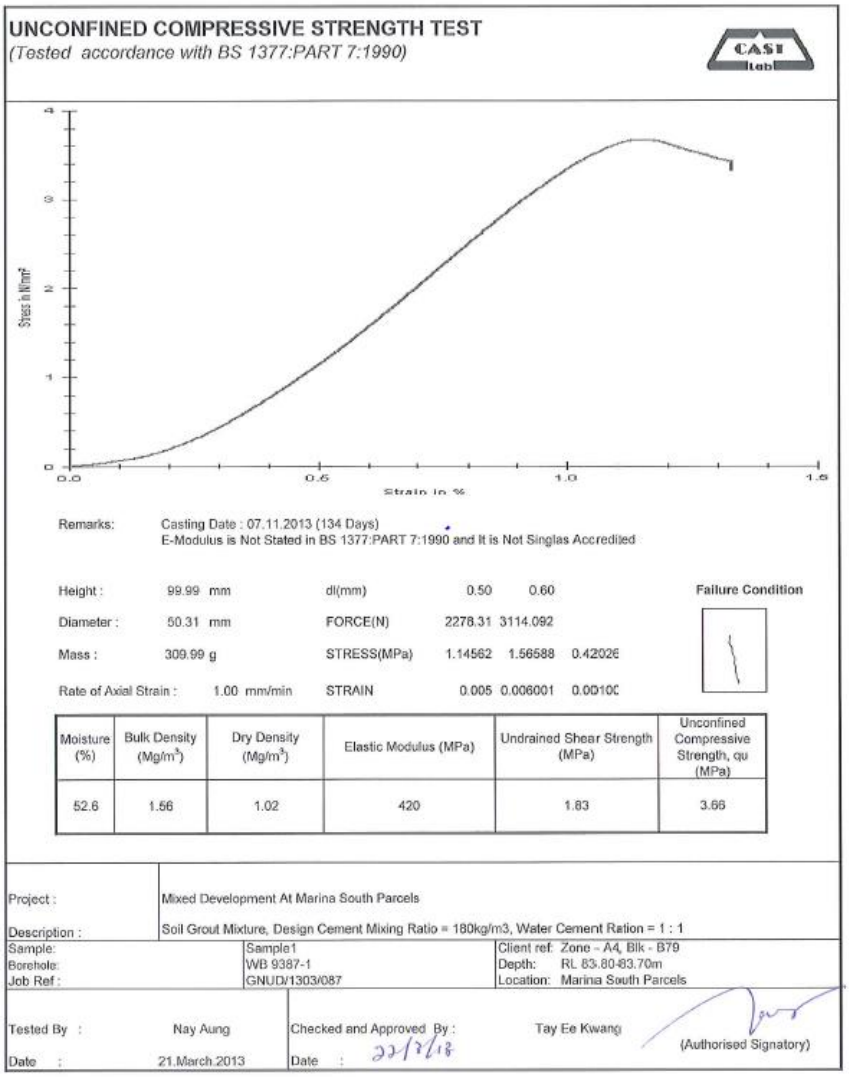

UNCONFINED COMPRESSIVE STRENGTH TEST
(Tested accordance with BS 1377:PART 7:1990)

CASI Lab

Stress in N/mm²

Strain in %

Remarks: Casting Date : 07.11.2013 (134 Days)
E-Modulus is Not Stated in BS 1377:PART 7:1990 and It is Not Singlas Accredited

Height :	99.99 mm	dl(mm)	0.50	0.60		Failure Condition
Diameter :	50.31 mm	FORCE(N)	2278.31	3114.092		
Mass :	309.99 g	STRESS(MPa)	1.14562	1.56588	0.42026	
Rate of Axial Strain :	1.00 mm/min	STRAIN	0.005	0.006001	0.001001	

Moisture (%)	Bulk Density (Mg/m³)	Dry Density (Mg/m³)	Elastic Modulus (MPa)	Undrained Shear Strength (MPa)	Unconfined Compressive Strength, qu (MPa)
52.6	1.56	1.02	420	1.83	3.66

Project :	Mixed Development At Marina South Parcels		
Description :	Soil Grout Mixture, Design Cement Mixing Ratio = 180kg/m3, Water Cement Ration = 1 : 1		
Sample:	Sample1	Client ref:	Zone - A4, Blk - B79
Borehole:	WB 9387-1	Depth:	RL 83.80-83.70m
Job Ref :	GNUD/1303/087	Location:	Marina South Parcels
Tested By :	Nay Aung	Checked and Approved By :	Tay Ee Kwang
Date :	21.March.2013	Date :	22/3/13

(Authorised Signatory)

Figure 3. 11 An example of core sampling report of Unconfined Compressive Strength lab test of cement treated soil in Marina One project.

According to site investigation report, the depth of boundary between reclaimed sand-fill and soft marine clay layer varies from 10 m to 15 m. In this study, only the cement-treated marine clay is considered. Thus, cement-treated soil samples from a depth of 15 m to 25 m were selected for further analysis. A total amount of 1149 improved soil samples from this layer were selected. Similarly, in-situ moisture content of natural soil samples in depth from 15m to 25m will be investigated later.

The histogram of UCS in cement–admixed soil in Marina One project is illustrated in **Figure 3.12**. Similar to UCS distribution in MBFC site, the distribution of UCS in Marina One is left-skewed, with a similar coefficient of variation of 0.423.

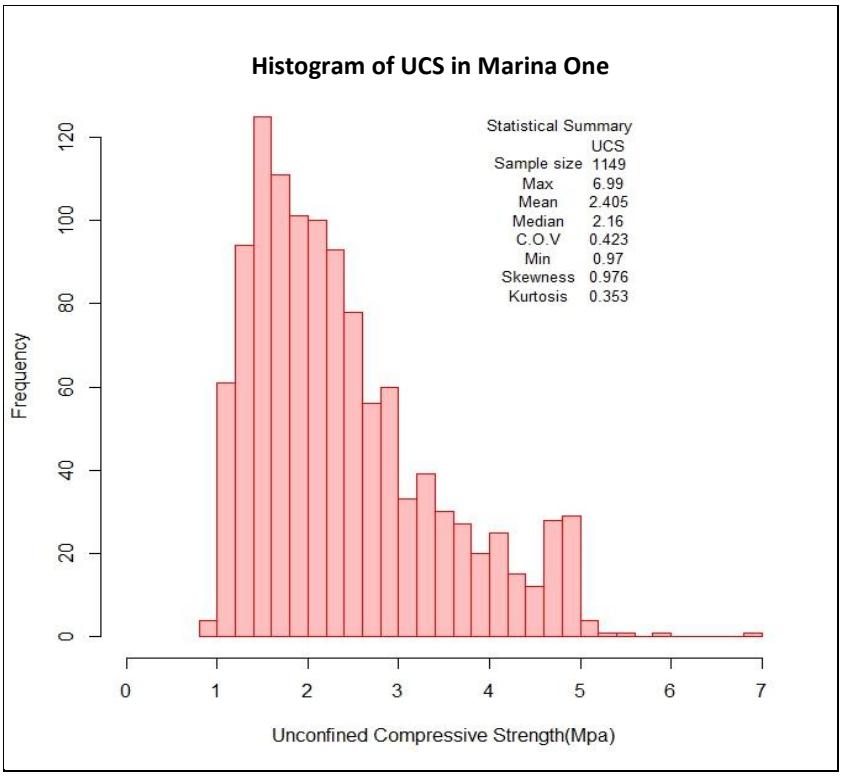

Figure 3. 12 Histogram of UCS after cement-treatment in Marina One

3.3. Data Processing Considerations

As mentioned before, there are many causative factors for the spatial variation in strength of cement-admixed clay. It is not possible to fully isolate the effect of each factor from core sample test report and site investigation report. For example, curing temperature and curing pressure (Bruce *et al.*, 2013) are rarely documented in engineering practice. In addition, uncertainties resulting from operational errors and random testing errors cannot be assessed from these reports. Due to the limitation of available information, these uncontrollable and undeterminable error sources will not be examined in this study.

In many experimental studies on trend and auto-correlation, large amount of data were taken in one bore-hole with small intervals (Cafaro and Cherubini, 2002; Firouzianbandpey *et al.*, 2014). This facilitates study on vertical spatiality of soil property within a single bore-hole. However, in this case study, only about four samples were taken in each bore-hole. Hence, instead of local spatial variability behaviour, an averaged global spatial variability in vertical direction was studied by assuming weak stationary in horizontal direction. This assumption implies that, for modelling purpose, soil properties in all bore-holes are assumed to be statistically similar, but not necessarily depth-invariant.

In such a study, it is often difficult to isolate the variation caused by one single factor while holding other variables constant. For example, when fitting time-strength correlation, variation caused by in-situ water content still exists; and vice versa. Only a lump-sum variation could be detected in site data. Hence, it is not surprise to see huge disparity in data. Moreover, regression by Least Square Method (LSM) may not be a good choice for this kind of data: the indicator of regression, coefficient of determination R^2 may not be meaningful. With presence of huge variation in data, R^2 is often too low to return a reliable result. Many researchers use local average method to control the variance caused by other irrelevant factors. Xiao *et al.* (2014), for instance, plotted average of measured UCS of each

curing time in their experimental studies. Similarly, Fenton and Griffiths (2008) proposed the use of local averaging to reduce variance. Thus, in first stage of data process of this project, local average method will be applied in regression fitting to eliminate variance caused by other factors.

The location of natural soil sample taken during site investigation is not the same as the location of cement-admixed soil samples taken for strength testing. Hence it is not feasible to conduct a one-to-one mapping between in-situ moisture content and strength of improved soil. Instead of studying correlation between in-situ water content and soil strength directly, an indirect mapping method was carried out herein: the trend of in-situ water content along depth, and the trend of UCS along depth will be studied separately. Finally, the correlation between in-situ water content and UCS of cement-treated soil will be related by depth.

4. Site Data Analysis: Variability Analysis of In-situ Water Content and Time Effect on Soil Strength

4.1. Impact of Curing Time on Soil Strength

Logarithmic equation

The logarithmic form represented by Eq.2.4 was firstly used to fit UCS in improved soil from the two sites. In order to reduce the variance caused by factors other than curing time, the algorithmic means of UCS at each curing time were plot in **Figure 4.1**. Fitting results led to 28-day equivalent UCS of 1.7 MPa and 2.2 MPa for MBFC and Marina One, respectively. In Eq.2.4, the normalized strength-gain path is fixed; this implies that the higher 28-day UCS in Marina One will also lead to a higher ultimate strength, compared to MBFC. This obviously ignores the differences in the strength gain patterns of Ordinary Portland Cement and Portland Blast Furnace Cement. As can be seen, for a curing time higher than 100 day, logarithmic form slightly over-estimates the strength-gain velocity in MBFC site, while under-estimating the strength-gain rate in Marina One site.

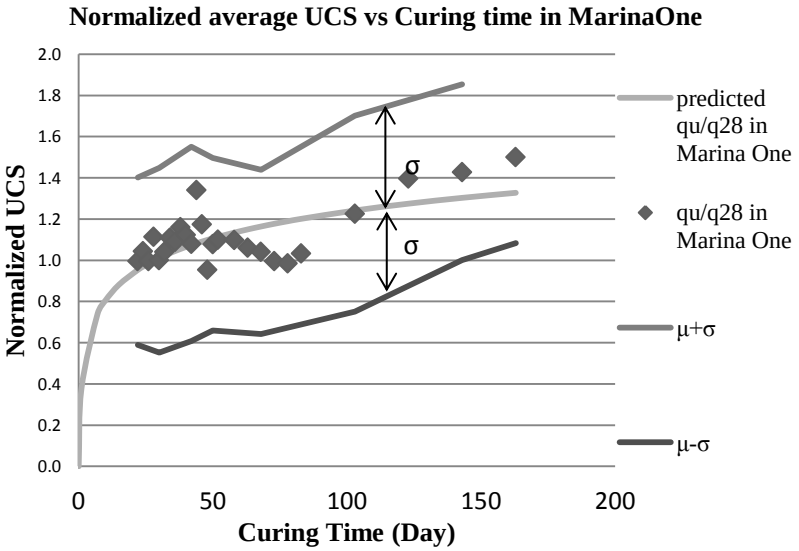

(a) Marina One

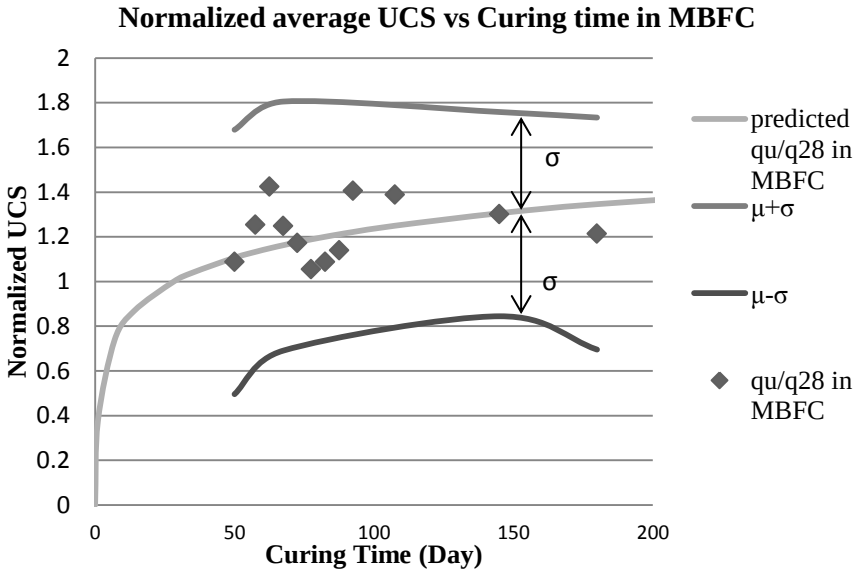

(b) MBFC

Figure 4. 1 Normalized average UCS versus curing time fitted by logarithmic form in Eq.2.4 with data from (a) Marina One; (b) MBFC. Normalized average UCS refers to $\mathbf{f_c}$ in Eqs. 2.4, the ratio of mean UCS over fitted 28-day equivalent UCS. σ refers to the standard deviation of UCS; and $\boldsymbol{\mu}$ is the mean of UCS at each curing time. Fitting Equation (Eqs. 2.4): f_c=0.187ln (t) +0.375

Generalized Hyperbolic Equation

As explained earlier, Xiao *et al.* (2014)'s generalized hyperbolic strength-gain model (Eq.2.7) can reflect the fact that the increment of strength in cement-treated soil may depend on other factors besides curing time.

Based on Eq.2.7, let:

$$q_1 = \mathrm{q}_\infty \left\{ \frac{\exp\left(\mathrm{m}\left(\frac{1}{A_w}\right)\right)}{\left(\frac{w}{c}\right)^{\mathrm{n}}} \right\} \tag{4.1}$$

In Eq.4.1, q_1 hence is independent of time. By substituting Eq.4.1 into Eq.2.7, the generalized hyperbolic relationship can be re-written in a linear form:

$$\frac{q_u}{q_1} = \frac{\left(\frac{\alpha t}{q_\infty}\right)^r}{1+\left(\frac{\alpha t}{q_\infty}\right)^r} \tag{4.2}$$

The left hand side of Eq.4.2 is purely a function of q_u whereas the right-hand side is purely a function of time. The plot of $\frac{q_u}{q_1}$ against $\frac{\left(\frac{\alpha t}{q_\infty}\right)^r}{1+\left(\frac{\alpha t}{q_\infty}\right)^r}$ should therefore be a unit gradient passing through the origin; this makes it much easier to fit than a generalized hyperbolic curve. Parameter α and q_∞ are then adjusted to find a better fitting of Eq.4.2.

In order to reduce the variance resulting from other factors, the mean values of UCS at each curing time were used in the fitting of Eq.4.2. As **Figure 4.2** shows, the plotted data from MBFC site and Marina One site are clustered along the straight line of $y = x$, it indicates that two fittings may be acceptable. The fitted parameters for generalized hyperbolic equation are summarized in **Table 4.1**. Parameters m, n and r are chosen as 0.3, 2.92 and 0.9 respectively, following Xiao *et al.* (2014).

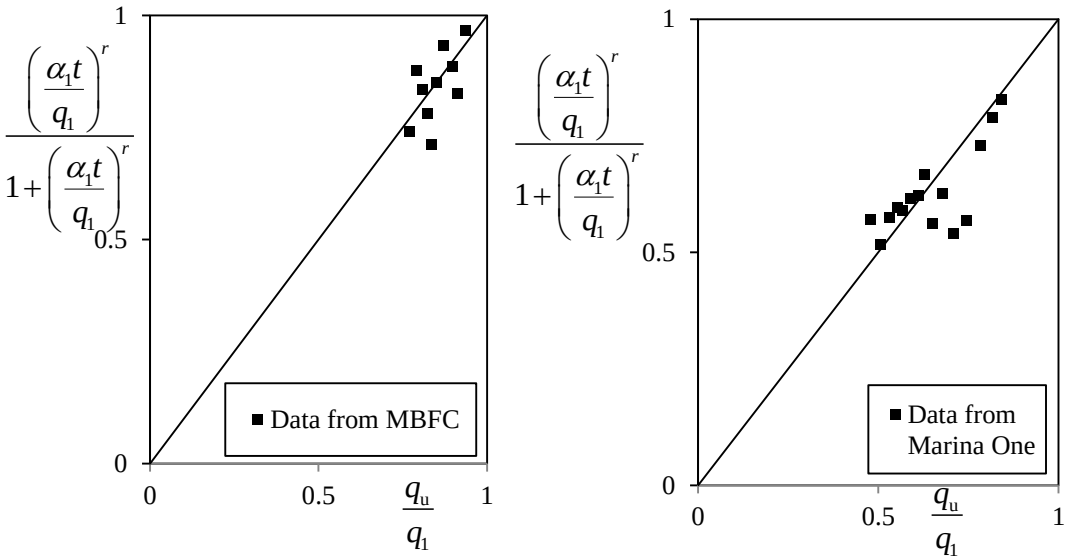

Figure 4. 2 Fitting of hyperbolic transformed linear Eq.4.2 by average UCS of cement-treated clay from MBFC and Marina One sites

Table 4.1. Parameters for strength prediction model ($\alpha_1 = \alpha \frac{q_1}{q_\infty}$ in unit of MPa/day)

Parameters	Projects		Unit
	MBFC	Marina One	
q_∞	20.8	15.7	Mpa
α	1.6	0.6	Mpa/day
r	0.9	0.9	-
q_1	2.5	4	Mpa
α_1	0.194	0.16	Mpa/day

Previously we assumed that water-cement-soil proportion is uniform over the whole site. As **Figure 3.5** and **Figure 3.9** shows, there is a variation in in-situ water content ranging from 20% to 80% over the depth of treated layers in the two sites. We can avoid the influence of various curing duration by normalizing UCS with 28-day equivalent value. According to Eq.2.7, the equivalent 28-day UCS can be calculated by setting time equal to 28 days:

$$q_{28} = q_\infty \left\{1 - \frac{1}{1+(\frac{\alpha \times 28}{q_\infty})^r}\right\} \left\{\frac{\exp(m(\frac{1}{A_w}))}{(\frac{W}{C})^n}\right\} \tag{4.3}$$

Hence the ratio of $q_u(t)$ over 28-day UCS will only depend on α and q_∞:

$$\frac{q_u(t)}{q_{28}} = \left\{1 - \frac{1}{1+(\frac{\alpha \times t}{q_\infty})^r}\right\} \Big/ \left\{1 - \frac{1}{1+(\frac{\alpha \times 28}{q_\infty})^r}\right\} \tag{4.4}$$

Figure 4.3 plots normalized ratio, $\frac{q_u(t)}{q_{28}}$ versus curing time. Since soil mixed with PBFC has slower strength-gain rate and higher ultimate strength than soil improved by Ordinary Portland Cement, it is rational to choose a lower α and higher q_1 for soil model in Marina One where PBFC was applied.

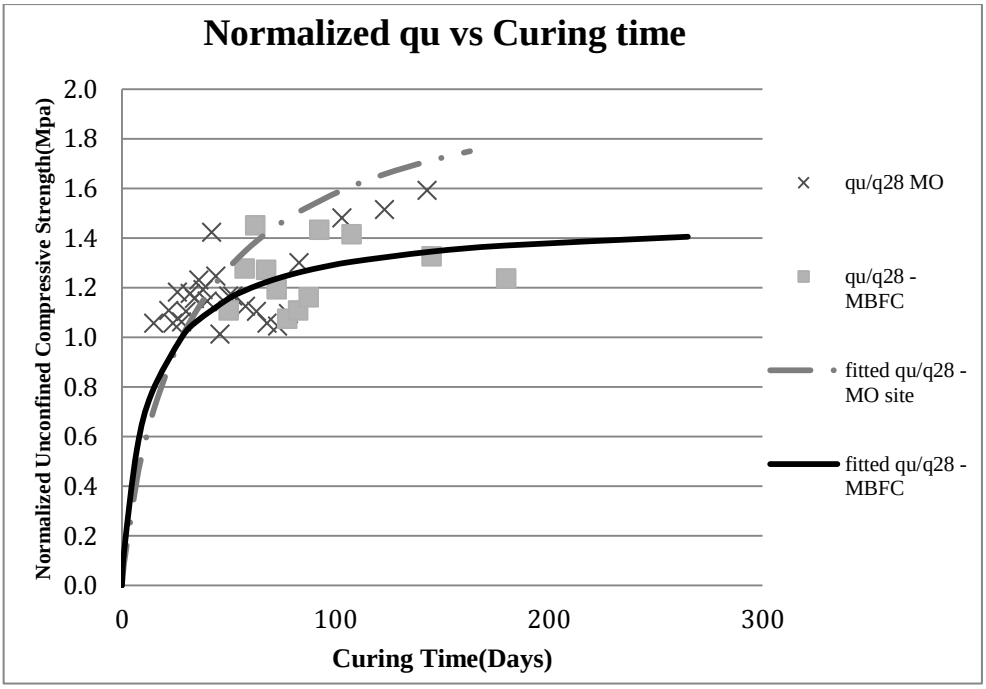

Figure 4. 3 Normalized UCS versus Curing Time, fitting of generalized hyperbolic curve by average data from MBFC and Marina One (MO: Marina One site)

q_∞ is a strength parameter related to the ultimate strength of cement-treated soil. As the curing time *t* approaches infinite, q_u approaches q_1:

$$\lim_{t\to\infty} q_u(t) = \lim_{t\to\infty} q_\infty \left\{1 - \frac{1}{1+\left(\frac{\alpha t}{q_\infty}\right)^r}\right\}\left\{\frac{\exp\left(m\left(\frac{1}{A_w}\right)\right)}{\left(\frac{W}{C}\right)^n}\right\} \tag{4.5}$$

$$\lim_{t\to\infty} q_u(t) = q_\infty \left\{\frac{\exp\left(m\left(\frac{1}{A_w}\right)\right)}{\left(\frac{W}{C}\right)^n}\right\} \tag{4.6}$$

$$\lim_{t\to\infty} q_u(t) = q_1 \tag{4.7}$$

Hence, q_1 is equal to the long-term UCS of the cement-treated soil.

Figure 4.4 plotted the average UCS of cement-treated soil with curing time, fitted by generalized hyperbolic curve with parameters listed in **Table 4.1**. It can be observed that fitted generalized hyperbolic curve can well predict the strength in long term: soil improved by PBFC (in Marina One site) steadily gains strength even at 100 days after mixing; while

soil treated by Portland Ordinary cement (in MBFC site) shows much smaller increment of strength after two-month curing.

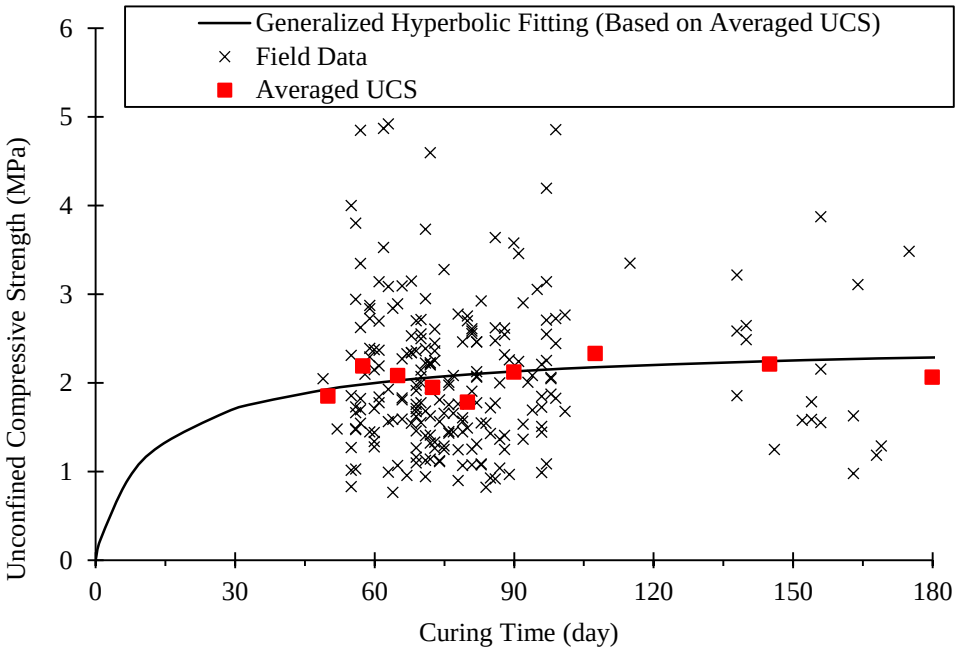

(a) MBFC site

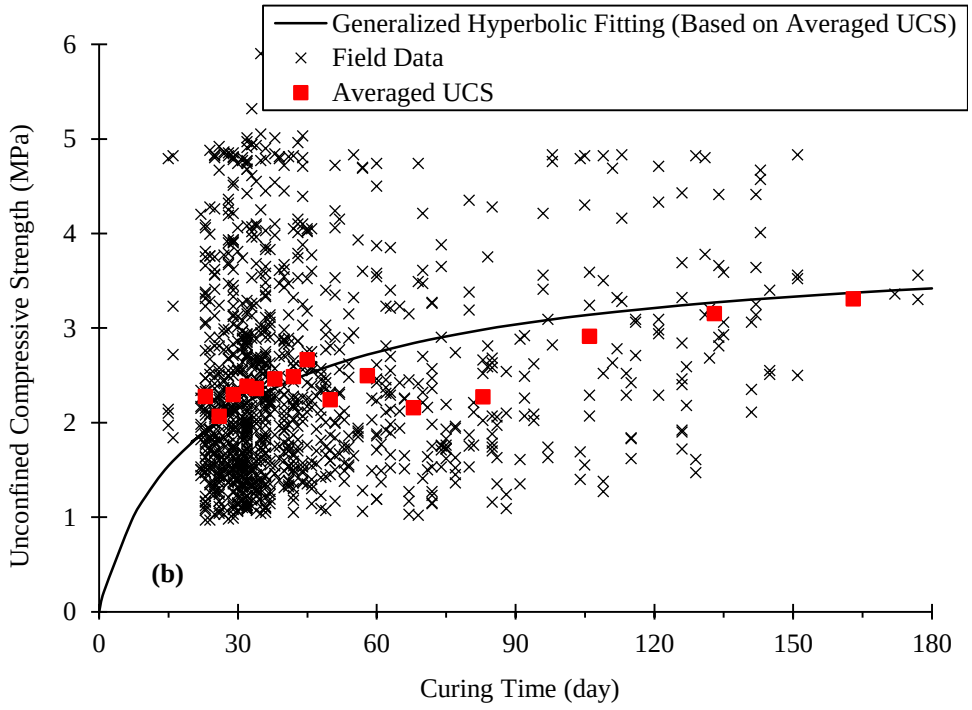

(b) Marina One site

Figure 4. 4 Fitting of generalized hyperbolic curve by field data of unconfined compressive strength from (a) Marina Bay Financial Centre, and (b) Marina One projects.

Comparison of Fitting Results

There are two main differences between Logarithmic relationship and generalized hyperbolic relationship.

Firstly, the generalized hyperbolic curve has greater flexibility - it can be adjusted to fit different strength-gain rate of cement-treated soil; whereas logarithmic curve pre-assumes that the strength-increment is proportional to final strength. As mentioned earlier, for a curing period up to 60 days, Verastegui Flores *et al.* (2011) concluded that the strength ratio of soil improved by quick-hardening and slow-hardening cement follow the same logarithmic curve. The above analysis indicates that this may not be applicable to strength gain in the longer term. In contrast, in generalized hyperbolic curve, parameter α controls the rate of strength-gain and another independent parameter q_∞ is related to the ultimate strength in long term while the index r allows non-linear early strength gain to be described.

Furthermore, the logarithmic relationship implies that, as curing time approaches infinity, so does the strength, which is counter-intuitive. On the other hand, the generalized hyperbolic curve defines a finite long-term strength q_1.

Hence, the generalized hyperbolic curve is chosen herein to describe the correlation between UCS and curing time.

Eq.4.4 motivates a method for normalizing UCS to a standard UCS at a prescribed curing time of, say, 28 days:

$$q_{28} = q_u(t) \times \left\{1 - \frac{1}{1+(\frac{\alpha \times t_{28}}{q_\infty})^r}\right\} \Big/ \left\{1 - \frac{1}{1+(\frac{\alpha \times t}{q_\infty})^r}\right\} \quad (4.8)$$

Figure 4.5 shows the histograms of UCS and 28-day equivalent UCS in cement-treated soil from the two sites. It can be seen that after normalization, the mean UCS drops by 16% and 20% in Marina One and MBFC sites, respectively; while the kurtosis and skew-ness increase. This implies that the normalized 28-day equivalent strengths in cement-treated soil

is within a narrower range. Since the coefficients of variation do not change significantly, the standard deviation (i.e. coefficient of variation times mean) is decreased.

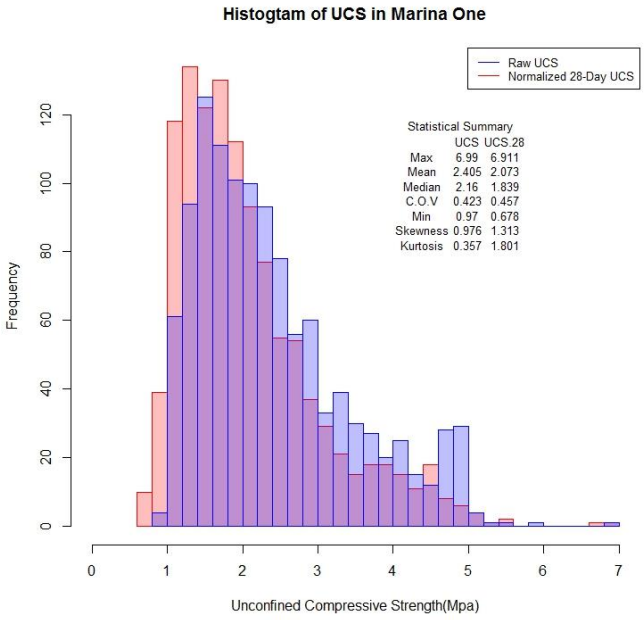

(a) Marina One

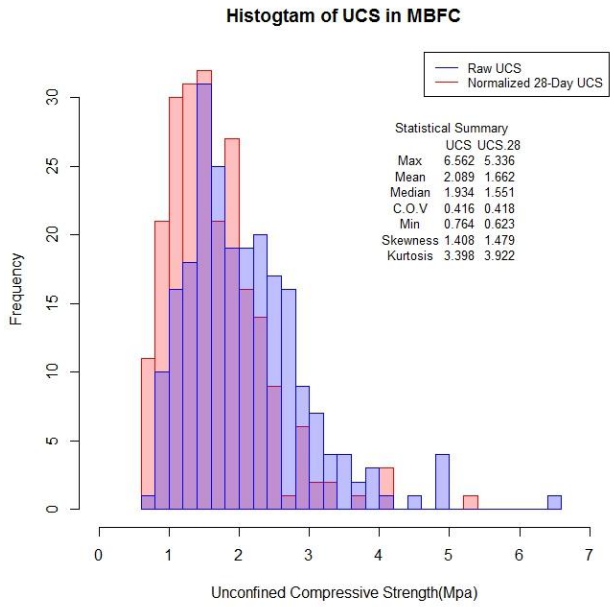

(b) MBFC

Figure 4. 5 Histogram of UCS and 28-day equivalent UCS normalized by generalized hyperbolic curve with parameters in table. 4.1 in (a) Marina One; (b) MBFC(red: normalized 28-day equivalent UCS; blue: original UCS; Purple: overlapping part for 28-day UCS and original UCS)

4.2. Spatial Analysis of In-situ Water Content

Random field theories

Soil properties vary due to a combination of geological, environmental and physical-chemical factors in soil formation (Phoon and Kulhawy, 1999). Spatially random soil property has been studied in recent years (Fenton and Griffiths, 2008; Li *et al.*, 2005).

A one-dimensional random process X(*t*) can be expressed by following relation (Fenton and Griffiths, 2008):

$$X'(z) = \frac{X(z)-\mu(z)}{\sigma_\varepsilon(z)} \tag{4.9}$$

Where: z is a variable, representing depth in this project;

$X(z)$ is a random process, representing measured soil properties herein;

$\mu(z)$ is a deterministic function giving mean soil property at z;

$X'(z)$ is a stationary random process with zero mean and unit variance everywhere;

$\sigma_\varepsilon(z)$ is the standard deviation of residual part.

The presence of trend, $\mu(z)$ in soil properties is observed in most cases of geotechnical parameters. It is associated to factors in geological formation, like overburden stress and stress history (Srivastava and Sivakumar Babu, 2009). The trend is generally defined as linear function or quadratic function of single variable, such as depth. Many methods have been proposed to find true trend of soil properties. Trend removal by least squares regression is one popular choice (Srivasta *et al.*, 2009); whereas "Cusum analysis" is proposed by Cafaro and Cherubini (2002) to select the best trend to obtain a sound of residuals.

Houlsby and Houlsby (2013) believe that the goal of fitting is "to distinguish the underlying signal - that is, the true layer structure –from the noise in the data". As shown in **Figure 4.6**, he illustrated typical errors in trending fitting in a schematic way.

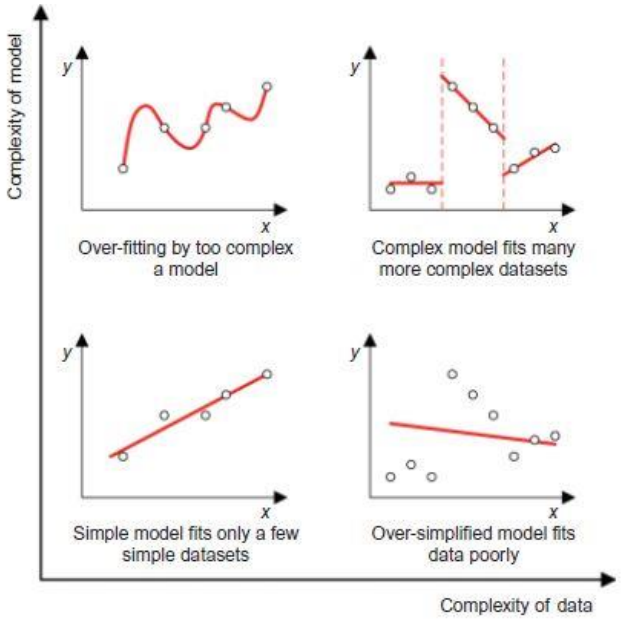

Figure 4. 6 Schematic diagram of relationship between complexity of data and complexity of model (after Houlsby and Houlsby, 2013)

A widely-hold view on soil spatial variability is the data stationarity of de-trended residual. In this context, weak stationarity is defined by: (1) constant mean (zero mean in $X'(z)$); (2) constant variance (constant σ_ε, not depend on z); and (3) correlation only depends on separation distance rather than spatial location (Vanmarcke, 1983). Likewise, Fenton (1999) and Fenton and Griffiths (2008) suggested that the trend, $\mu(z)$ shall be optimized to allow accurate representation of $X(z)$ in such a way that $X'(z)$ could obtain zero mean and small variance with constant covariance structure. Similarly, Phoon and Kulhawy (1999) highlighted that the fluctuations of random residual shall be approximately uniform to satisfy the condition of zero mean (**Figure 4.7**).

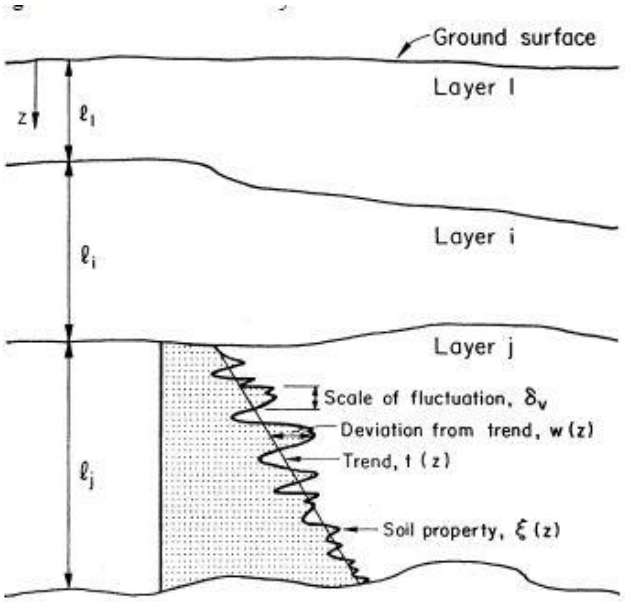

Figure 4. 7 Model of variability of inherent soil (after Phoon and Kulhawy, 1999) z: Depth

Horizontal trends were observed in cement-treated soil column. Kawasaki *et al.* (1984) observed a decreasing trend of direct shear strength along radial distance in horizontal direction within one cement-treated column (see **Figure 4.8**). Similarly, Larsson (2001) observed a decreasing trend of Calcium Oxide concentration, along radial distance in a lime-cement column (see **Figure 4.9**). Calcium Oxide concentration is positive correlated to the strength of lim-cement column. However, vertical trend of variation of strength or properties in cement-treated soil has not been widely studied so far.

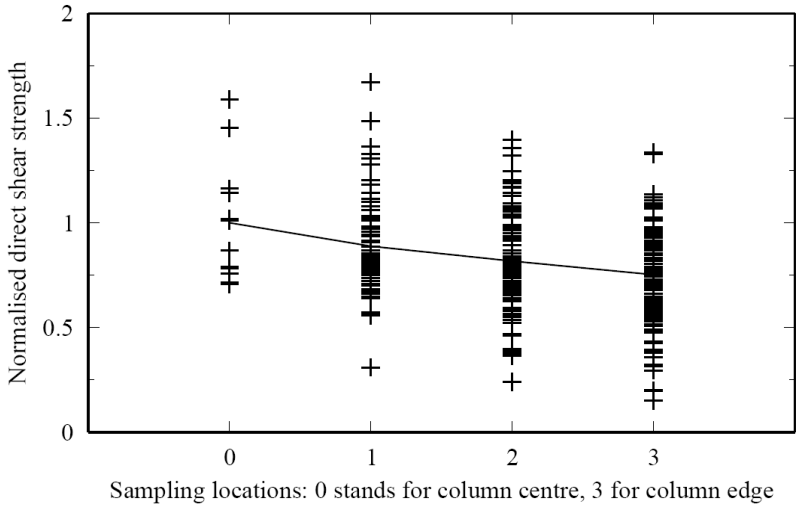

Figure 4. 8 Decreasing trend of direct shear strength along radial distance in horizontal direction (after Kawasaki *et al.*, 1984)

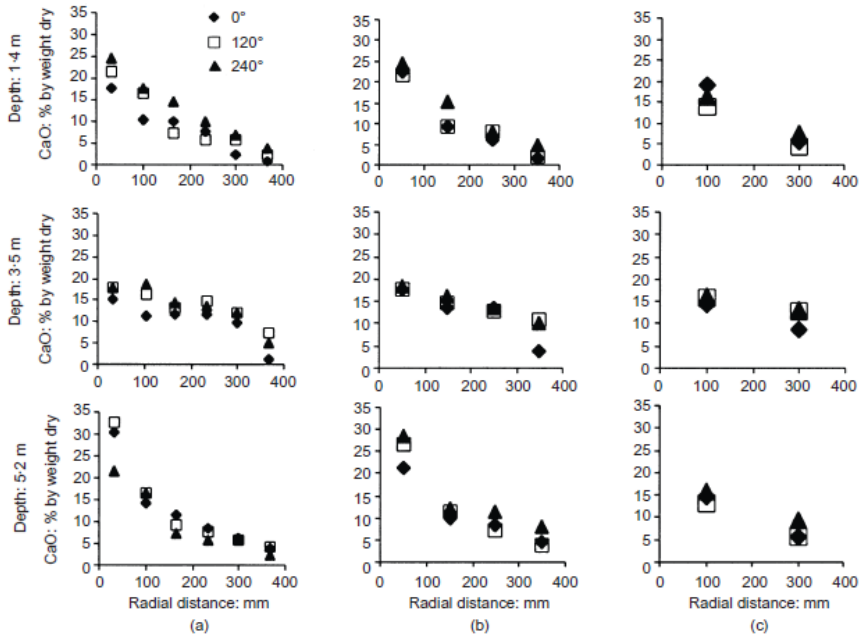

Figure 4. 9 Chemical analysis of Calcium Oxide concentrates in the samples from column B1: (a) small size; (b) medium size; and (c) large size (after Larsson, 2001).

The variance of soil property, σ_x^2, consists of two independent parts: variance of trend σ_μ^2 in x direction, and variance stochastic residual σ_ε^2. Their relationship is shown as follows:

$$\sigma_x^2 = \sigma_\mu^2 + \sigma_\varepsilon^2 \tag{4.10}$$

Based on this variance model, Phoon and Kulhawy (1999) proposed the coefficient of variation as a useful dimensionless representation of inherent variability by ratio of standard deviation σ_ε over mean trend, given by

$$COV_\varepsilon = \frac{\sigma_\varepsilon}{\mu} \tag{4.11}$$

Since variation of residual is constant and *μ(z)* is the mean property trend, COV_ε only depends on depth.

Field data application

Figure 3.5 and **Figure 3.9** suggests that trend is relatively more prominent in vertical direction than in horizontal direction. Therefore, trend analysis can be conducted previously for the vertical direction. However, the disparity of in-situ water content in horizontal direction may disturb the fitting quality of vertical trend. Hence, instead of raw data, average in-situ water content in each depth was used to fit vertical trend in each soil layer.

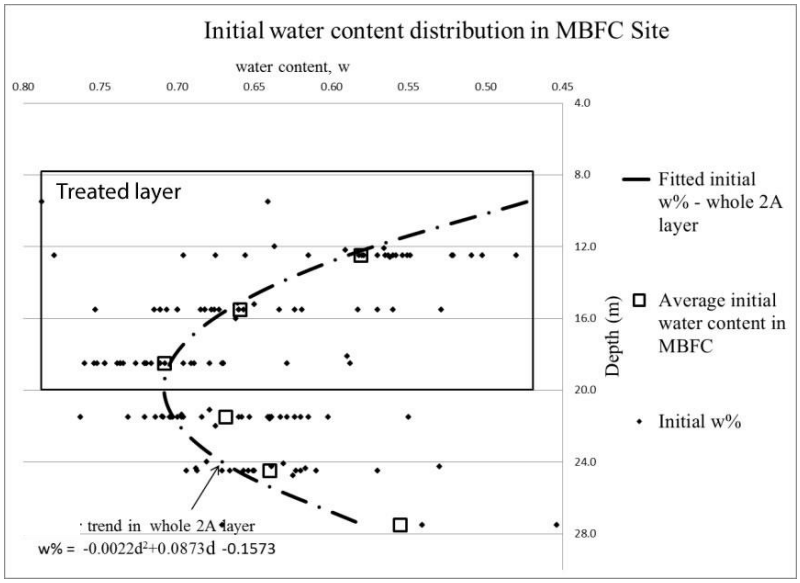

(a) MBFC site

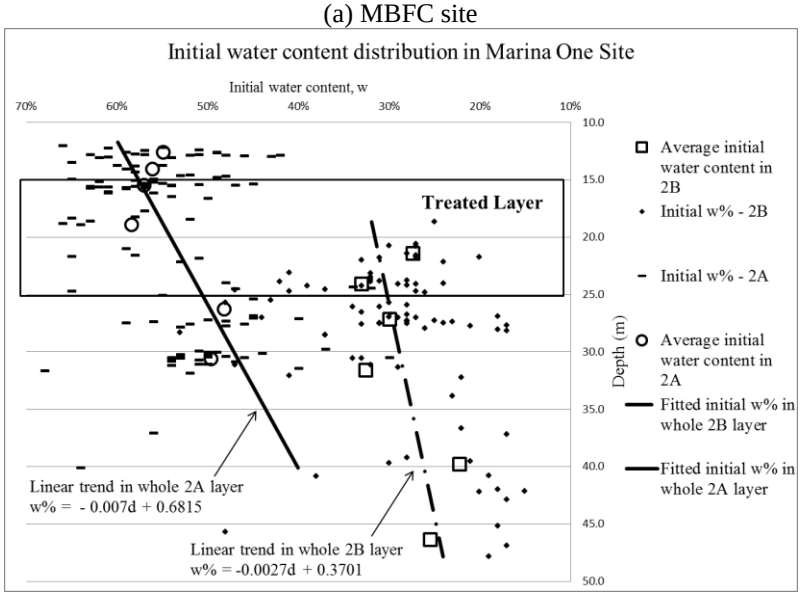

(b) Marina One site

Figure 4. 10 Distribution of in-situ water content along depth in (a) MBFC site; (b) Marina One site. Fittings of trends were based on average in-situ water content at each depth. 2A: upper marine clay layer; 2B: lower marine clay layer.

As **Figure 4.10** shows, in both clay layers of Marina One site, linear correlations exist between the averaged in-situ water content and depth. Part of the reason could be the presence of residual excess pore pressure from the reclamation works. Due to the continuous reclamations since 1970s, the marine clay in upper layer of MBFC site has been experienced further consolidation caused by loading from the sand fill. As **Figure 4.10(a)** shows, rather than a straight line, a curve appears to better describe the trend of in-situ water content in MBFC site; this is consistent with the notion of residual excess pore pressure at the mid-layer region. **Table 4.1** summarized statistical characteristics of water content in both sites before and after fitting. Residual water content is defined as the difference between measured water content and fitted trend. Following Phoon and Kulhawy (1999)'s definition, the equivalent COV (coefficient of variation) is defined as the ratio of standard deviation of residual water content to fitted water content at the middle of the cement-treated layer.

Table 4. 1 Summary of fitting results of in-situ water content, classified by soil type in improved-soil layer. Data source: Site Investigation report of two sites.

		Marina One		MBFC
		2A	2B	2A
Sample Size		122	91	134
Depth of whole layer(m)		12 – 40	18-48	9-30
Depth of treated layer(m)		15-25		8-20
In-situ water content in treated layer, w_0	Mean	0.56	0.31	0.66
	Standard deviation	0.096	0.142	0.077
	Coeff. of Variation	0.18	0.43	0.12
Trend of In-situ water content in treated layer, w_μ	Fitted trend of whole soil layer	$w_\mu\% = -0.007 \cdot d + 0.68$	$w_\mu\% = -0.0027 \cdot d + 0.37$	$w_\mu\% = -0.002 \cdot d^2 + 0.087 \cdot d - 0.157$
	$w_{\mu mid}$: value at middle of treated layer	**0.54**	**0.31**	**0.65**
	Minimum	0.40	0.24	0.47
	Maximum	0.60	0.32	0.70
Residual water content in treated layer , ε_w	Mean	0.0017	0.001	-0.0038
	σ_{ε_w} (Standard deviation)	0.07	0.063	0.064
	Minimum	-0.19	-0.111	-0.15
	Maximum	0.142	0.166	0.31
$Equivalent\ COV = \frac{\sigma_{\varepsilon_w}}{w_{\mu mid}}$		**0.13**	**0.20**	**0.10**

Auto-correlation

In the study of the spatial variation in the properties of cement-treated soil, the autocorrelation distance or scale of fluctuation is often used (e.g. Honjo 1982; Fenton and Griffiths, 2008). The covariance between the two values of a measured parameter (e.g. strength) X(z') and X(z*) at two locations separated by a distance of $\tau = z^*\text{-}z'$ can be estimated (Fenton and Griffiths, 2008) as follows:

$$C(z', z^*) = \mathrm{Cov}[X(z'), X(z^*)] \tag{4.12}$$

$$= E[X(z') - \mu_X(z')][X((z^*) - \mu_X(z^*)] \tag{4.13}$$

When the covariance is large, it means that the two values are strongly correlated statistically. For a set of discrete data, autocorrelation is also calculated as (Fenton, 1999):

$$\hat{C}(i_j) = \frac{1}{n}\sum_{i=1}^{n-j+1}(x_i - \hat{\mu}_X)(x_{i+J-1} - \hat{\mu}_X),\ j=1, 2, \ldots, n \tag{4.14}$$

Where: $\hat{\mu}_X = \frac{1}{n}\sum_{i=1}^{n} x_i$ is the estimator of mean μ_X.

The auto-correlation is obtained by normalizing covariance by cross-product of the standard deviation at z' and z^* (Fenton and Griffiths, 2008):

$$\rho\left(z', z^*\right) = \frac{C\left(z', z^*\right)}{\sigma_X(z')\,\sigma_X(z^*)} \tag{4.15}$$

Where the standard deviation $\sigma_X(z)$ is calculated as:

$$\sigma_X(z) = \sqrt{\frac{1}{n}\sum_{i=1}^{n}(x_i(z) - \hat{\mu}_X(z))^2} \tag{4.16}$$

In the study of spatial variability of soil, it is commonly assumed that the soil is spatially and statistically homogeneous (i.e. the statistical properties do not change from one region

to another), but can be anisotropic (Fenton, 1999). That implies that spatial auto-correlation can be simplified and de-constructed into two independently one-dimensional random processes, in horizontal (i.e. along x-axis or y-axis) and vertical direction (along z-axis), respectively. Likewise, Popescu *et al.* (2005) argued that mechanism of soil deposit formation leading to different spatial variability structure of natural soil layer in horizontal and vertical directions. Hence, the auto-correlation in horizontal and vertical directions should be considered separately.

The scale of fluctuation (SOF) is an important indicator of strength of auto-correlation. It is defined as a separation distance beyond which soil properties are largely uncorrelated (Fenton, 1999). **Table 4.2** lists six different correlation functions summarized by Rackwitz (2002), which are plotted in **Figure 4.11**. It can be seen that the performances of six models are quite similar in small distance, but differ around scales of fluctuations.

Table 4. 2 One-dimensional models for correlation function and spectral density (after Rackwitz, 2002) $\boldsymbol{\rho}$: distance lag; $\boldsymbol{a}$: Scale of Fluctuation

Type of auto-correlation function	Autocorrelation function $R(\rho)$	Spectral density function $G(\kappa)$
I	$\sigma^2 \exp[-a\lvert\rho\rvert]$	$\sigma^2 \frac{2a}{\pi(a^2+\kappa^2)}$
II	$\sigma^2 \exp[-a\lvert\rho\rvert]\cos(b\rho)$	$\frac{2\sigma^2 a(a^2+\kappa^2+b^2)}{\pi(\kappa^4+2\kappa^2(a^2-b^2)+(a^2+b^2)^2}$
III	$\sigma^2 \exp[-a\rho^2] J_0(b\rho)$	$2\int_0^\infty \sigma^2 \exp[-a\rho^2] J_0(b\rho)\cos(\kappa\rho)\mathrm{d}\rho$
IV	$\sigma^2 \exp[-a\rho^2]$	$\frac{\sigma^2}{\sqrt{\pi a}} \exp\left[-\frac{\kappa^2}{4a}\right]$
V	$\sigma^2 \frac{(a\rho)^b K_b(a\rho)}{2^{b-1}\Gamma(b)}$	$\frac{2\sigma^2\Gamma(b+1/2)a^{2b}}{\pi^{1/2}\Gamma(b)(a^2+\kappa^2)^{b+1/2}}$
VI	$\begin{cases} \sigma^2(1-\lvert\rho\rvert/a) & for\lvert\rho\rvert \geqslant a \\ 0 & for\lvert\rho\rvert > a \end{cases}$	$\frac{2}{\pi}\frac{1-\cos(a\kappa)}{a\kappa^2}$

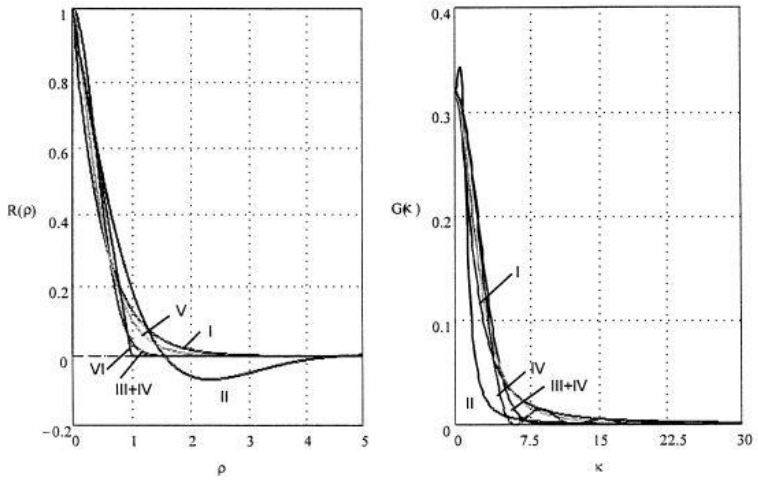

Figure 4. 11 One-dimensional autocorrelation functions and their spectral densities (after Rackwitz, 2002). I-IV correspond auto-correlation function types in Table 4.2**.**

The scales of fluctuation (SOF) of UCS in cement-treated soil have been reported variously, as summarized in **Table 4.3**. Honjo (1982) reported scale of fluctuation of UCS in cement-treated soil from three sites ranging from 0.4 m to 4 m (See **Figure 4.12**) in vertical direction. He also concluded that cement-treated clay usually has a longer SOF than sandy soil.

Table 4. 3 Summary on scale of fluctuation of UCS in recent papers. Some of the data were from: Chen, 2014

Reference	**Horizontal (m)**	**Vertical (m)**	**Mixing type**	**Definition**
Matsuo *et al.*, 1977	-	0.6-1.3	-	Auto-correlation distance
Honjo, 1982	-	0.4-4	wet	Auto-correlation distance
Navin, 2005	~12	-	wet	Scale of fluctuation
Larsson, 2005	0.5	Widely scatted	dry	Scale of fluctuation
Larsson et Nilsson, 2009	0.9-1.8 (> column spacing)	-	dry	Scale of fluctuation

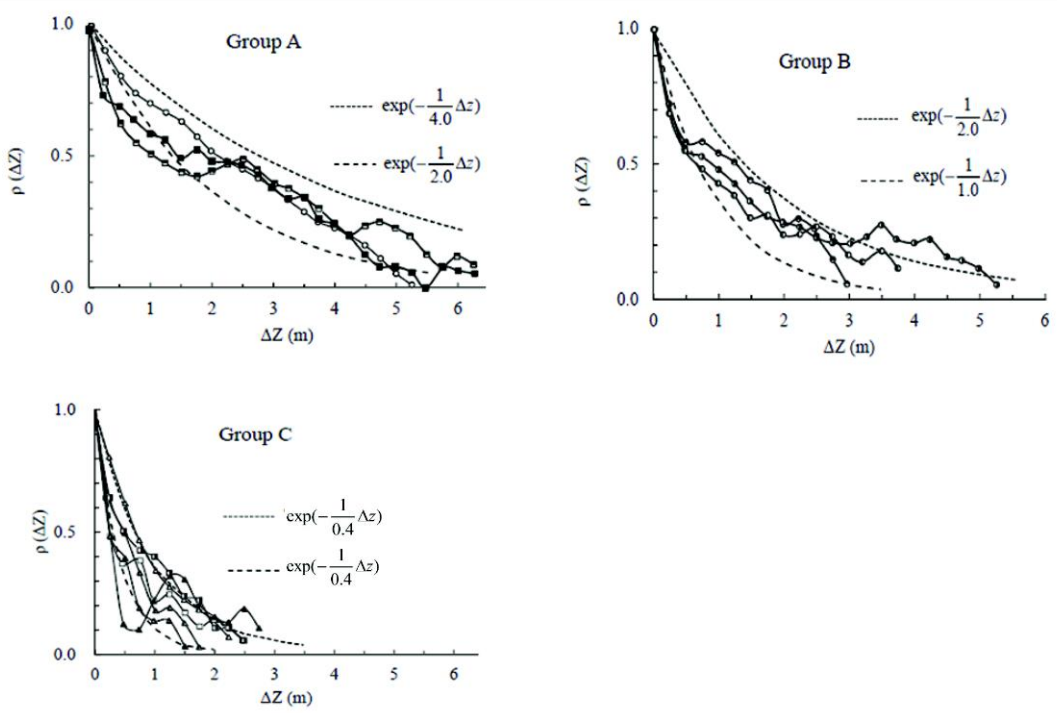

Figure 4. 12 Auto-correlation functions of shear strength in different locations. Group A: Hiroshima Port and Tokyo; Group B: Yokohama Port; Group C: Chiba Port. The scales of fluctuation are: Group A: 2.0 m -2.4 m; Group B: 1.0 m – 2.0 m; Group C: 0.4 m – 1 m (Source: Honjo, 1982)

In terms of natural soil properties, Popescu *et al.* (2005) found that the correlation distance (same concept as scale of fluctuation, but follow different definition) in horizontal direction is around one order of magnitude larger than the one in the vertical direction. The same conclusion was drawn by Phoon and Kulhawy (1999). **Table 4.4** cites some of typical scale of fluctuation in UCS and water content in inherent soil summarized by Phoon and Kulhawy.

Table 4. 4 Summary of scale of fluctuation of natural soil property (data source: Phoon and Kulhawy, 1999)

			Scale of Fluctuation (m)	
Property	**Soil type**	**Direction**	**Range**	**Mean**
Undrained shear strength (Van Shear Test)	clay	Vertical	2.0-6.2	3.8
		Horizontal	46-60	50.7
Undrained shear strength	clay	Vertical	0.8-6.1	2.5
Water content	clay	Vertical	1.6-12.7	5.7
		Horizontal	-	170

As can be seen in **Table 4.3** and **Table 4.4**, the scale of fluctuation (SOF) of natural soil properties is generally much larger than the SOF in cement-treated soil. Auto-correlation

function shall be applied to de-trended data, which represent the true inherent correlation structure of soil.

SOF of original data is generally higher than the one of de-trended data. For example, Cafaro and Cherubini (2002) plots auto-correlation of original data and de-trended data from same bore-hole (**Figure 4.13**). Significant trend presents in original data, which result in an over-estimation of SOF.

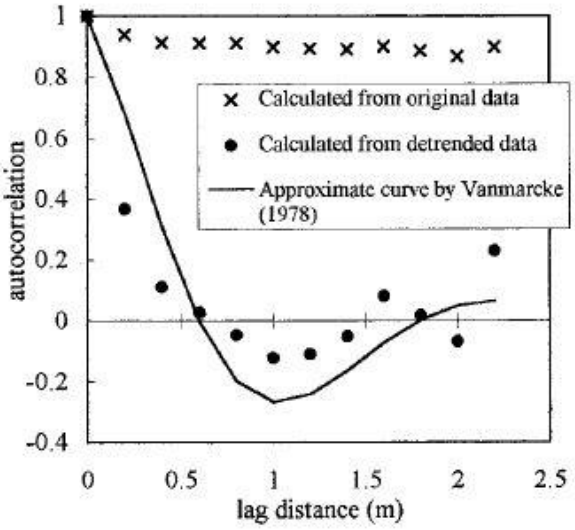

Figure 4. 13 Auto-correlation function for G3 lower cone profile (after Cafaro and Charubini, 2002)

Field data application

The auto-correlation functions of residual water content in both sites are plotted in **Figure 4.14**. Markov autocorrelation function is selected to fit autocorrelation data from sites, which is in the following form:

$$\rho(\tau) = e^{\frac{-2\tau}{\theta}} \tag{4.18}$$

where θ is the scale of fluctuation, and τ is the distance lag between samples. As can be seen in **Figure 4.14**, very few data points on in-situ water content are available to evaluate its vertical autocorrelation in short distance, hence data from two sites were combined into

one group to achieving sufficient large sample size. Combined data from two sites show that the vertical SOF is about 6 m, which is smaller than most core-sample intervals, hence measured de-trended water content data can be considered as identical and independent data (*i.i.d*) herein.

By comparison, the horizontal autocorrelation is significantly stronger. As can be seen in **Figure 4.14**, in both sites, horizontal SOFs of residual water are approximated in scale of hundreds of metres, which coincides with the one measured by Phoon and Kulhawy (1999), where the SOF of natural water content in the vertical direction was observed to be from 1.6 m to 12.7 m .

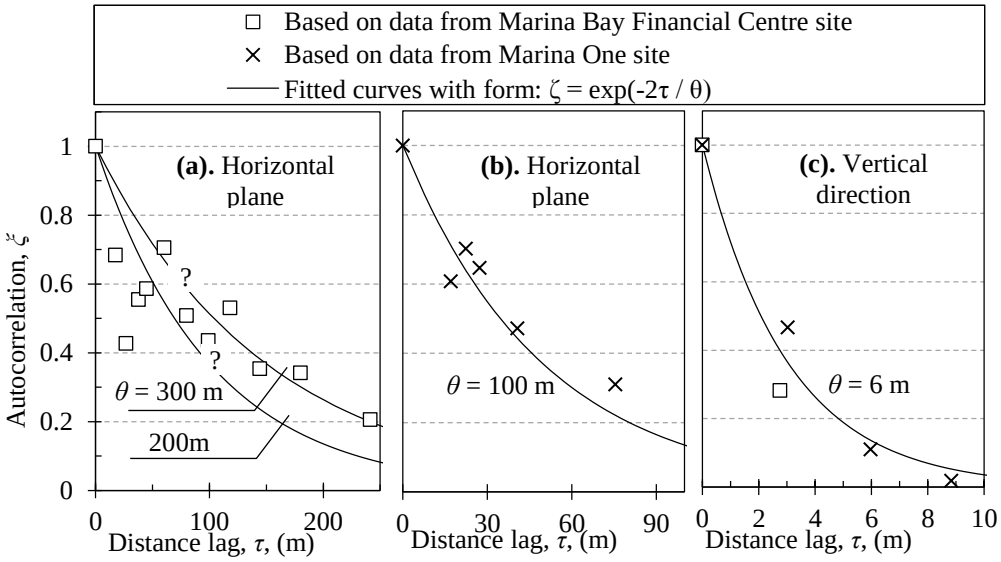

Figure 4. 14 Auto-correlation structures of in-situ water content (θ: scale of fluctuation)

Impact of In-situ Water Content on Soil Strength

The spatial distribution of 28-day equivalent UCS in cement-treated soil is also investigated. As can be seen in **Figure 4.15**, the strength of soil is classified by colours. Compared to spatial distribution of in-situ water content, the distribution of UCS in improved soil is much more chaotic and scattered.

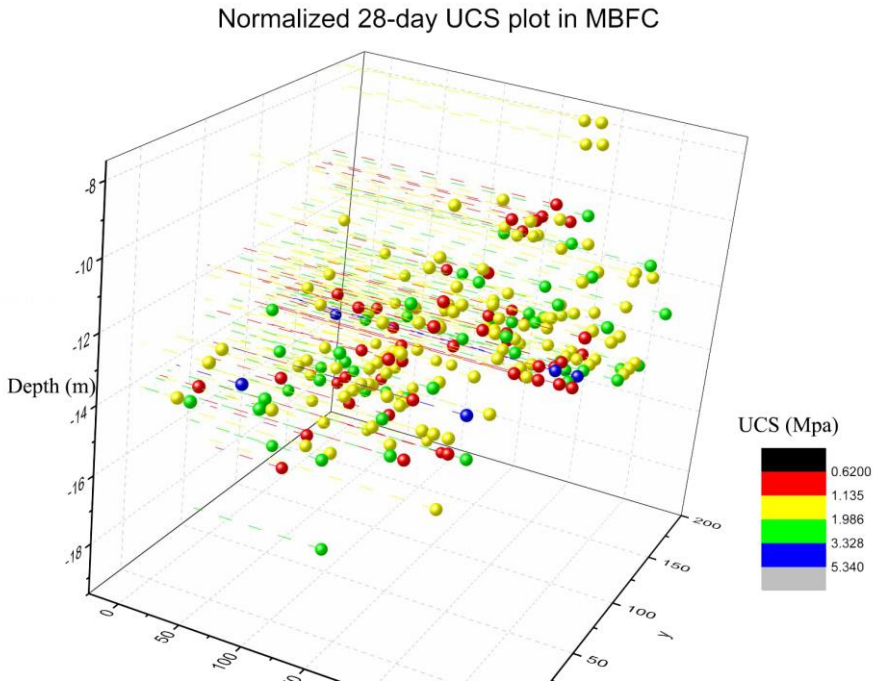

(a) MBFC

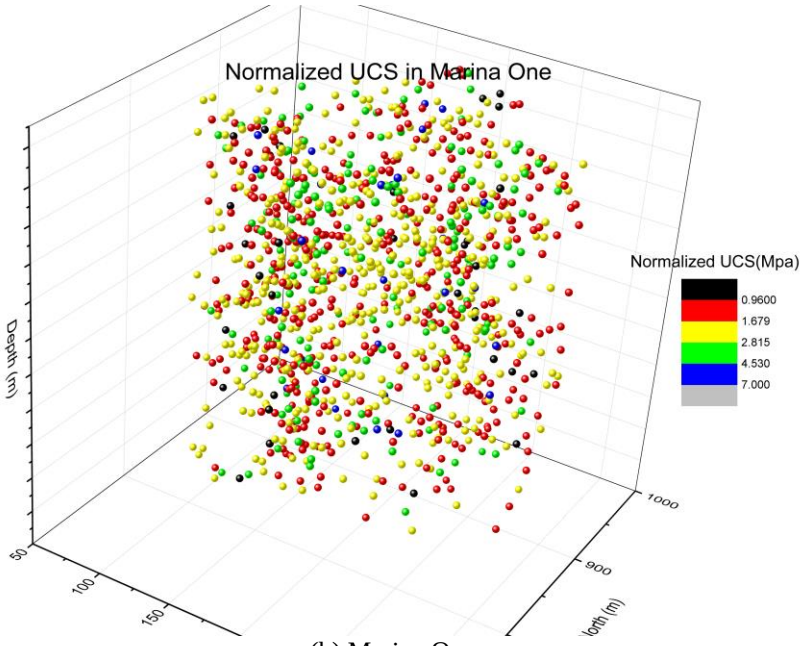

(b) Marina One

Figure 4. 15 3-dimensional scatter plot of 28-day equivalent UCS in (a) MBFC; (b) Marina One.

In order to make a comparison between in-situ water content and UCS in terms of their spatial distribution, vertical trend of 28-day equivalent UCS was extracted based on average UCS in each depth. **Figure 4.16** shows the vertical trend of 28-day equivalent UCS in two sites. In general, the local average values of UCS in two sites fall into a narrow linear band which increases along depth.

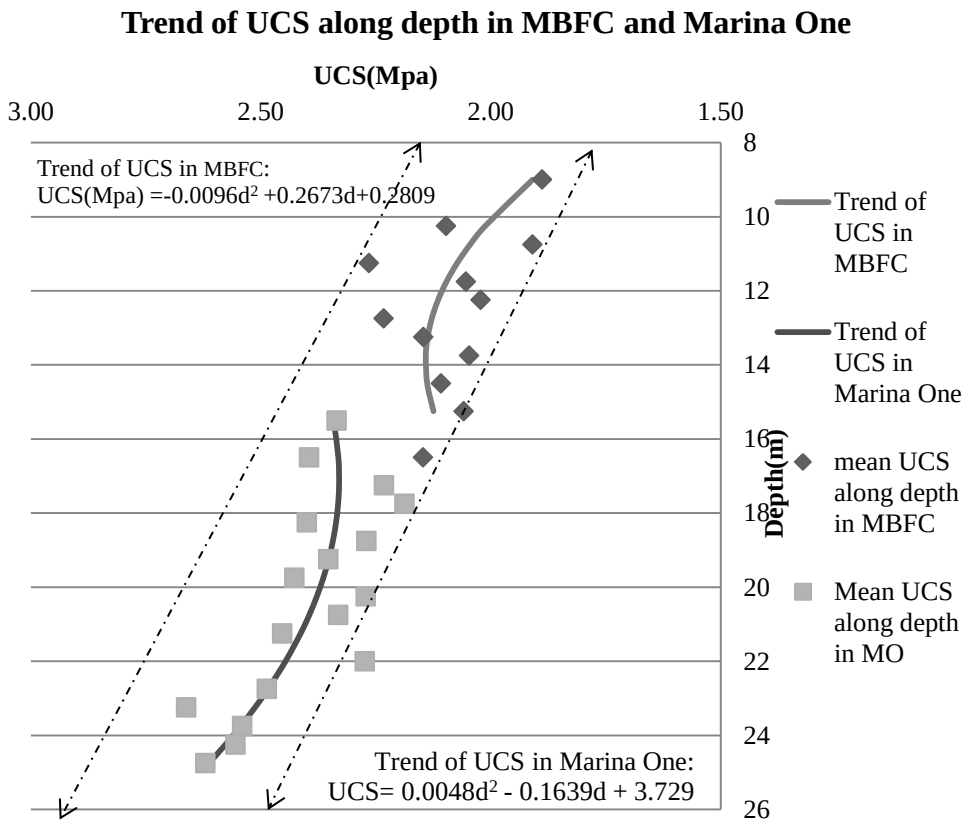

Figure 4. 16 Trend of UCS, fitted by average UCS in each depth. (MO: Marina One)

In the Marina One site, the cement-treated layer overlaps across two marine clay layers with significantly different in-situ water contents. However, the boundary between two marine clay layers cannot be clearly distinguished in UCS core strength data. In order to link UCS and in-situ water content, a polynomial is used herein to describe the trend of in-situ water content in the cement-treated layer. As can be seen in **Figure 4.17**, similar to UCS, the in-situ water content decreases significantly with depth. Furthermore, the in-situ water content in MBFC is generally higher than that of Marina One, and cement-treated soil in MBFC is generally weaker than soil in Marina One. This is consistent with the notion that higher the in-situ water content leads to higher overall water content of the treated soil and thus lower strength.

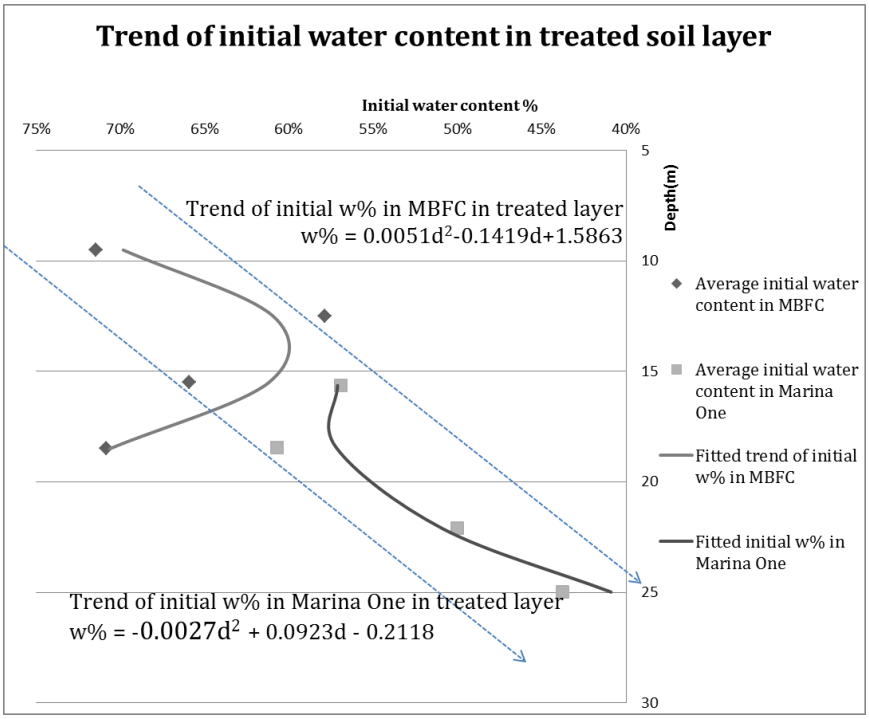

Figure 4. 17 Trend of in-situ water content considering data in treated- zone only.

The fitted water-depth trends in **Figure 4.17** are listed as follows:

In MBFC:

$$w_\mu = 0.0051 \cdot z^2 - 0{,}419 \cdot z + 1.5863 \tag{4.19}$$

where z is the depth in metre. For Marina One:

$$w_\mu = -0.0027 \cdot z^2 + 0.0923 \cdot z - 0.2118 \tag{4.20}$$

The corresponding fitted UCS-depth relationships in **Figure 4.17** are:

In MBFC:

$$q_\mu = -0.0096 \cdot z^2 + 0.2673 \cdot z + 0.2809 \tag{4.21}$$

Where q_u is the UCS measured in MPa. In Marina One:

$$q_\mu = 0.0048 \cdot z^2 - 0.1639 \cdot z + 3.729 \tag{4.22}$$

In this correlation exercise, the depth *z* can be considered as a common variable to relating the in-situ water content and UCS. Based on Eqs. 4.19 – 4.22, fitted water-content-UCS-depth relationships can be plotted as shown in **Figure 4.18**. The black line at left side of w%-UCS-Depth space is defined by Eq.4.19 and Eq.4.21, which describe the relationship of fitted w%-UCS-depth in MBFC. Similarly, the black dashed line at right hand side is constrained by Eq.4.20 and Eq.4.22 for water-strength in Marina One. The projection of water-content-UCS-depth relationship on the base plane is the in-situ water content-UCS relationship, as shown in **Figure 4.19**.

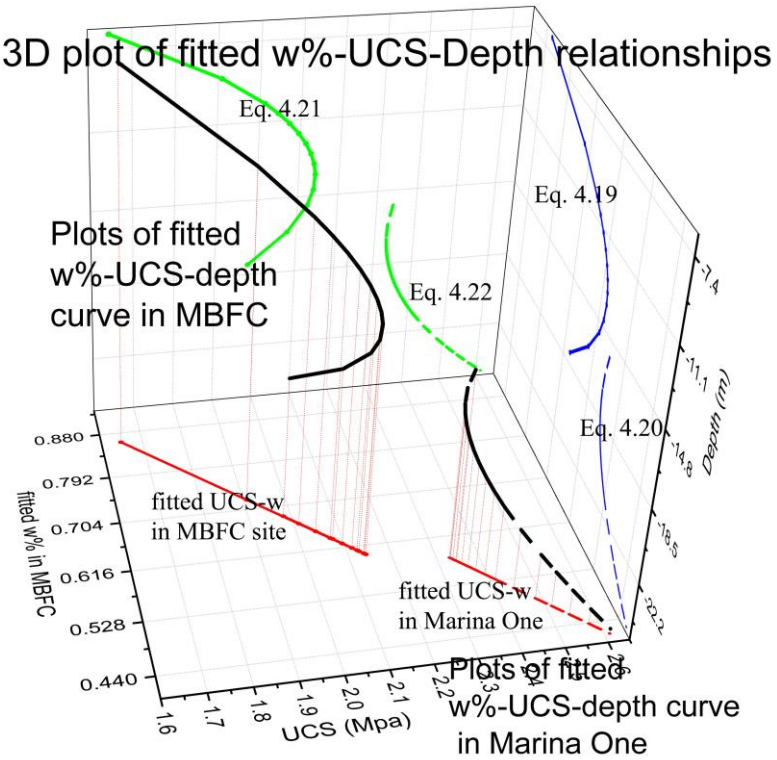

Figure 4. 18 3D plot of fitted w%-UCS-depth relationships in treated zone

As can be seen, the projected water-depth relationship is remarkably close to straight line (**Figure 4.19**). We can observe a remarkable negative linear correlation between UCS and in-situ water content. More importantly, the linear relationships from two sites, MBFC and UCS are quite consistent. This implies that although soil improvement activities in two sites might have used different equipment, cement type and operational parameters, a certain

degree of continuity nonetheless exists in the correlation between in-situ water content and UCS of cement treated clay.

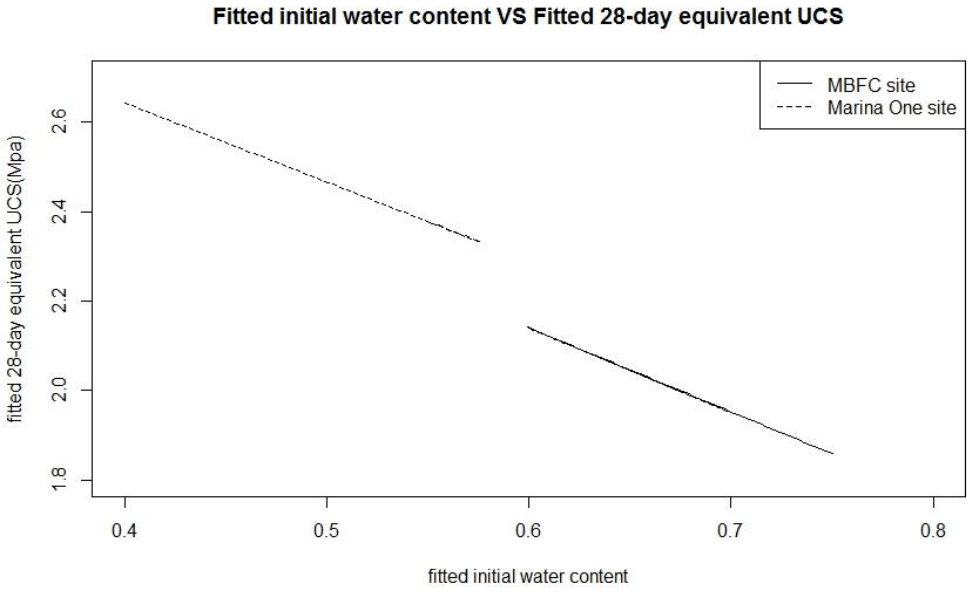

Figure 4.19 Projected UCS-w% relationship based on Fig 4.18.

5. A Two-Parameter Model for the Effect of in-situ water content and Cement Slurry concentration on UCS

In order to separate the effects of curing time and mixing ratio separately, Eq.2.7 can be re-written as:

$$q_u = q_0(t) \cdot r(w,c) \tag{5.1}$$

Where:

$$q_0 = q_\infty \left\{ 1 - \frac{1}{1 + \left(\frac{\alpha t}{q_\infty} \right)^r} \right\} \tag{5.2}$$

And

$$r = \frac{e^{mx}}{(wx + a)^n} \tag{5.3}$$

in which x is defined as : $x = \frac{1}{A}\left(\frac{1}{c} - 1\right)$ and $A = \frac{1+w}{1+a}$.

c is the cement slurry concentration, the mass ratio of cement to cement-column; *w* is the in-situ water content, defined as the mass ratio of water to soil in soil; and *a* is the water-cement ratio in cement slurry. The lower power part at right hand side of Eq.5.3, *wx+a* is actually equal to $\frac{W}{C}$, the mass ratio of total water to cement defined in Eq.2.7; while *x* herein is equal to $\frac{1}{A_w}$, the cement-soil ratio. Assuming that q_∞ and α are constants for given type of cement and soil, the curing time is the only variable for q_0. Similarly, water-cement ratio, *a* in a well-mixed cement slurry can be considered as a constant, hence the

variability of r results from the variability of w and c . Eq.5.3 can be rewritten as a general function of *c* and *w*:

$$r = g(c, w) \tag{5.4}$$

Figure 5.1(a) shows the strength ratio *r* calculated using Eqs. 5.3 and 5.5 with fixed water-cement ratio (*a*) in cement slurry as 0.9. The *c*-*r* and *w*-*r* relationships are plotted in solid lines in **Figure 5.1(b)** and **Figure 5.1(c)**, respectively. **As Figure 5.1(b)** shows, the strength ratio calculated using Eq.5.3 increases drastically at low cement slurry concentration, which is counter-intuitive, since one would expect low strength with low cement-content in soil column. Lee *et al.* (2005) and Xiao *et al.* (2014) tested soil samples with in-situ water content higher than 71% and 86%, cement slurry concentration higher than 10% and 20%, respectively. Both of these cement slurry concentrations are not sufficiently low to allow this anomalous trend to be manifested. Deep mixing generally uses cement slurry concentrations that are well above 0.2. Hence, this anomaly does not affect Eq.5.3 when one is considering mean cement slurry concentration typically encountered in deep mixing. However, when analysing the non-uniformity in cement-treated soil column, locations with very low cement slurry concentration cannot be discounted and Eq.5.3 would allow these locations to have spurious high strength. To avoid anomalous results during strength distribution computation, a modified relationship was used which involves removing the higher order terms from the exponential Taylor series. This leads to a modified relationship as:

$$r(c, w) = \frac{1 + mx + (mx)^2}{(wx + a)^n} \tag{5.5}$$

where: $x = \frac{1}{A}\left(\frac{1}{c} - 1\right)$ and $A = \frac{1+w}{1+a}$

Eq.5.5 is plotted in solid line in **Figure 5.1.** Eq.5.5 predicts strength decreasing monotonously as cement slurry concentration declining. For cement slurry concentration higher than 20%, Eq.5.5 gives almost the same strength ratio of Eq.5.3. The maximum tolerance on difference of predicted r by Eq.5.3 and Eq.5.5 is assumed to be 0.02, which is drawn as a dotted line in **Figure 5.1**. On right side of dotted line, the value of modified r is accepted within maximum tolerance of 0.02.

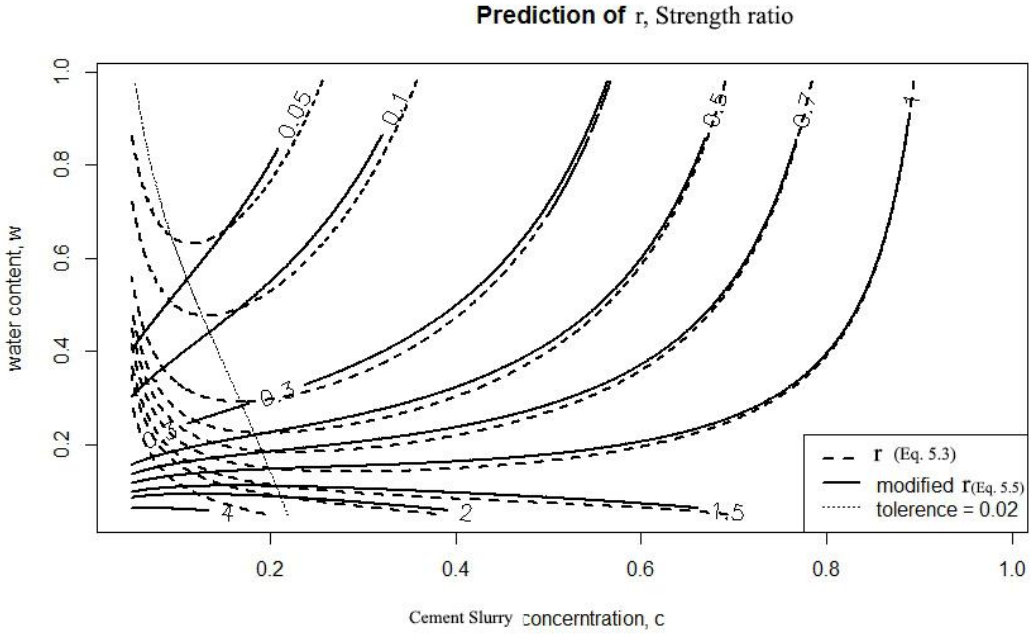

(a) Contours of *r*, the strength ratio as a function of *w* and *c*. *r* is for Eq.5.3; while modified *r* is for Eq.5.5s

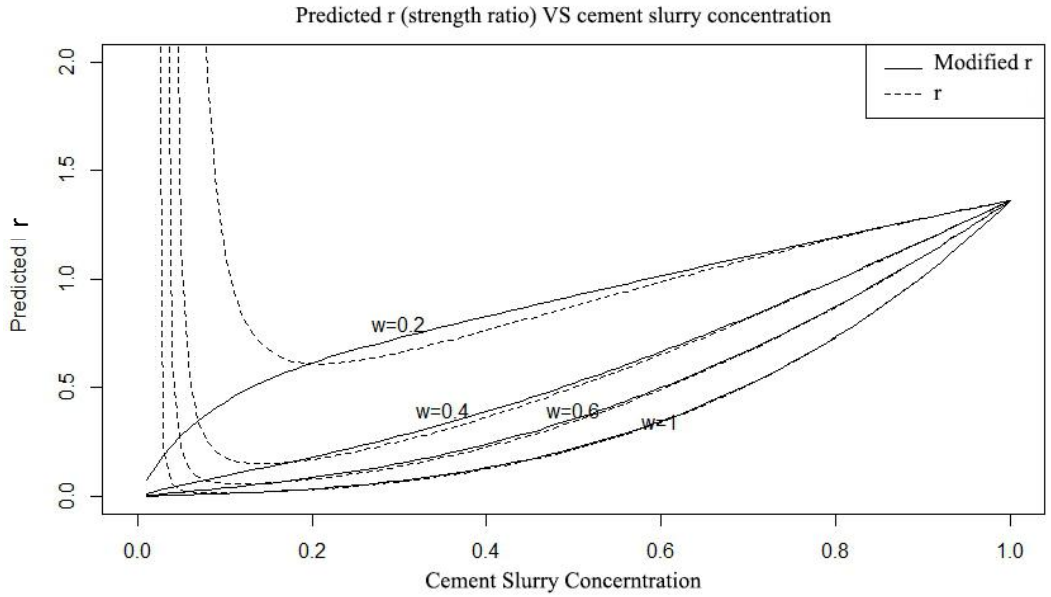

(b) Plot of cement slurry concentration-*r*. *r* is strength ratio for Eq.5.3, while modified *r* is for Eq.5.5 (w: in-situ water content)

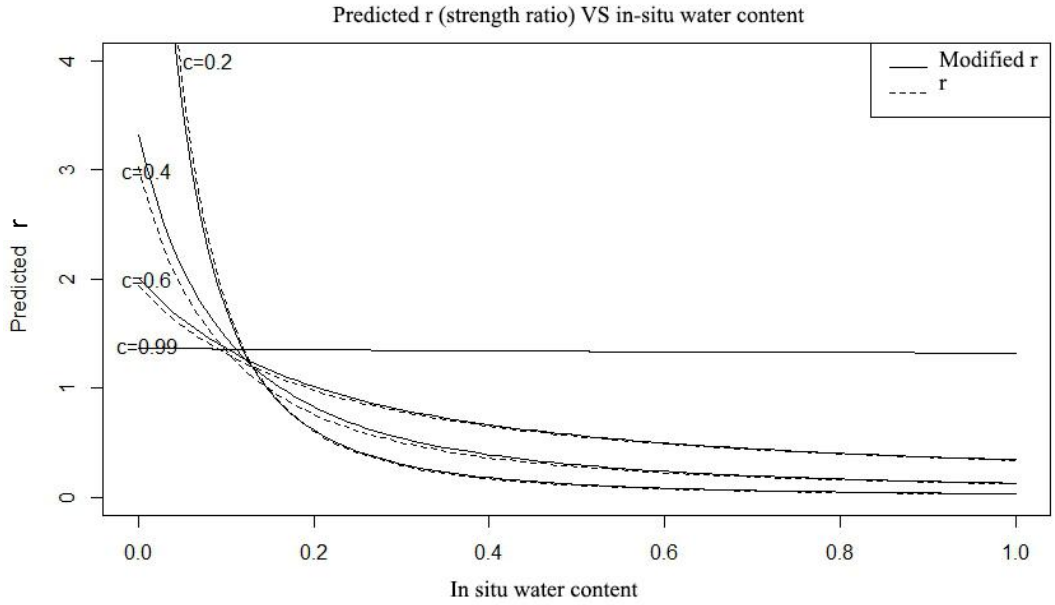

(c) Plot of in-situ water content-*r*; *r* is strength ratio for Eq.5.3, while modified *r* is for Eq.5.5 (c: cement slurry concentration).

Figure 5. 1 plots on in-situ water content, cement slurry concentration and *r* (strength ratio), according to Eq.5.3 and Eq.5.5

The fitted UCS-*w* relationships in **Figure 4.19** were transformed and plotted as fitted *r*-*w* relationship in **Figure 5.2**. As can be seen, the measured *r*-UCS relationships fall in the range of predicted *r*-UCS relationships with cement slurry concentration from 0.2 to 0.4.

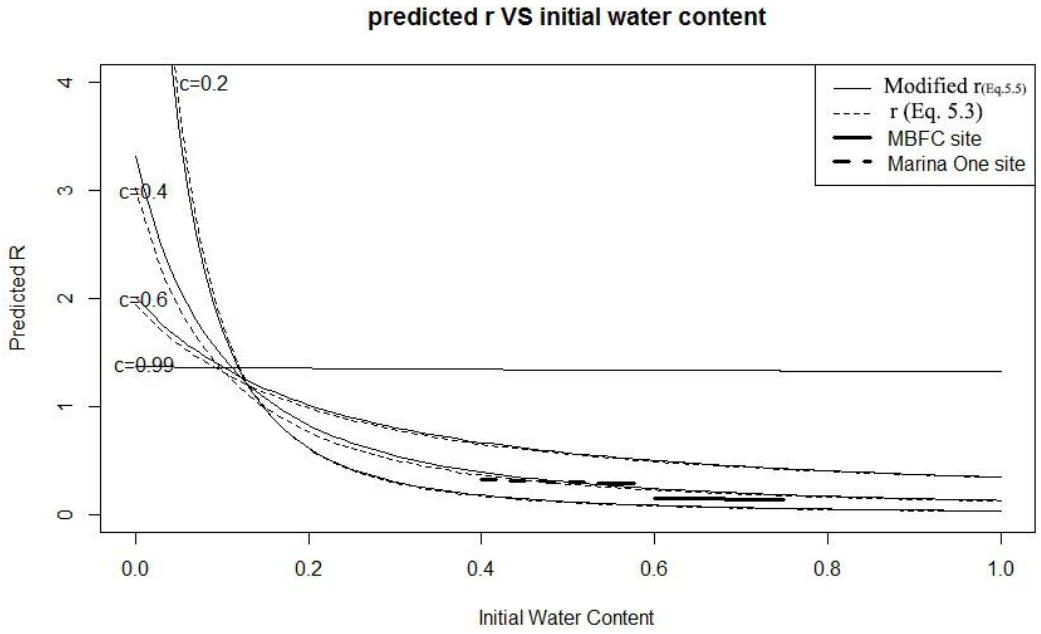

Figure 5. 2 Relationship of Predicted *r* (strength ratio)and *w* (in-situ water content) according to Eq.5.3 & Eq.5.5. The fitted UCS-*w* relationship in Figure 4.19 was transformed accordingly and plotted in bold line.

5.1. Mean and Variance Estimation

Expanding Eq.5.3 in a Taylor series about the mean values $(\bar{c}, \bar{w})$ yields:

$$r = g(\bar{c},\bar{w}) + \left[(c-\bar{c})\frac{\partial}{\partial c} + (w-\bar{w})\frac{\partial}{\partial w}\right] g(\bar{c},\bar{w}) + \frac{1}{2!}\left[(c-\bar{c})\frac{\partial}{\partial c} + (w-\bar{w})\frac{\partial}{\partial w}\right]^2 g(\bar{c},\bar{w}) + \ldots \tag{5.6}$$

One can truncate Eq.5.6 to a certain order and thereby estimate the mean and variance of *r* provided that the corresponding order of moments in *c* and *w* are available. However, calculation of the skewness or higher order moments require a large sample size, which might not be available for geotechnical data from site. Thus, from a practice point of view,

the mean and variance in *c* and *w* can be employed to predict the mean and variance, that is the first and second moments, in *r*. This is also in line with common statistical analyses.

The second-order approximate mean of *r* is:

$$E[r] \approx g(\bar{c}, \bar{w}) + \rho_{cw}\sigma_c\sigma_w \frac{\partial^2 g(\bar{c}, \bar{w})}{\partial c \partial w} + \frac{1}{2}\sigma_c^2 \frac{\partial^2 g(\bar{c}, \bar{w})}{\partial c^2} + \frac{1}{2}\sigma_w^2 \frac{\partial^2 g(\bar{c}, \bar{w})}{\partial w^2} \quad (5.7)$$

The first-order approximate variance of *r* is:

$$Var[r] \approx \sigma_c^2 \left[\frac{\partial g(\bar{c}, \bar{w})}{\partial c}\right]^2 + \sigma_w^2 \left[\frac{\partial g(\bar{c}, \bar{w})}{\partial w}\right]^2 + 2\rho_{cw}\sigma_c\sigma_w \frac{\partial g(\bar{c}, \bar{w})}{\partial c}\frac{\partial g(\bar{c}, \bar{w})}{\partial w} \quad (5.8)$$

where σ_c and σ_w are the standard deviations of *c* and *w*, respectively; ρ_{cw} is the correlation coefficient between *c* and *w*, of which the value is zero in this study, as *c* and *w* are independent random variables. It shall be noted that if the second-order is to be used herein to approximate variance of *r*, the fourth-order statistics in *c* and *w* are required, which is usually unavailable.

Thus, Eq.5.7 and Eq.5.8 can be respectively rewritten as:

$$E[r] \approx g(\bar{c}, \bar{w}) + \frac{1}{2}\sigma_c^2 \frac{\partial^2 g(\bar{c}, \bar{w})}{\partial c^2} + \frac{1}{2}\sigma_w^2 \frac{\partial^2 g(\bar{c}, \bar{w})}{\partial w^2} \quad (5.9)$$

$$Var[r] \approx \sigma_c^2 \left[\frac{\partial g(\bar{c}, \bar{w})}{\partial c}\right]^2 + \sigma_w^2 \left[\frac{\partial g(\bar{c}, \bar{w})}{\partial w}\right]^2 \quad (5.10)$$

The approximate mean and variance of r predicted by Eq.5.9 and Eq.5.10 involve mean and variation of *c* and *w*. The first and second order derivations of Eq.5.9 and Eq.5.10 in terms *c* and *w* are:

$$\frac{\partial g(\bar{c},\bar{w})}{\partial c}=\frac{-1}{\bar{A}\left(\bar{c}\right)^{2}}\left(m-\frac{n\bar{w}}{\left(\bar{w}\bar{x}+a\right)}\right)g(\bar{c},\bar{w}) \tag{5.11}$$

$$\frac{\partial g(\bar{c},\bar{w})}{\partial w}=\xi\cdot g(\bar{c},\bar{w}) \tag{5.12}$$

$$\frac{\partial^{2} g(\bar{c},\bar{w})}{\partial c^{2}}=\left[\frac{-2}{\bar{c}}+\frac{1+a}{\left(1+\bar{w}\right)\left(\bar{c}\right)^{2}}\left(-m+\frac{n\bar{w}}{\bar{w}\bar{x}+a}-\frac{n\bar{w}^{2}}{\left(\bar{w}\bar{x}+a\right)\left(m\bar{w}\bar{x}+ma-n\bar{w}\right)}\right)\right]\frac{\partial g(\bar{c},\bar{w})}{\partial c} \tag{5.13}$$

$$\frac{\partial^{2} g(\bar{c},\bar{w})}{\partial w^{2}}=\left[\frac{2m\bar{B}}{\left(1+\bar{w}\right)^{3}}+\frac{n\bar{B}\left(\bar{B}+2\bar{w}\bar{B}+2\left(1+\bar{w}\right)a\right)}{\left[\bar{w}\left(1+\bar{w}\right)\bar{B}+\left(1+\bar{w}\right)^{2}a\right]^{2}}+\xi^{2}\right]g(\bar{c},\bar{w}) \tag{5.14}$$

Where: $\xi=\frac{\bar{B}}{\left(1+\bar{w}\right)^{2}}\left[-m-\frac{\left(1+\bar{w}\right)n}{\bar{w}\bar{B}+\left(1+\bar{w}\right)a}\right]$ (5.15)

$$\bar{A}=\frac{1+\bar{w}}{1+a} \tag{5.16}$$

$$\bar{B}=\left(1+a\right)\left(\frac{1}{\bar{c}}-1\right) \tag{5.17}$$

Following Xiao *et al.* (2014)'s study, parameters m and n in Eq.5.3 are equal to 0.3 and 2.92, respectively. At the MBFC site, the water-cement ratio, *a* in cement-slurry is 0.9 (Liu *et al.*, 2015). Based on data from centrifuge model tests and the deep mixing operational parameters for the MBFC site, Liu *et al.* (2015) estimate the mean and coefficient of variation of cement slurry concentration to be 0.28 and 0.18, respectively. **Figure 5.**3 also suggests that when in-situ water content is low (0.3 or below), *r* is relatively insensitive to the variation in cement slurry concentration. Although information on water-cement ratio

and cement slurry concentration is missing in Marina One site, we can make a weak assumption that they are consistent in two sites herein.

This two-parameter model implies that the expectation and variation of UCS in cement-treated soil depend on four parameters: μ_w, μ_c, σ_c and σ_w. For example, a parametric study of mean prediction is investigated in **Figure 5.3**: Four cases were considered:

1) Deterministic case with zero variation (Bolded black line, same as Eq.5.3);

2) COV_c =0; COV_w =0.3 (Red dashed line);

3) COV_c =0.3; COV_w =0 (Blue dashed line);

4) COV_c =0.3; COV_w =0.3 (Green dashed line).

As can be seen in **Figure 5.3,** when water content is high, variations in cement slurry concentration and water content significantly influences the predicted UCS. On the other hand, the influence of water content variation is not so evident at low mean water content.

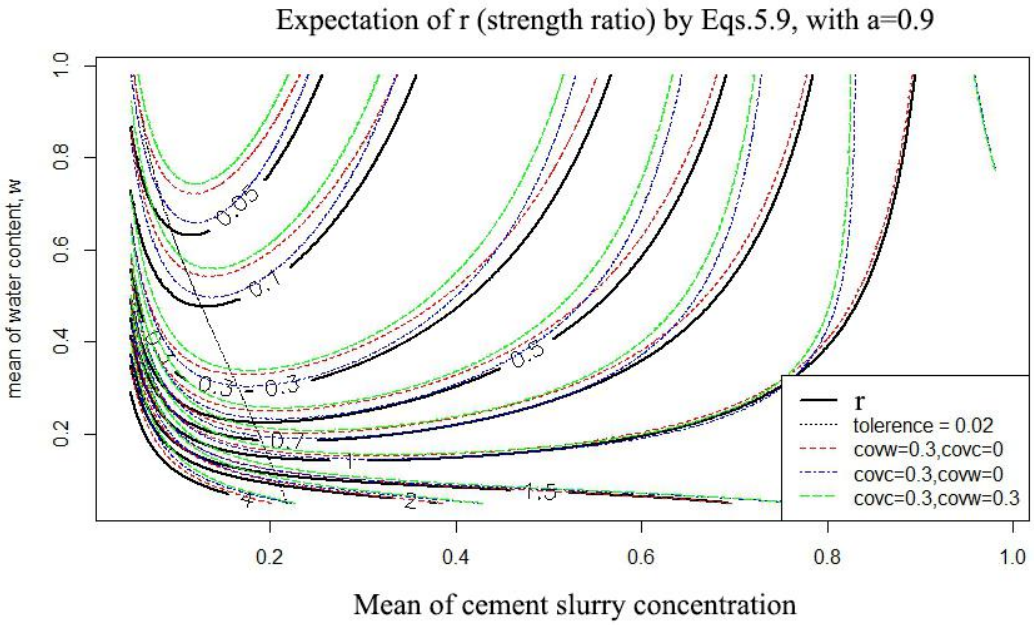

Figure 5. 3 Predicted mean of *r* (Eq.5.3) in four cases: (1) $\boldsymbol{cov_c}$=0; $\boldsymbol{cov_w}$=0, same as Eq.5.3 (black line), (2) $\boldsymbol{cov_c}$ =0; $\boldsymbol{cov_w}$=0.3 (Red dashed line); (3) $\boldsymbol{cov_c}$=0.3; $\boldsymbol{cov_w}$=0 (Blue dashed line); (4) $\boldsymbol{cov_c}$=0.3; $\boldsymbol{cov_w}$=0.3 (Green dashed line).

For same values of parameters m and n herein, the components comprising the strength ratio *r* in Eqs. 5.9 & 5.10 with in-situ water content and cement slurry concentration are shown in **Figure 5.4.** Once the mean and variance of in-situ water content and cement concentration are measured, Fig.5.4 offers a practical method to predict mean and variance of strength ratio in accordance with Eqs.5.9 and Eqs.5.10. For reference purpose, three different values of *a*, water-cement ratio of cement slurry are considered herein: 0.9, 1.0 and 1.1, respectively.

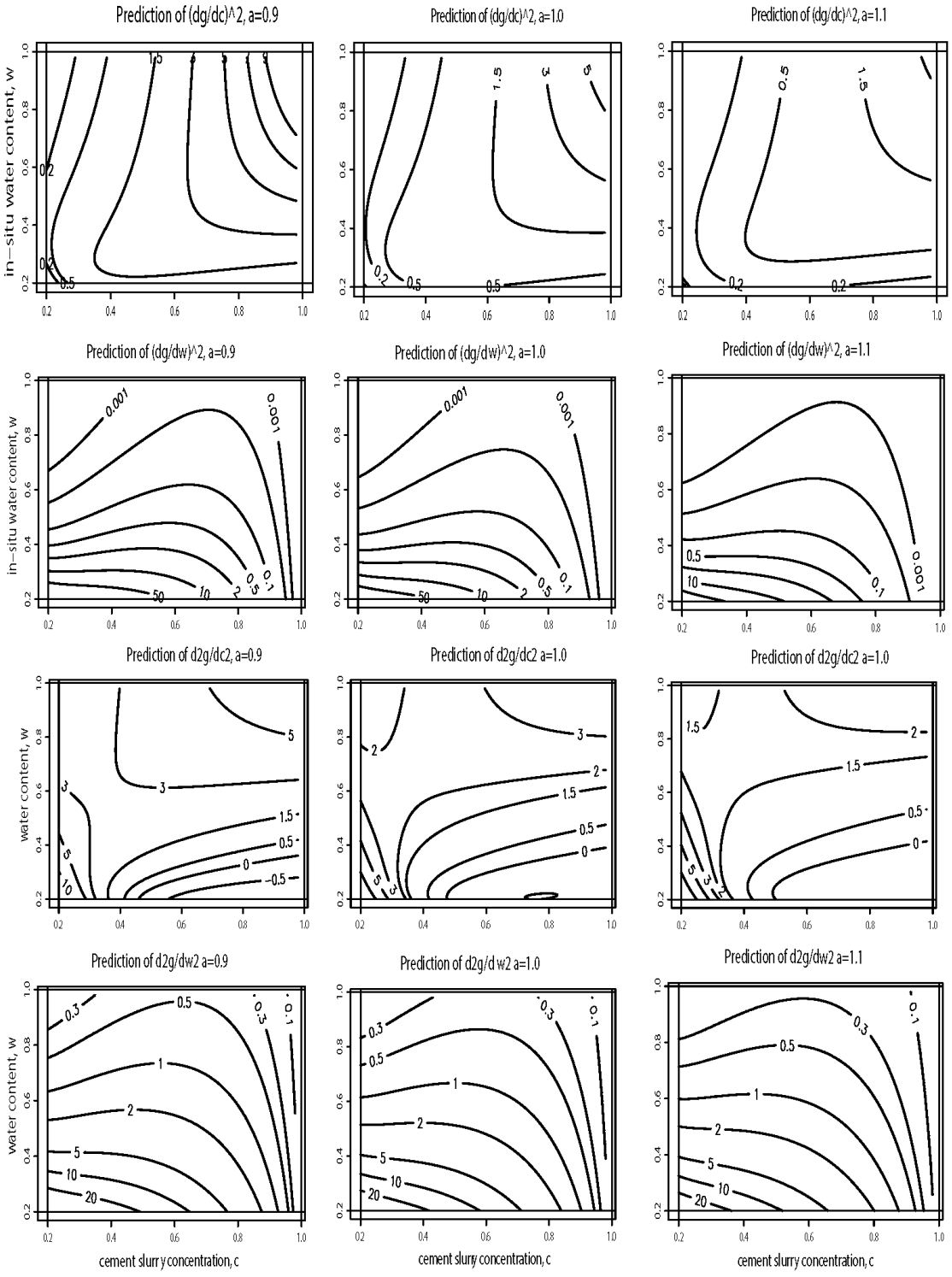

Figure 5. 4 Plot of derivation: (a) Plot of $\left[\frac{\partial g(\bar{c},\bar{w})}{\partial c}\right]^2$ in Eq.5.11; (b) Plot of $\frac{\partial^2 g(\bar{c},\bar{w})}{\partial c^2}$ in Eq.5.13; (c) Plot of $\left[\frac{\partial g(\bar{c},\bar{w})}{\partial w}\right]^2$ in Eq.5.12; (d) Plot of $\frac{\partial^2 g(\bar{c},\bar{w})}{\partial w^2}$ in Eq.5.14.

Field data comparison

In this field data comparison, the mean and COV of the in-situ water content from the two sites are employed here to estimate the mean and variance of the strength ratio, *r* by Eqs.5.9 and 5.1, respectively. In the Marina One site, the improved soil layer consists of two clay layers with distinguishable water contents. Such disparity results in divergent mean and variance of associated *r* in two soil layers. Assuming that core sample were taken uniformly over whole improved soil layer during site investigation, the proportion of treated soil from two marine layers can be approximated by ratio of amount of data of in-situ water content from two clay layers. That is to say, in Marina One site, the "weighted UCS" of whole treated layer can be predicted by the sum of predicted UCS from two layers, 2A and 2B in proportion. In other words, the mean and standard deviation of whole site, $\mu_{combined}$ and $\sigma_{combined}$ are derived as:

$$\mu_{combined} = \frac{N_{2A}\mu_{2A} + N_{2B}\mu_{2B}}{N_{2A} + N_{2B}} \tag{5.18}$$

$$\sigma_{combined} = \sqrt{\frac{N_{2A}\sigma_{2A}{}^2 + N_{2B}\sigma_{2B}{}^2}{N_{2A} + N_{2B}} + \frac{N_{2A}N_{2B}}{\left(N_{2A} + N_{2B}\right)^2}\left(\mu_{2A} - \mu_{2B}\right)^2} \tag{5.19}$$

where N_{2A} and N_{2B} are the sample sizes of in-situ water content data from upper and lower marine clay layers, respectively; while μ_{2A}, μ_{2B}, σ_{2A} and σ_{2B} are mean and standard deviation of predicted *r*, strength ratio, from upper and lower marine clay layers, respectively.

Eq.4.3 suggests that q_0 corresponding to a curing time of 28 days, hereafter denoted by $q_0(28)$ is a constant value, hence mean and standard deviation of equivalent 28-day normalized UCS can be obtained by multiplying mean and standard deviation of *r* by value

of $q_0(28)$ from two sites. **Table 5.1** listed predicted mean and variation of 28-day equivalent UCS by Taylor-expansion.

Table 5. 1 Summary of mean and variance of predicted 28-day equivalent UCS of two sites (unit of q_u: MPa)

		Marina One		MBFC
		2A	**2B**	
Mean w		0.54	0.31	0.65
mean c		0.28	0.28	0.28
cov w		0.13	0.20	0.10
cov c		0.18	0.18	0.18
Number of data for SI per soil type		N_{2A} = 42	N_{2B} = 30	78
Proportion of predicted r per soil type		58%	42%	100%
Predicted R by Taylor's Expansion Per soil layer	mean	μ_{2A} = 0.17	μ_{2B} = 0.41	-
	COV	0.30	0.12	-
Predicted R by Taylor's Expansion	mean	$\mu_{combined}$ = 0.27		0.12
	COV	0.55		0.30
Predicted $q_u(t = 28day)$ by Taylor's Expansion	mean	2.15		1.70
	COV	**0.55**		**0.30**
Measured $q_u(t = 28day)$	mean	2.13		1.66
	COV	**0.44**		**0.42**

5.2. Probability Density Function of Strength Ratio

Derivation of Probability Density Function

Based on Eq.5.5, one can write slurry concentration *c* as a function of strength ratio *r* and in-situ water content *w*:

$$w = g(r, c) \tag{5.20}$$

The cumulative distribution function (CDF) of *r*, $F_R(r)$, can be defined as

$$F_R(r) = P\left[r(c, w) \le r\right] \tag{5.21}$$

where *P*[*] is the probability of a combination of the concentration *c* and in-situ water content *w*.

Since *r* is an increasing function of *w*, Eq.5.21 can be calculated as:

$$\begin{aligned} F_R(r) &= P\left[r(c, w) \le r\right] \\ &= \int_{w=-\infty}^{\infty} \int_{c=-\infty}^{g(r,w)} f_{CW}(c, w)\, dc\, dw \end{aligned} \tag{5.22}$$

where $f_{CW}(c, w)$ is the joint probability density function (PDF) of *c* and *w*.

Since the variables *c* and *w* are independent, thus we have:

$$f_{CW}(c, w) = f_C(c)\, f_W(w) \tag{5.23}$$

Substituting Eq.23 into Eq.5.22 yields:

$$F_R(r) = \int_{w=-\infty}^{\infty} \int_{c=-\infty}^{g(r,w)} f_C(c)\, f_W(w)\, dc\, dw \tag{5.24}$$

The PDF of *r*, $f_R(r)$, can be expressed as

$$f_R(r) = \frac{dF_R(r)}{dr} = \int_{w=-\infty}^{\infty} \frac{dg(r,w)}{dr} f_C\left[g(r,w)\right] f_W(w) dw \tag{5.25}$$

Since the function cannot be explicitly expressed, Eq.5.25 cannot be solved in a mathematically closed-form manner. Instead of continuous integration, the probability density function of *r* is approximated by discrete integration (see **Appendix A**).

Truncated Normal Distribution

The normal distribution is a widely-accepted distribution to fit the histogram of soil properties (Honjo, 1982; Matsuo, 2002; Usui, 2005; Namikawa and Koseki, 2013; CEN, 2002). However, negative values can be introduced in normal distribution since it is unbounded. This is meaningless for water content and cement slurry concentration since they are always positive. To accommodate this restricted range, the normal distribution was truncated to the interval [0, 2μ], where μ is the mean value (Barr and Todd, 1999). For distributions with low coefficient of variation, the coverage of truncated normal distribution will be high and that the truncation is unlikely to affect a significant number of data points on the upper end of the distribution. Thus, the probability density function of cement slurry concentration and in-situ water content, $f_H(h)$, can be expressed as the truncated normal distribution (Elishakoff, 1999) in the following form:

$$f_H(h) = \begin{cases} \dfrac{1}{G(2\mu) - G(0)} g(h) & \text{for } 0 < h < 2\mu \\ 0 & \text{Otherwise} \end{cases} \tag{5.26}$$

in which *g(h)* and *G(h)* are the probability density and cumulative distribution functions of normal distribution, respectively. *h* herein refers to *w* and *c*.

In this study, the truncated-normal distributions of the in-situ water content and cement slurry concentration are two variables discussed herein to predict probability density function of 28-day equivalent UCS, $q_u(t = 28day)$. As shown in **Figure 5.5**, same means and COVs employed in previous Section 5.1 are selected to generate truncated-normal distribution of in-situ water content and cement slurry concentration in each soil layer:

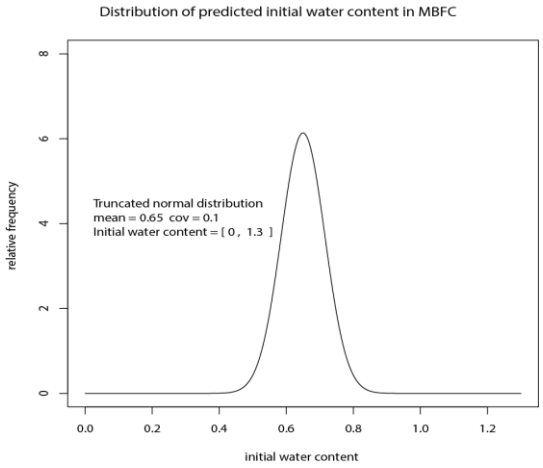

(a) Truncated normal distribution of in-situ water content in MBFC site

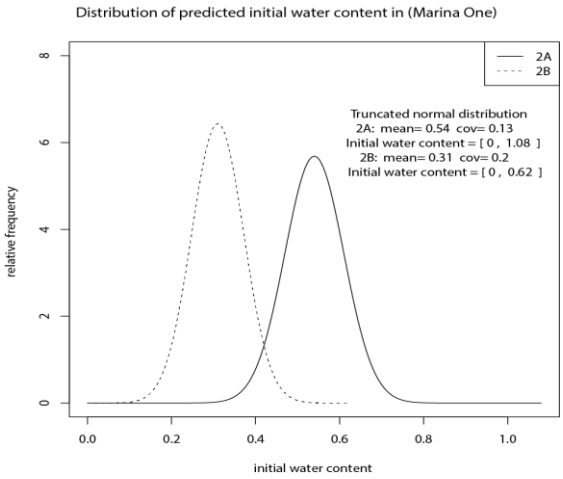

(b) Truncated normal distribution of in-situ water content in Marina One site; Solid line: Upper marine clay layer(2A); Dashed line: Lower marine clay layer(2B)

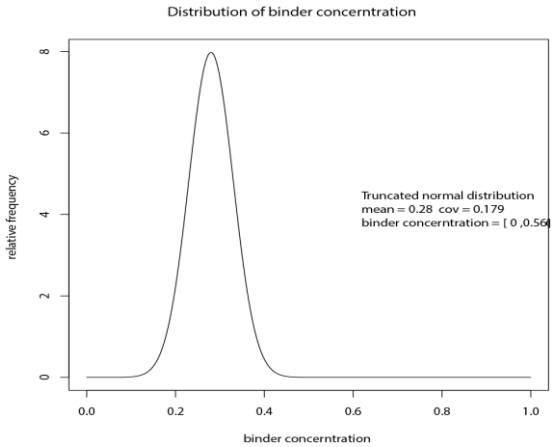

(c) Truncated normal distribution of cement slurry concentration in two sites.

Figure 5. 5 Distribution of input variables: (a)Truncated normal distribution of in-situ water content in MBFC site; (b) Truncated normal distribution of in-situ water content in Marina One site; Solid line: Upper marine clay layer (2A); Dashed line: Lower marine clay layer (2B) ; (c) Truncated normal distribution of cement slurry concentration in two sites.

Field data application

In Marina One site, probability density functions (PDF) of 28-day equivalent UCS in each soil layers were predicted separately; following same idea of "proportional combination" in section 5.1, a weighted PDF of UCS is calculated by combining PDFs from two soil layers in proportions.

Figure 5.6(a) and **5.6(b)** compares the predicted $q_0(28)$ and the equivalent 28-day UCS inferred from core strength data, $q_u(28)$, in MBFC and Marina One site, respectively; **Table 5.2** summarizes statistical characteristics of UCS predicted by PDF. Comparing **Tables 5.1** and **5.2**, mean and variation of UCS predicted by PDF and Taylor's Expansion are quite similar. The general uniformity of results by two methods confirms the consistency between the two methods.

The two-sample Kolmogorov-Smirnov test was employed to evaluate the quality of prediction by PDF. For a significance level α, the null hypothesis that two samples were drawn from same population can be rejected if the maximum difference of two cumulative distribution functions is higher than D_a:

$$D_a = c(a)\sqrt{\frac{n_1 + n_2}{n_1 n_2}} \tag{5.27}$$

Where n_1 and n_2 are sizes of two samples. For α = 0.05 (i.e. 5% significance level), $c(a)$ = 1.36; D_a is equal to 0.056, 0.127 for Marina One and MBFC site, respectively. Although the null hypothesis in MBFC cannot be rejected, null hypothesis in the Marina One site is rejected at 95% confidence interval. This is due to the fact that the Marina One data set shall pass a more discriminating criteria due to the larger sample size than the MBFC site.

As shown in **Table 5.2**, compared to the variation of measured UCS in MBFC site, COVs predicted by both methods, Taylor's Expansion and PDF, are slightly under-estimated. In

this soil model, only two variables, that is in-situ water content and cement slurry concentration, are used to predict the distribution 28-day equivalent UCS. Other factors which may also contribute to the total variation of strength in cement-treated soil are not considered. Hence, it is not surprising that, in MBFC site, the predicted COV by both methods is lower than measured COV of UCS. Notwithstanding this, the predicted PDF for the MBFC site appears to be remarkably similar to the measured PDF, at least qualitatively. Given the large number of variables in this problem, the agreement appears to be surprisingly good.

However, the predicted COVs of UCS in Marina One site are evidently higher than measured COV. Over-estimation of variation probably results from "proportional combination" of two soil layers with largely differed means. In reality, soil portions from different soil layers might be mixed together in up- and-down mixing process, in such a way that the disparity of in-situ water content may have a smaller influence. In addition, this hypothesis can explain the difference between predicted and measured PDFs: two sets of in-situ water content distribution bring two peaks in combined distribution of UCS; although real distribution of UCS has only one peak. There are many possible reasons for such discrepancy. One of the main reasons is that the deep mixing parameters for the Marina Site are assumed to be same as that for the MBFC. This includes the parameters q_0, m and n of the UCS-cement slurry relation, which has a direct and very significant effect on the predicted PDF. In addition, it is quite plausible that the values of q_0 are different for the upper and lower marine clay.

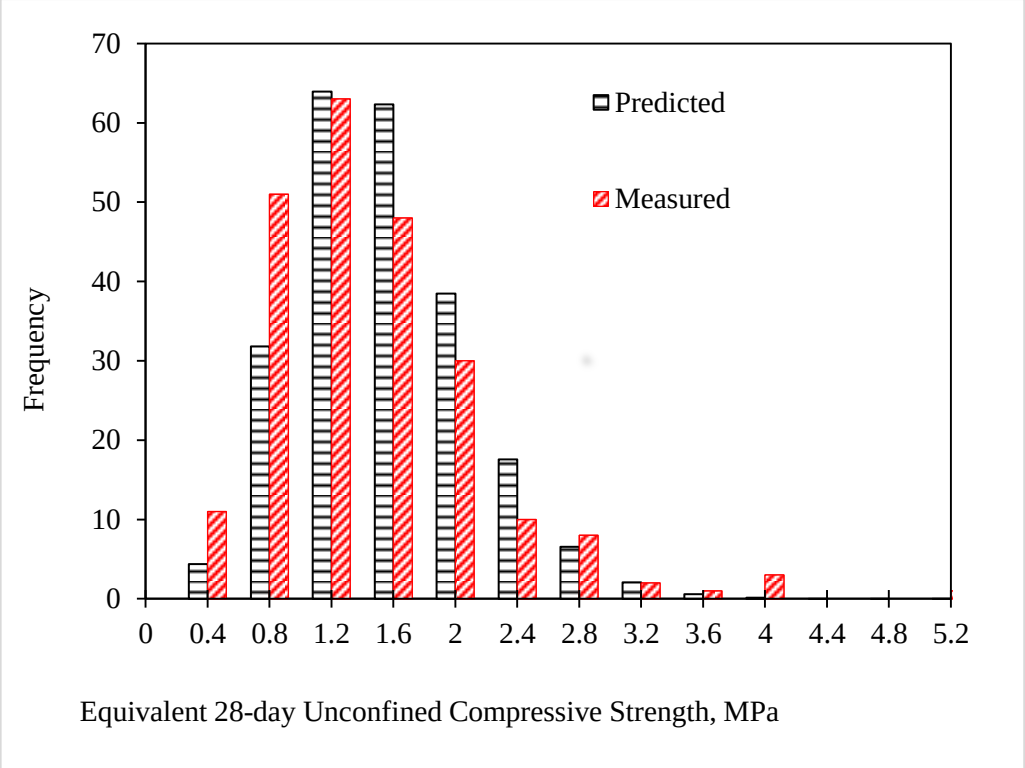

(a) MBFC site

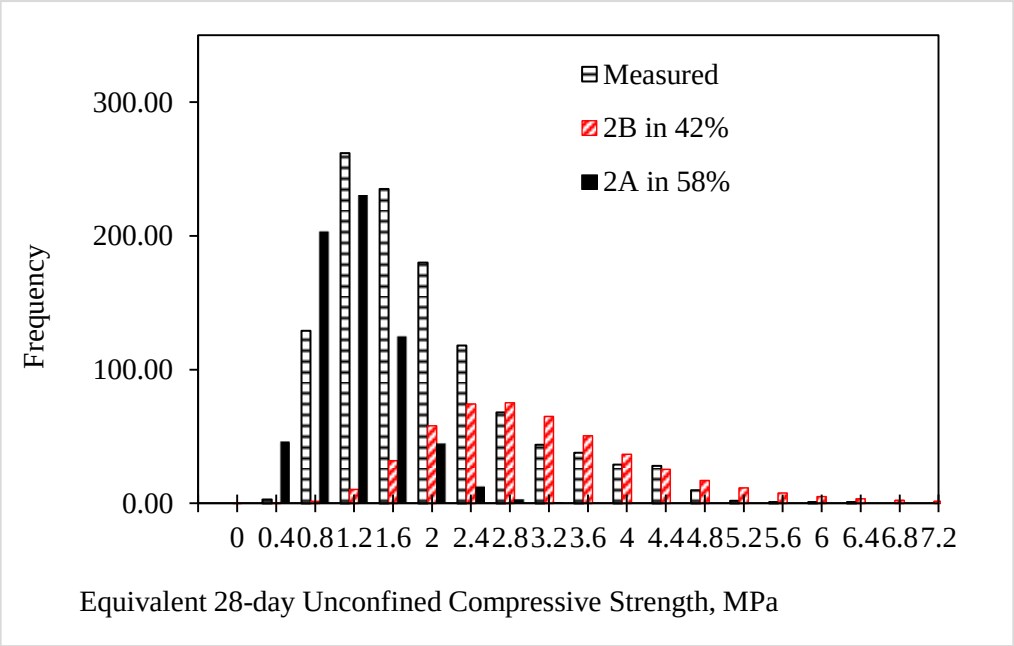

(b)Marina One site

Figure 5. 6 Predicted probability density functions of 28-day equivalent UCSs by Eq.5.25 in (a) MBFC site; (b) Marina One site. (**Measured**: normalized 28-day equivalent UCS from measured site data; **Predicted**: Predicted UCS based on truncated normal distributed w with mean and standard deviation measured from MBFC site. **2A:** Predicted UCS based on truncated normal distributed *w* with mean and standard deviation measured from upper marine clay layer; **2B**: Predicted UCS based on truncated normal distributed *w* with mean and standard deviation measured from lower marine clay layer.)

Table 5. 2 Summary of predicted result by Probability Density Function (2A: Upper marine clay layer; 2B: Lower marine clay layer) unit of q_u : MPa

Properties		**Marina One**		**MBFC**
		2A	**2B**	
Mean of *w*		0.54	0.31	0.65
mean of *c*		0.28	0.28	0.28
COV of *w*		0.13	0.20	0.10
COV of *c*		0.18	0.18	0.18
Number of data for SI per soil type		N_{2A} = 42	N_{2B} = 30	78
Proportion of predicted *r* per soil type		58%	42%	100%
Predicted $q_u(t = 28day)$ by PDF per soil layer	mean	1.334	3.294	-
	COV	0.336	0.378	-
Predicted $q_u(t = 28day)$ by PDF	mean	2.16		1.66
	COV	**0.61**		**0.33**
Measured $q_u(t = 28day)$	mean	2.13		1.66
	COV	**0.44**		**0.42**

5.3 Scale of Fluctuation Estimation

By definition, the autocorrelation function of strength ratio, ζ_r, can be estimated as

$$\zeta_r(\tau) = \frac{c_r(\tau) - \bar{r}}{\mathrm{Var}(r)} \tag{5.28}$$

in which $c_r(\tau)$ can be calculated by

$$c_r(\tau) = \int_{-\infty}^{\infty}\int_{-\infty}^{\infty} x_1 x_2 f(x_1, x_2;\ \tau) dx_1 dx_2 \tag{5.29}$$

where f is the joint PDF of UCS with spatial lag τ. The joint PDF is a function of the PDFs of in-situ water content and cement slurry mass fraction, in form of Eq.5.25. Again, both the in-situ water content and cement slurry concentration (Chen, 2011) can be assumed to follow the same truncated normal distribution listed in **Figure 5.6**. Therefore, the autocorrelation function in Eq.5.28 can be obtained by numerical Monte-Carlo integration, from which the scale of fluctuation, θ_r, can be calculated by definition (Vanmarcke 1983):

$$\theta_r = 2\int_0^{\infty} \zeta_r(\tau) d\tau \tag{5.30}$$

Considering the range of SOF of in-situ water content, it is reasonable to assume that the water content within a deep mixing / jet grouting column is constant in horizontal direction. In this case, the relationship between SOF of cement slurry concentration and strength ratio was tabulated in **Figure 5.7(a),** from which can be seen that the SOF is almost equivalent in cement slurry mass fraction and strength ratio, for both equal to 0.8 and 1.0. In Marina One and MBFC sites, the minimum horizontal spacing between UCS samples is around 10 m. There is no observable strong correlation structure from field data. This implies that the horizontal SOF of UCS is probably less than 10 m.

In vertical direction, the in-situ water content may not be necessarily constant, and its SOF is likely to affect the results. **Figure 5.7(b)** plots the contours of SOF of strength ratio as a function of SOF of in-situ water content and cement slurry concentration. As the figure shows, the SOF of strength was dominated by that of the in-situ water content. For example, for SOF of in-situ water content equal to 6 m, the SOF of strength is predicted to be in the range of 2 m to 3 m. **Figure 5.8** shows that in two sites, the vertical SOF of strength in cement-treated soil is observed to be about 3.3 m, which is very close to the predicted result in **Figure 5.7(b)**.

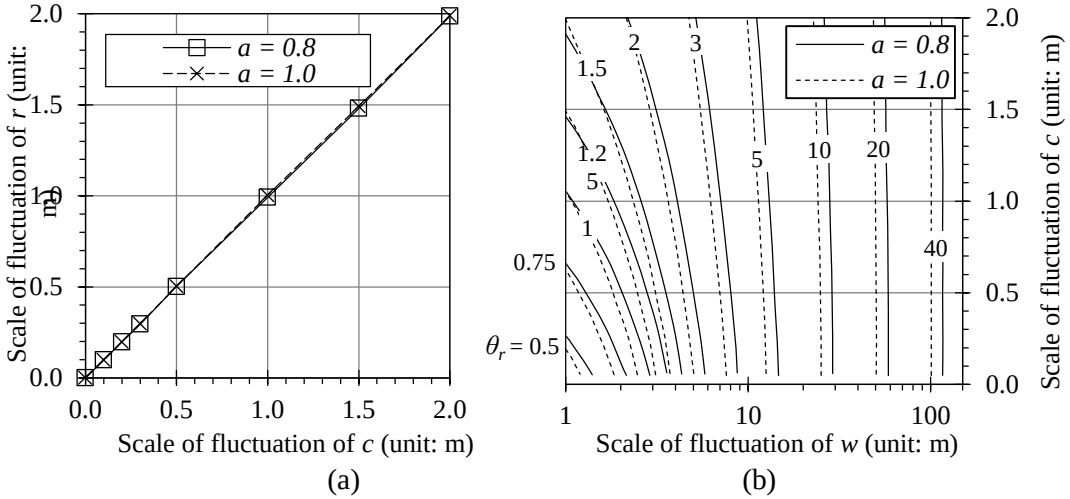

Figure 5. 7 Relationship among scales of fluctuation in strength ratio, *r*, cement slurry concentration, *c*, and in-situ water content, *w*. (a) *w* is constant; (b) both *w* and *c* have scales of fluctuations.

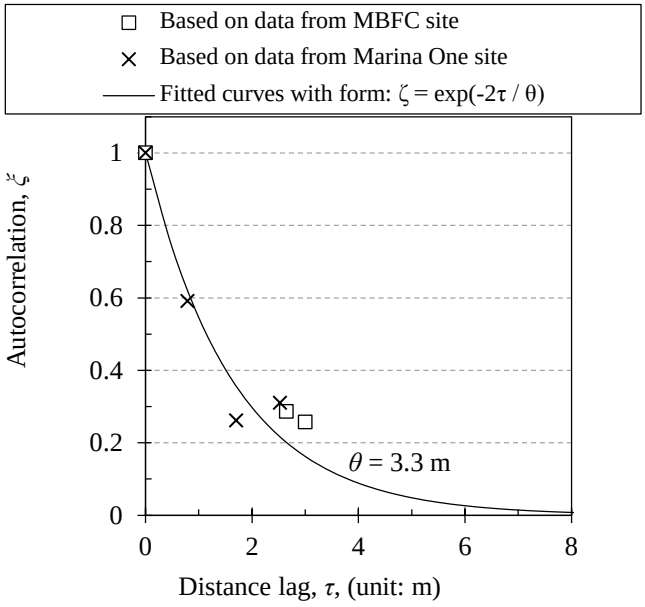

Figure 5. 8 Autocorrelation function of unconfined compressive strength of cement-admixed soils in vertical direction

6. Criteria and Sample Size of Mass Property Characterization

The previous chapter proposed a model to predict the spatial distribution of cement-treated soil based on cement slurry and in-situ water content variation. This chapter deals with monitoring and quality control. The most commonly used method of quality control is core strength measurement. However, there remains many aspects of core strength measurement which have not been studied and regularized. Chapter 4 already dealt with the issue of curing time normalization. This chapter uses the field data to examine two related issues in the monitoring, which are as follows:

(a) The number of samples which are needed to make a robustness assessment of the representative UCS of the treated soil mass.
(b) A statistically robust approach to defining a representative UCS of the treated soil mass.

These two may be related since different ways of defining a representative UCS may require different number of samples to ensure stability.

6.1. Previous and Related Studies

Distribution Fitting

As mentioned before, the strength in cement-treated soil is highly variable. Histograms can vary from site to site. Many researchers proposed various forms of distributions to fit the histogram of UCS in cement treated soil, such as normal distribution (Honjo, 1982; Futaki *et al.*, 2002; Matsuo, 2002), lognormal distribution (Fenton, 1999; Liu *et al.*, 2008) and beta distribution (Harr, 1977). The probability distribution to fit the material property has a

significant effect on the failure probability of a structural component; two different probability distributions for strength are likely to result in difference in failure probabilities over an order of magnitude (Ellingwood, 1994).

The normal and lognormal distributions are popular choices for the distribution fitting of UCS. Honjo (1982) found that in most of the cases of cement-improved soil, normal distribution fits well of field data of soil properties, although a few distributions with significant skewness cannot be well-fitted using a normal distribution. Similarly, normal distribution was employed in many projects of deep-cement mixing (Futaki *et al.*, 2002; Matsuo, 2002; Usui, 2005) to fit the histogram of UCS. By investigating the deep-cement-mixed soil in coast area of Japan, Namikawa and Koseki (2013) found that both lognormal and normal distributions can pass the distribution-fitting test of UCS at the 10% significant level.

However, Schultze (1972) had noticed that UCS of many natural clays are poorly fitted by the normal distribution, although many other soil properties can be fitted by normal distribution. Fenton (1999) also pointed out that normal distribution leads to a negative UCS for some samples, which is obviously unrealistic. He hence proposed that non-Gaussian distributions like lognormal distribution and gamma distribution might be more reasonable to predict certain soil properties. Besides normal distribution, lognormal distribution is preferred for its simplicity and non-negative property. Based on the assumption that the water-cement ratio is lognormal-distributed, Liu *et al.* (2008) proposed that a lognormal distribution could be employed to fit the distribution of UCS of cement-treated soil by transforming the empirical formula Eq.2.2. Similarly, Santoso *et al.* (2013) drew a similar conclusion by following another empirical formula applicable for clay at high water content, which was proposed as (Miura *et al.*, 2001):

$$q_u = \frac{A}{B^{W/C}} \tag{6.1}$$

where A and B are empirical fitted parameters, and *W* and *C* are water content and cement content, respectively. He also noted that according to Anderson-Darling goodness-of-fit test, the lognormal distribution fitted the histogram of UCS better than normal distribution (**Figure 6.1**).

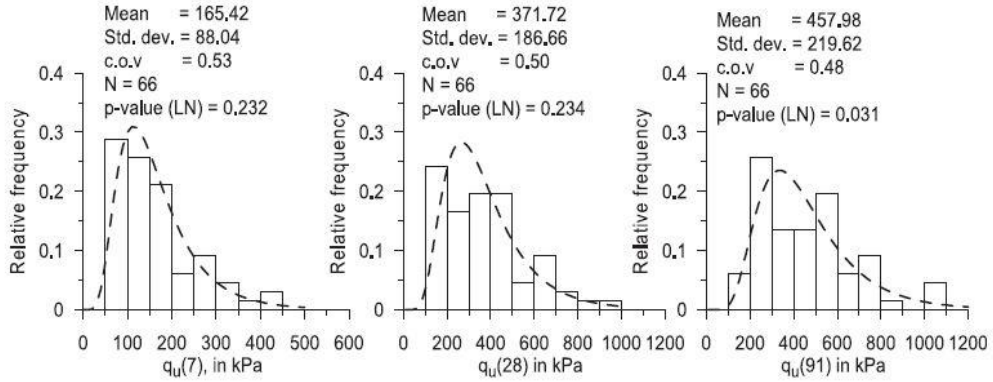

Figure 6. 1 Histogram of unconfined compressive strength (UCS) at 7, 28, and 91 days. N is the size of data, p-value is the type 1 error from the Anderson-Darling goodness-of-fir test. (Source: Santoso *et al.* 2013)

Besides the lognormal and normal distributions, the four-parameter beta distribution (Pearson's Type I) can also be employed for UCS of cemented soil. Harr (1977) suggested that, compared with the normal distribution, the beta distribution is more consistent with observed properties of materials. Two main reasons were stated by Harr: (a) Symmetry is not required in the beta distribution; (b) It is bounded by upper limit and lower limit in beta distribution. Harr also noted that Lamb (1970) reported that cohesion parameter of soil strength is quite likely to be fitted by a skewed-beta distribution, although the central section of this distribution can also be approximated by a normal distribution. By modelling the behaviour of individual particles in uniformed soil, Kingsley (1986) proved through a theoretical approach that c and φ, cohesion and friction angle of drained strength respectively, are beta - distributed. Similarly, Popescu (2005) adapted a symmetric beta distribution to approximate the distribution of strength in over-consolidated soil.

In this study, four probability distribution functions were examined, namely, the normal, lognormal, Weibull and beta distributions. **Table 6.2** summarized those distributions in fitting material properties from different literatures. The first three distributions are two-parameter models and the beta distribution is a four-parameter model. The Kolmogorov–Smirnov (KS) test was used to assess the goodness-of-fit of these distributions to the field data.

The details of these distributions and KS test results are summarized in **Table 6.2**. For the MBFC project, all the four distributions pass the KS test at 5% significant level; however, only the lognormal distribution and beta distribution pass the K-S test for the Marina One project at a 5% significance level. The difference in fitting results can be attributed to the different sample sizes of these two projects. The MBFC has 232 data points, which corresponds to a critical KS statistic D_0 (maximum vertical difference between empirical and fitted cumulative distribution functions) value of 0.09 at the 5% significance level. On the other hand, the Marina One sample has 1149 data points, so the corresponding critical D_0 value reduces to 0.04. That is to say, the Marina One data set shall pass a much stricter test than the MBFC data.

Table 6. 1 Summary of probability distribution types on soil strength in literature reviews

Reference	**Probability Distribution**	**Material Property**
Honjo, 1982	Normal	UCS of cement-admixed soils
Futaki *et al.*, 2002		
Matsuo, 2002		
Usui, 2005		
Namikawa and Koseki, 2013		
Fenton, 1999	Lognormal	
Griffiths *et al.*, 2001		
Al-Naqshabandy, 2012		
Santoso *et al.*, 2013		Undrained shear strength of soils
Vahdatirad *et al.*, 2014		
Lamb, 1970	Beta	
Harr, 1977		
Kingsley, 1986		
Popescu, 2005		
Liu *et al.*, 2014		UCS of cement-admixed soils
Trustum and Jayatilaka, 1983	Weibull	Strength of brittle material
Department of Defense, 2002		Composite material strength
Zureick *et al.* 2006		Properties of fiber-reinforced polymer
CEN, 2002 (Eurocode 0)	Lognormal or Weibull	Material and structural resistance parameters

Distribution	Parameters	MBFC Project	Marina One Project
	Sample size	232	1145
Critical D_0 at 0.05 significance level		0.09	0.04
Normal	Variable Range	$-\infty < x < \infty$ (unit: Mpa)	
	PDF $f_X(x)$	$f_X(x) = \frac{1}{\sigma\sqrt{2\pi}} \exp\left[-\frac{1}{2}\left(\frac{x-\mu}{\sigma}\right)^2\right]$	
	Fitted Parameters	μ = 1.67; σ = 0.71	μ = 2.14; σ = 0.94
	D_0 #	0.0818	0.1083
Lognormal	Variable Range	$0 \le x < \infty$ (unit: Mpa)	
	PDF $f_X(x)$	$f_X(x) = \frac{1}{x\xi\sqrt{2\pi}} \exp\left[-\frac{1}{2}\left(\frac{\ln x-\lambda}{\xi}\right)^2\right]$	
	Fitted Parameters	λ = 0.43; ξ = 0.39	λ = 0.67; ξ = 0.41
	D_0	0.0395	0.0383
Weibull	Variable Range	$0 \le x < \infty$ (unit: Mpa)	
	PDF $f_X(x)$	$f_X(x) = \left(\frac{\beta}{\alpha}\right)\left(\frac{x}{\alpha}\right)^{\beta-1} \exp\left[-\left(\frac{x}{\alpha}\right)^{\beta}\right]$	
	Fitted Parameters	α = 1.88; β = 2.46	α = 2.42; β = 2.39
	D_0	0.0733	0.0872
Beta *	Variable Range	$a \le x \le b$ (unit: Mpa)	
	PDF $f_X(x)$	$f_X(x) = \frac{(x-a)^{p-1}(b-x)^{q-1}}{\mathrm{B}(p,q)\times(b-a)^{p+q-1}}$, where $\mathrm{B}(p,q) = \int_0^1 t^{p-1}(1-t)^{q-1}\,\mathrm{d}t$	
	Fitted Parameters	p = 2.35; q = 11.2 a = 0.56; b = 6.94	p = 1.42; q = 8.48 a = 0.67; b = 8.28
	D_0	**0.0322**	**0.0368**

Note: Field data were normalized to 28-day values for both projects to eliminate time effect. # D_0 is a Kolmogorov–Smirnov statistic representing the maximum vertical difference between empirical and fitted cumulative distribution functions. * Four parameters of the Beta distribution in fitting a data set were determined based on the method in Liu *et al.* (2006). PDF = probability density function.

Table 6. 2 Probability distributions with Kolmogorov–Smirnov statistic D_0

Amongst four distributions, the beta distribution also yields minimal D_0 value in KS test for both projects. That implies that the beta distribution fit the distribution of 28-day normalized UCS from sites better than the other three distributions. In addition, the upper and lower bounds of the beta distribution is intuitively more meaningful, since the lower bound of UCS in cement-treated soil should be greater than zero and the upper bound strength must remain finite. For above-mentioned reasons, the UCS was assumed to follow the Beta distribution (see **Figure 6.2**) hereafter.

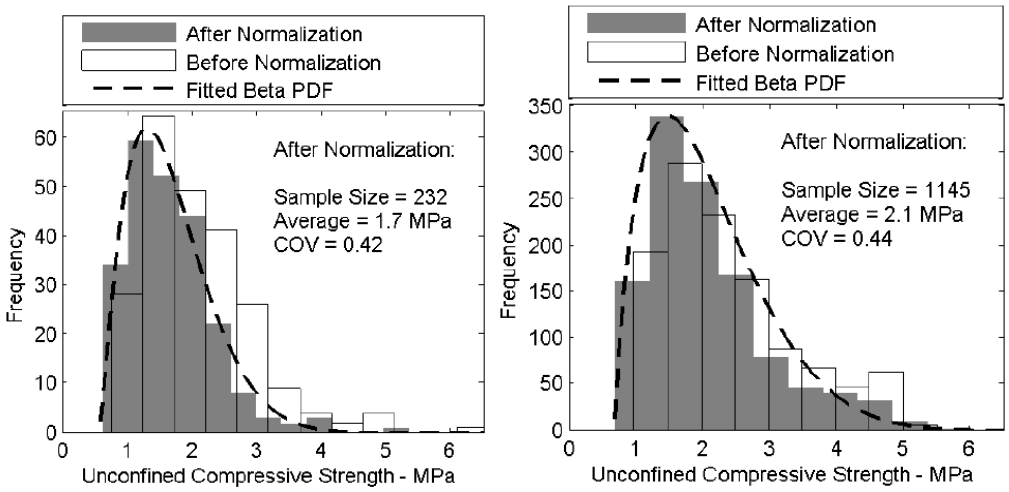

(a) MBFC Project (b) Marina One Project

Figure 6. 2 Histograms of unconfined compressive strength and fitted probability density function (PDF). COV = coefficient of variation. Fittings of PDF were based on histograms after normalization.

Characteristic value and robust criteria

Due to the inherent heterogeneity and spatial variation of soil structure, the strength of cement-admixed soil adopted in design is often several times lower than the laboratory-measured strength using the same mix proportion (e.g. Chew *et al.*, 2004). Various criteria for determining the design strength from core sample data can be found in literature and practice. Currently in Singapore, public agencies (e.g. LTA, 2010) often require that the strength of all of the tested cores must not be lower than the design strength. This is equivalent to using the sample minima as the design strength.

Alternatively, the specified strength is determined as a low-value percentile, typically 5% to 10%, of all the core sample data (e.g. Bertero *et al.*, 2012; Bruce, 2013). In particular, the 5% quantile in the lower tail of the distribution function is adopted by Eurocode 7 (CEN, 2004) to determine the characteristic value of a material property with spatial variation.

The characteristics values of geotechnical data are adapted in Eurocode 0 (CEN, 2002) to determine the design value of a material property with spatial variation. This characteristic value is determined from the core sample data by subtracting a multiple of the standard deviation from the mean strength (e.g. Futaki and Tamura, 2002, Bond *et al.*, 2013):

$$X_k = X_m(1 - k_n V_x) \tag{6.2}$$

where X_m is the mean value of measured property, V_x is the coefficient of variation, and k_n is a statistical coefficient depending on size n, the probability of X and whether V_x is known. Schneider (1999) suggested setting k_n in Eq.6.2 as 0.5 for undrained shear strength so that

$$c_{u,m,k} = c_{u,m} - 0.5 s_{cu} \tag{6.3}$$

$c_{u,m,k}$ is the characteristic value; $c_{u,m}$ is the mean value of samples; s_{cu} is the standard deviation. Schneider proposed that Eq.6.3 had been proven its simplicity and workability in practise since its first trial in 1989.

The second criterion (i.e. percentile criterion) is actually an alternative form of the third criterion (i.e. mean-COV criterion), in that tolerable percentage in the former can be expressed in the form of the latter by adjusting the multiple of the standard deviation. For example, in **Figure 6.3**, the 5% lower quantile of normal distribution is mathematically equal to the third criterion by setting the multiple of standard deviation k_n to 1.65 (Bond and Harris, 2008) . Both the second and third criteria can be also unified in the framework of reliability-based design with the concept of reliability index (Sivakumar Babu and Srivastava, 2011).

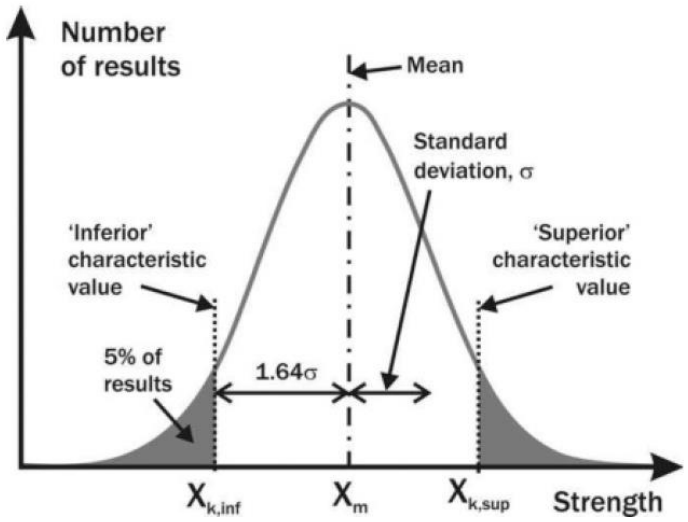

Figure 6. 3 The normal distribution of strength (after Bond *et al.*, 2008). The left dash line represents the inferior characteristic value, which is equal to the 5% lower quantile (criterion 2), as same as the third criterion by adjusting the multiple of standard deviation $\mathbf{k_n}$ to 1.65.

6.2. Robustness of Criteria

The three criteria for evaluating design value are as follows:

- Criterion 1: Minima of core sample data
- Criterion 2: Low-value percentile
- Criterion 3: Mean-standard-deviation linear combination

Criterion 3 can be expressed as:

$$z = \mu - h \cdot S \tag{6.4}$$

in which z is the design strength; μ and S are the mean and standard deviation of sample, respectively; and h is a reduction coefficient.

The test is conducted by randomly selected sub-sets of different sizes out of the two data sets and then calculating the design strength using the three criteria above. By repeatedly and randomly re-selecting different sub-sets from the two data sets, different design

strengths will be obtained. For a given criterion, a coefficient of variation (COV) of the design strength can thus be calculated; this can be used as the criterion to compare the robustness of different criteria; the smaller the COV of the design strength, the more robust is the criterion. This method of randomly selected sub-sets of samples with replacement (i.e. placing the sampled data back into the overall data set prior to re-sampling) is equivalent to the statistical method of "bootstrapping" (Efron, 1979). The underlying condition for using the bootstrapping method is that the sample (i.e. field data in this study) should comprise independent and identically distributed data, this might not be fully satisfied because the existence of autocorrelation. However, previous study shows that the autocorrelation in the field data herein is not significant. Bearing this in mind, the bootstrapping method was used, and the repeated sampling number was set as 3000 for each resampling test.

In this study, the 28-day equivalent UCS datasets from the two sites were randomly re-sampled with replacement by bootstrapping method (**Appendix B**). The resampling process was repeated for 3000 times, so that 3000 design values was obtained for each criterion, from which the COVs of design values can be calculated.

Figure 6.4 illustrates the COVs of these three criteria against various sample sizes, where Criteria 2 and 3 adopt 5th (10th) percentile. As the figures show, compared to other two criteria, Criterion 1 yields the largest difference in COVs of two sites. For the Marina One data set, the COVs in Criterion 1 is much higher than the COV for the other two criteria. On the other hand, for the MBFC data, the calculated COV using all the criteria are very close. The phenomenon indicates that Criterion 1 is more sensitive to the sample size than other two criteria. That is to say, for a given resampling size (i.e. *n* in **Figure 6.5**), the minima of randomly resampled data sets from a larger data pool (i.e. field data from Marina One site) is likely to have a larger variation. In contrast, Criteria 2 and 3 yield more stable results: the calculated values are more consistent for the data from both sites. **Table 6.3** summarizes the necessary sample size for Criteria 1 - 3 to achieve certain values of COV in results based on

the two field data sets, where the sample size for the larger COV was chosen for a conservative consideration.

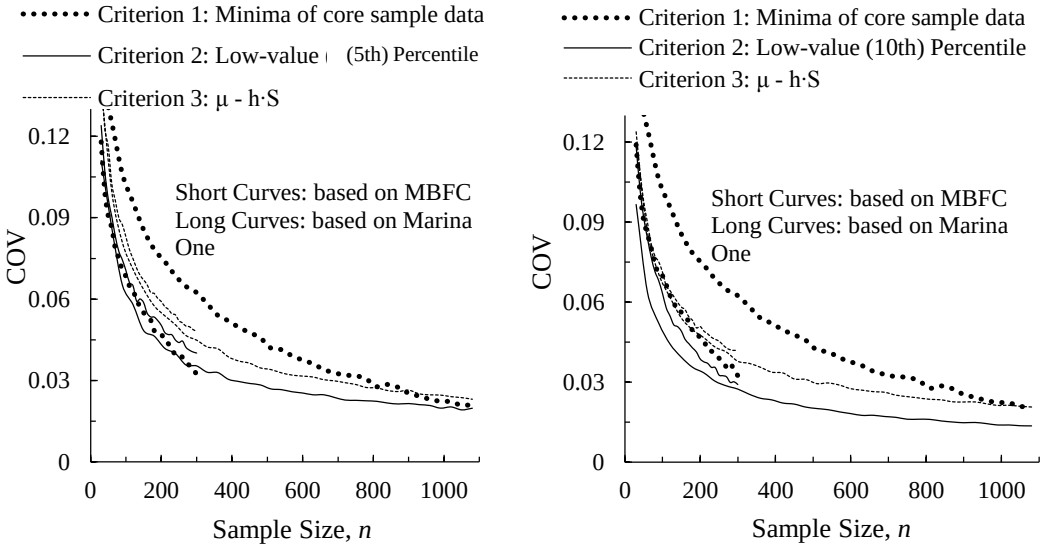

Figure 6. 4 Coefficient of variation (COV) in design values evaluated from different criteria. (a) 5^{th} percentile; (b) 10^{th} percentile. (For Criterion 3, *h* was so chosen that the probability of data being approximately equal to the corresponding percentile.)

Table 6. 3 Recommendations in sample size based on maximum tolerable COVs.

Type of criteria		**Minimum sample size**	
		COV = 0.1	**COV = 0.05**
Criterion 1: Minima of core sample data		100	415
Criterion 2: Percentile	5^{th}	45	205
	10^{th}	45	145
Criterion 3: μ - $h\times\sigma$	h = 1.1 (~ 5^{th} percentile)	65	270
	h = 1.0 (~ 10^{th} percentile)	45	200

Note: COV = coefficient of variation, which was used herein for the variables calculated by the three criteria.

The reliability of Criterion 1 may depend on the distribution of lower percentile end of the data set. **Table 6.4** lists the smallest 10 data points of two sites in order. In both sites, first three data are smaller or equal to 0.7 Mpa. That us to say, in MBFC site, there is a probability of 3/232 to get the value under Criterion 1 not higher than 0.7 Mpa at each picking-up; whereas this probability reduces to 3/1149 based on data from Marina One site.

Hence, in small sample size, the resample obtained from MBFC site data is of a higher probability to get a lowest value close to lower limit.

Table 6. 4 First 10 data points from ordered field data sets

	MBFC Site (Unit: Mpa)		**Marina One Site** (Unit: Mpa)	
No.	B *	A *	B	A
1	0.76	0.62	0.97	0.68
2	0.82	0.65	0.98	0.69
3	0.83	0.68	0.99	0.7
4	0.9	0.72	1.02	0.73
5	0.91	0.72	1.03	0.74
6	0.92	0.72	1.03	0.76
7	0.94	0.73	1.03	0.76
8	0.96	0.75	1.03	0.77
9	0.98	0.77	1.04	0.77
10	0.99	0.77	1.04	0.8

Note: * A = after normalization; B = before normalization

In order to determine the impact of low-end outliers on the robustness of the three criteria, an additional outlier point was artificially added into each of the data sets from MBFC and Marina One sites to change the distribution of lower tail. Three data points of 200 kPa, 400 kPa and 600 kPa were considered to represent weak zones with different degrees of defects in an improved ground. At each time, only one of them was added in the field data sets to ensure the outlier point accounting for a very small portion of the data volume. **Figure 6.5** and **Figure 6.6** illustrate the results from data sets from MBFC and Marina One sites, respectively, where the 5^{th} percentile was chosen for Criteria 2 and 3. As the figures show, Criterion 1 is affected significantly by the additional outlier data point; the influence is more evident with a smaller outlier. It is attributable to the fact that this criterion only considers the minimum of a data set but the added data point may not be necessarily sampled in every resampled data set. In contrast, Criteria 2 and 3 yield consistent results regardless of the value of the added data point, since one data point is unlikely to affect the mean and standard deviation significantly.

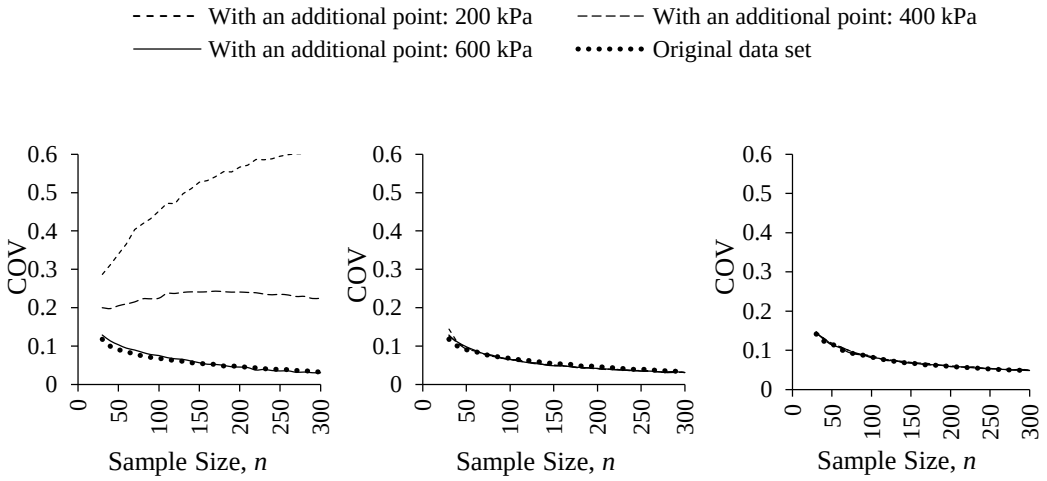

Figure 6. 5 Robustness comparisons among different criteria subjected to an additional point in data set from MBFC project. (left) Criterion 1, (middle) Criterion 2 under 5th percentile and (right) Criterion 3 with h = 1.1.

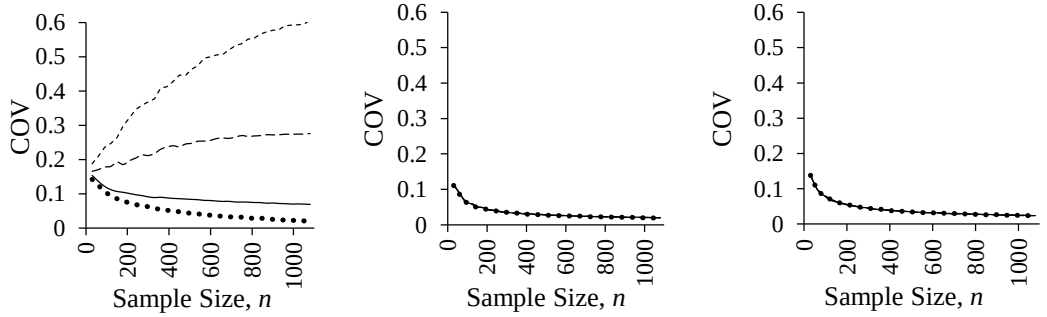

Figure 6. 6 Robustness co Mparisons among different criteria subjected to an additional point in data set from Marina One project. (left) Criterion 1, (middle) Criterion 2 under 5th percentile and (right) Criterion 3 with h = 1.1.

In summary, comparison of non-parametric bootstrapping estimation using the three criteria shows that Criterion 1 is most sensitive to the low-end of the distribution, especially on single extremely low outlier. In contrast, the results obtained using Criteria 2 and 3 are more stable. In addition, Criterion 1 may yield over-conservation design values especially in large sample size since it treats the whole cement-treated domain as weak as the weakest point. It may be noted in this regard that some guidelines (e.g. Bruce *et al.*, 2013) permit a certain percentage of test results to be lower than the design strength, that is, adopting Criteria 2 or 3.

6.3. Further modifications on robust criteria

Modified Criterion 1

When choosing the sample-minima type of design criterion, it is widely accepted that the strength should have a non-negative lower bound. Similarly in this case, the minimal strength in cement-treated soil should be equal to or greater than that of natural soil.

Based on an ordered sample (i.e. $X_1 < X_2 \ldots < X_n$) of a random variable, x, the following formula can be used to estimate the lower bound of the variable (Robson and Whitlock, 1964):

$$X_0 = X_1 - \frac{\alpha}{1-\alpha}\left(X_2 - X_1\right) \tag{6.6}$$

where X_0 denotes an "estimated" lower bound of x; X_1 and X_2 are the lowest and second lowest values in the ordered sample; α is the confidence level. A schematic demonstration of Eq.6.6 is illustrated in **Figure 6.7**. Since α is a value between 0 and 1, the estimated lower bound is always smaller than the minimum of sample data, X_1. This is physically reasonable, because the minimum of sample data is always higher that of the corresponding population-n and the degree of overestimation decreases as the sample size increases. For the extreme case where sample size tends to infinitely large, both X_1 and X_2 converge in probability towards the lower bound; that is, the minimum of sample data is consistent with that of the corresponding population. In this study, instead of the minimum value X_1, the lower bound X_0 is suggested to be used as modified Criterion 1 so that the confidence lower can be accounted for.

Following Zureick *et al.* (2006), the confidence level α in Eq.6.6 could be chosen as 80%. This level is lower than the suggested confidence level of 95% by Eurocode 7 (CEN, 2004), which is recommended to determine the characteristic value of a geotechnical parameter.

Eurocode 7 states that "*... a cautious estimate of the mean value is a selection of the mean value of the limited set of geotechnical parameter values, with a confidence level of 95% ...*".

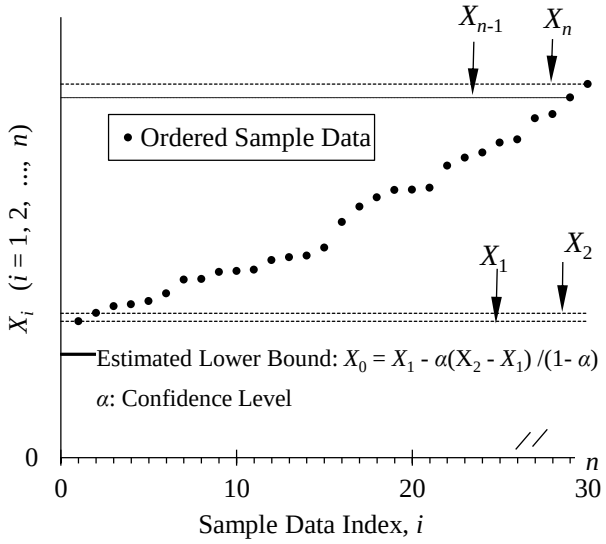

Figure 6. 7 A schematic demonstration on determination of lower bound for random variable according to Eq.6.6.

By adapting Eq.6.6, both the sample size and confidence level of design value can be considered by adopting X_0 as the design value. The concept of the "bootstrap" can be used again as for illustration purpose: by randomly sampling with replacement from the 1145 data points from the Marina One site, the estimator X_0 can be calculated from each re-samples with different number of data points, ranging from 30 to 1000. The whole process was repeated *3000* times so that the statistical properties in X_0 can be assessed. As the **Figure 6.8** shows, the mean of estimated lower bound increases with the sample increasing and tends to the minimum of site data point; whereas the COV of X_0 decreases with more sample size.

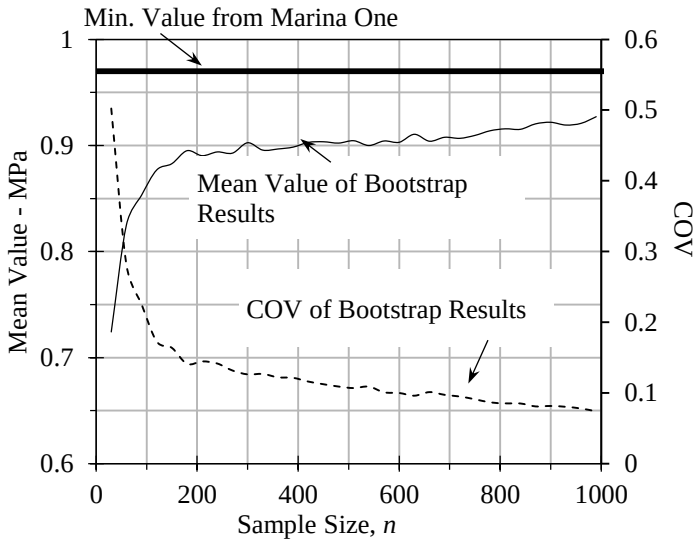

Figure 6. 8 Statistic characteristics of sample-minimum type of criterion (confidence level is chosen as 80%)

Modified Criterion 2 & 3

When a PDF is considered, the Criterion 2 and Criterion 3 can be equivalent by adjust the reduction coefficient *h* in Eq.6.4 to a prescribed percentile. In order to consider the variation in the random variable *z* in Eq.6.4, a modified form to evaluate the design value can be proposed:

$$z' = \bar{\mu} - A \cdot h \cdot \sigma_{\mathrm{u}} \tag{6.7}$$

where *A* is the data confidence factor accounting for the variation in the random variable *z*; $\bar{\mu}$ and σ_{u} are the population mean and population standard deviation of UCS, respectively. The factor *A* correlated with the confidence level. **Figure 6.9** illustrates the basis of Eq.6.7, whereby the data confidence factor *A* can be calculated as

$$A = \frac{\Phi^{-1}(\alpha) \times \sigma_z + h \cdot \sigma_{\mathrm{u}}}{h \cdot \sigma_{\mathrm{u}}} \tag{6.8}$$

where Φ is the CDF (Cumulative Density Function) of standard normal distribution; α is the confidence level; σ_z is the standard deviation of variable z. Substituting Eq.C.6 (see **Appendix C**) into Eq.6.8 yields

$$A = \frac{\Phi^{-1}(\alpha) \times \sqrt{\frac{1}{n} + \frac{h^2}{4n}\left(\kappa - \frac{n-3}{n-1}\right)} + h}{h} \tag{6.9}$$

Eq.6.9 implies that the data confidence factor A depends on the percentile-related h, confidence level α, sample size n and kurtosis of UCS κ. Based on the field data from Marina One site, where the sample size is relatively large, the shape parameters of the Beta distribution for UCS can be 1.42 and 8.48, which implies that the κ has a value of 4.3 (Johnson and Kotz, 1970). Based on this value, **Figure 6.10** tabulates the data confidence factor A under different conference levels.

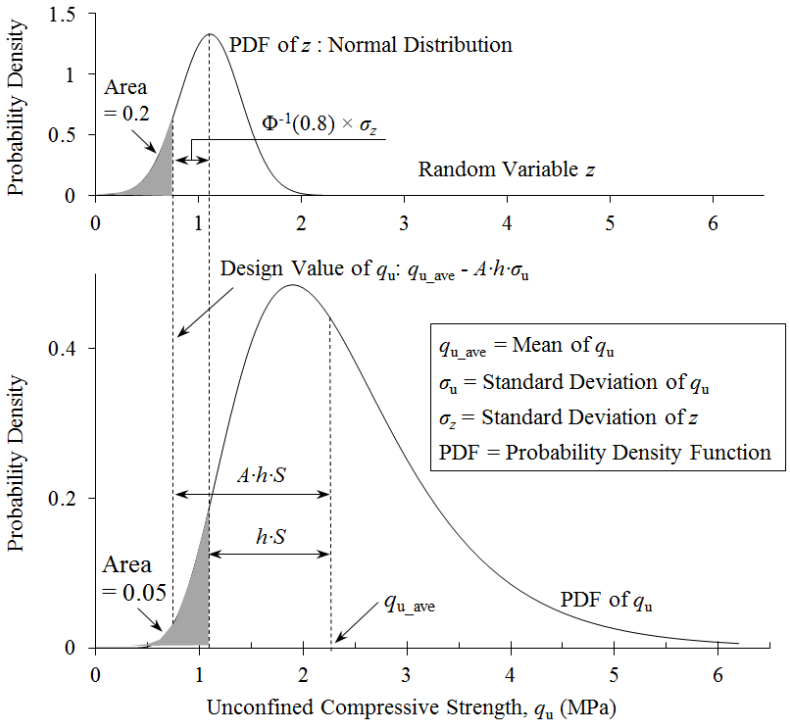

Figure 6.9 Illustration of modified mean-standard deviation type of criterion

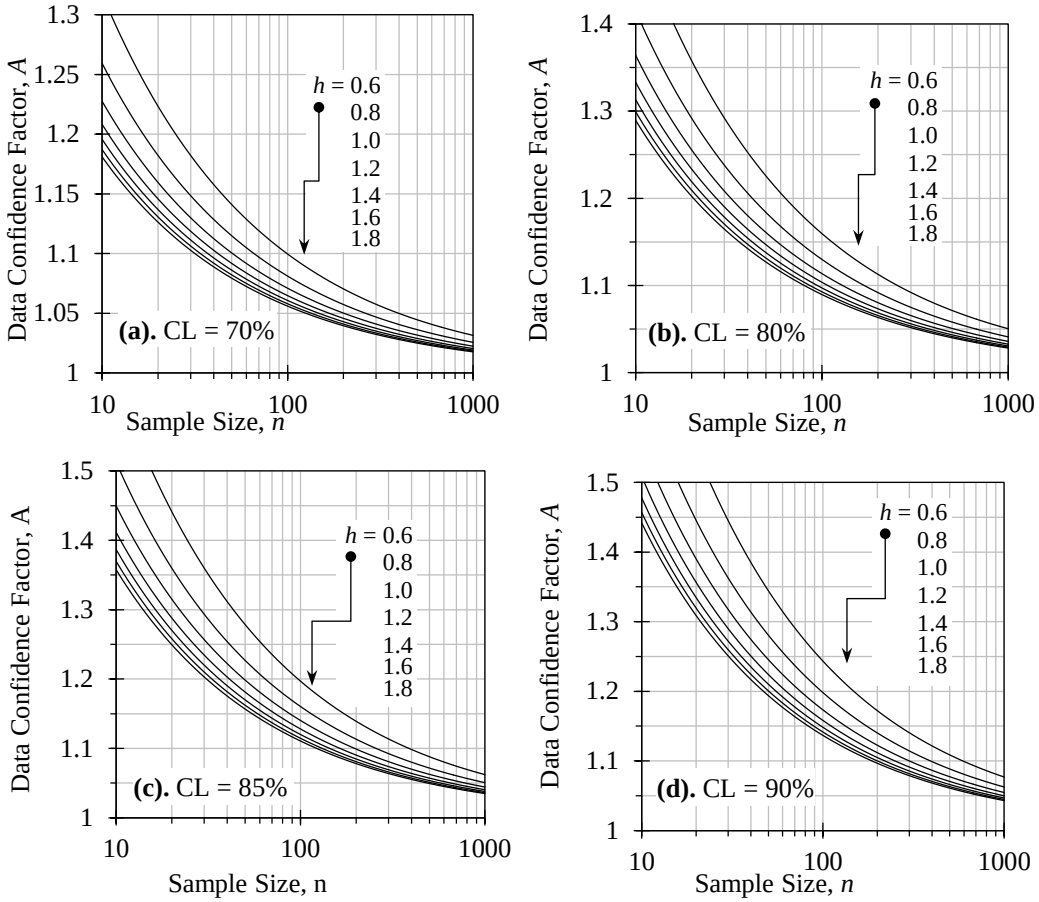

Figure 6. 4 Data confidence factor in modified mean-standard deviation type of criterion under different confidence levels.

6.4. Robustness of modified criteria based on field data

The original and modified criteria for evaluating design strengths were applied on the normalized 28-day equivalent UCS data sets, with results summarized in **Table 6.5**. For both the original and modified forms of Criteria 2, the design strengths for the Marina One project are approximately 15% larger than those of the MBFC project. However, the corresponding differences obtained from the original and modified Criteria 1 are 28% and 78%, respectively, for the Marina One and MBFC projects. It implies that both the original and modified form of Criterion 2 is likely to yield more consistent and stable results than the

corresponding form of Criterion 1. The difference in these two types of criteria is probably due to the fact that Criterion 1 only includes one or two values (i.e. X_1 and X_2 in **Figure 6.8**), which is likely to vary significantly depending on these two values from case to case. On the other hand, the modified form of criteria always yield smaller design strengths than the corresponding original criteria. The reduction of design strengths in the modified criteria were used to account for the statistical uncertainty – the variation in the variables arising from insufficiently large sample sizes. For these reasons, the modified Criterion 2 would be recommended for evaluating design strength.

Table 6. 5 Comparison of Criteria based on site data

Basic Parameters	**Site / Project**			
	MBFC		**Marina One**	
Sample Size	232		1145	
Mean value	2.1 Mpa		2.4 Mpa	
COV	0.42		0.42	
X_1 of ordered statistics (see Fig 6.8)	0.76 Mpa		0.97 Mpa	
X_2 of ordered statistics (see Fig 6.8)	0.82 Mpa		0.98 Mpa	
Prescribed confidence level (see Fig 6.10)	0.8		0.8	
Prescribed percentile (see Fig 6.10)	5%	10%	5%	10%
h (see Fig 6.10)	1.25	1.07	1.25	1.07
Data confidence factor *A* (see Fig 6.10)	1.06	1.07	1.03	1.03
Design Strengths - Mpa				
Original Criterion 1	0.76		0.97	
Modified Criterion 1	0.52		0.93	
Original Criterion 2	1.00	1.16	1.14	1.32
Modified Criterion 2	0.93	1.09	1.10	1.29

7. Conclusions

7.1. Summary of Finding

The key findings of this study are related to the high spatial variability in cement-treated soils.

1. Influence of time between installation and core testing on the measured strength

The average UCS of cement-treated soil in two sites, MBFC and Marina One were plotted against curing time, logarithmic form of Eq.2.4 and generalized hyperbolic curve of Eq.2.7 were employed to fit the time-strength relationship. Based on fitting results, it was concluded that generalized hyperbolic curve is more flexible than logarithmic form to describe the behaviour of strength in cement treated soil. Generalized hyperbolic curve can specify long-term strength-gain rate and ultimate strength of cement-treated soil with two independent parameters, α and q_∞, respectively. Eq.4.8 proposed a simplified method to normalize UCS in cement-treated soil in site to 28-day equivalent strength.

In conclusion, influence of time between installation and core testing on measured strength can be evaluated by generalized hyperbolic relationship with flexible fitting parameters. In such a way that not only 28-day equivalent strength can be normalized, but ultimate strength of cement-treated soil can be predicted.

2. Effect of in-situ water content on UCS in cement-treated marine clay

The effect of in-situ water content on measured strength in cement-treated marine clay was determined by two approaches.

Firstly, based on fitted polynomial trends of in-situ water content and UCS in cement-treated clay along depth, a negative linear relationship of in-situ water content and UCS of cement-treated clay was derived with link of depth. This fitted result is in accordance with theoretical derivation in **Figure 5.2**.

Secondly, based on Eq.5.28, the autocorrelation of UCS can be predicted by the one in in-situ water content and cement slurry concentration. It is observed both from site data and theoretical interpretation (**Figure 5.7(b**)) that the auto-correlation of UCS is about half of w's auto-correlation in vertical direction.

Since high in-situ water content may result in insufficient strength in cement-treated soil, few issues shall be aware of: Firstly, before ground improvement, site investigation is essential to detect the "weak zone" with high water content. Secondly, more attention shall be paid to the weal zone during improvement works. Finally, in strength assessment, core sample shall be taken in the "weak zone", from which the lower tail of strength often occurs.

3. Strength prediction by Two-parameter model

The prediction of strength ratio involves two variables: in-situ water content and cement slurry concentration. The former is one key parameter of in-situ soil condition, whereas the latter is related to operational control.

Firstly, the mean and variance of *r*, the strength ratio is predicted by Taylor's expansion as a function of mean and variance of in-situ water content and cement slurry concentration. Secondly, the histogram of *r* can be predicted by probability density function of in-situ water content and cement slurry concentration. Compared the predicted results to the field data, it shows a remarkable consistency between modelling and site observation.

Therefore, based on the result in this field data study, this generalized hyperbolic model is recommended to predict and assess UCS in cement-treated soil.

4. Reliability of robust criteria of characteristic soil strength in small sample size

Three criteria of characteristic soil strength were discussed herein: Minima of core sample data; Low-value percentile and Mean-standard-deviation linear combination. The first criterion is currently applied in Singapore, whereas the rest are recommended in Eurocode 7.

With the help of non-parametric bootstrapping method and Mont-Carlo simulation, the reliability of three criteria was assessed in different sample size with field data in Marina One site. It is observed that Minima-type criterion is relatively sensitive to the sample size and distribution of low tail; whereas the percentile-type and mean-variation-type show a more stable performance in small sample size. In addition, modified criteria are proposed to improve the accuracy and reliability of assessment. Based on bootstrapping result with field data, criterion 2, the low-value percentile is recommended.

7.2. Further Works

The findings of this study may be limited to the field data from two adjacent sites in Singapore. In future, it is better to conduct assessment on the spatial variability in cement-treated soil in other sites, in such a way that more field information could be involved.

The autocorrelation structure and linear trend of UCS in cement-treated soil has been measured from site. In future, based on measured results, a random UCS field can be realized in numerical simulation; hence failure mechanism in random soil model can be studied in random finite element method (RFEM). Based on RFEM method, reliability-base-design can be conducted, in which safety factor can be studied in a statistical method.

Bibliography

Al-Naqshabandy, M. S. (2011). *Strength variability in lime-cement columns and its effect on the reliability of embankments.* Licentiate Thesis, KTH Royal Institute of Technology, Department of Civil and Architectural Engineering,Division of Soil and Rock Mechanics, Stockholm.

Al-Tabbaa, A. (2003). Soil mixing in the UK 1991–2001: state of practice report. *Ground Improvement , 7*(3), 117-126.

Amundaray, J. I. (1994). *Modeling geotechnical uncertainty by bootstrap resampling(Thesis for Doctor of Philosophy).* Purdue University.

Ang, A. H.-S., & Tang, W. H. (1975). *Probability concepts in engineering planning and design, Vol. 1: basic principles.* New York: John Wiley & Sons.

Arulrajah, A., & Bo, M. W. (2008). Characteristics of Singapore Marine Clay at Changqi. *Geotech Geol Eng, 26*, 431-441.

B/526. (2011). *BS EN 12716:2001 Execution of special geotechnical works. Jet grouting.* BSI.

Babasaki, R., Terashi, M., Suzuki, T., Maekawa, A., Kawamura, M., & Fukazawa, E. (1997). JGS TC Report: Factor influencing the strength of improved soil. *Grouting and Deep Mixing, The second international conference on ground improvement geosystems* , (pp. 913-918).

Barr, D. R., & Todd, S. E. (1999). Mean and variance of truncated normal distributions. *The American Statistician, 53(4)*, 357–361.

Bertero, A., Leoni, F. M., Filz, G., Nozu, M., & Druss, D. (2012). Bench-scale testing and quality control/quality assurance testing for deep mixing at Levee LPV 111. *Grouting and Deep Mixing 2012, Proceedings of the 4th International Conference on Grouting and Deep Mixing* (pp. 694-705). Reston,VA: Geotechnical Special Publication 228.

Bond, A. J., Schuppener, B., Scarpelli, G., & Orr, T. L. (2013). *Eurocode 7: Geotechnical Design Worked Examples.* Dublin: Luxembourg: Publications Office of the European Union, ISBN 978-92-79-33759-8.

Bond, A., & Harris, A. (2008). *Decoding Eurocode 7.* Oxon: Taylor & Francis.

Bourdeau, P. L., & Amundaray, J. I. (2005). Non-parametric simulation of geotechnical variability. *Geotechnique, 55(2)*, 95-108.

Bruce, M. E., Berg, R. R., Collin, J. G., Filz, G. M., Terashi, M., & Yang, D. S. (2013). *Federal Highway Administration Design Manual: Deep Mixing fo rEmbankment and Foundation Support.* Washington.

Cafaro, F., & Cherubini, C. (2002). Large Sample Spacing in Evaluation of Vertical Strength Variability of Clayey Soil. *Journal of Geotechnical and Geoenvironmental Engineering, 128*, 558-568.

CEN. (2002). *EN 1990 (2002) - Eurocode, Basic of structural design.* Brussels: European Committee for Standardization.

CEN. (2004). *EN 1997-1: Eurocode 7 – Geotechnical design – Part 1: general rules.* Brussels: European Committee for Standardization.

Chen, J., Lee, F. H., & Liu, Y. (2014). A statistical model for the unconfined compressive strength of deep mixing columns(proceeding).

Chen, J., Lee, F. H., & Ng, C. C. (2011). Statistical analysis for strength variation of deep mixing columns in Singapore. *GeoFrontier 2011:Advances in Geoyechnical Engineering*, 576-584.

Chew, S. H., Kamruzzaman, A. H., & Lee, F. H. (2004). Physicochemical and engineering behavior of cement treated clays. *Journal of Geotechnical and Geoenvironmental Engineering*, *130*(7), 696 - 706.

Chin, K. G. (2006). *CONSTITUTIVE BEHAVIOUR OF CEMENT TREATED MARINE CLAY-Doctoral Thesis.* Singapore: National University of Singapore.

Chong, P. T. (2002). *CHARACTERISATION OF SINGAPORE LOWER MARINE CLAY-Doctoral Thesis.* Singapore: National University of Singapore.

Davison , A. C., & Hinkley, D. V. (1997). *Bootstrap methods and their applications.* Cambridge: The press syndicate of the university of cambridge.

Defense, D. o. (2002). Volume 1. Polymer matrix composites guidelines for characterization of structural materials. In *Composite Materials Handbook.* Lancaster: Technomic Publishing Co., Inc, and Materials Sciences Corporation in cooperation with ASTM.

Efron, B. (1979). Bootstrap methods: another look at the Jackknife. *The Annals of Statistics, Volume 7, Number 1*, 1 - 26.

Efron, B., & Tibshirani, R. (1986). Bootstrap Methods for Standard Errors, Confidence Intervals, and Other Measures of Statistical Accuracy. *Statistic Science, 1(1)*, 54-75.

Elishakoff, I. (1999). *Probabilistic Theory of Structures.* New York: Dover Publications.

Ellingwood, B. R. (1994). Probability-based codified design: past accomplishments and future challenges. *Structural Safety, 13*, 159-176.

Fenton, G. A. (1999). Estimation for Stochastic Soil Models. *Journal of Geotechnical and Geoenvironmental Engineering, 125*(6), 470-484.

Fenton, G. A. (2003). Bearing Capacity Prediction of Spatially Random Soils. *Canadian Geotechnical Journal, 40(1)*, 54-65.

Fenton, G. A., & Griffiths, D. V. (2008). Chapiter 3, Random Fields. In G. A. Fenton, & D. V. Griffiths, *Risk Assessment in Geotechnical Engineering*, (pp. 91-122).

Firouzianbandpey, S., Griffiths, D. V., Isben, L. B., & Andersen, L. V. (2014). Spatial Correlation Length of Normalized Cone Data in Sand: Case Study in the North of Denmark. *Canadian Geotechnical Journal, 51*, 844-857.

Futaki, M. a. (2002). The quality control in deep mixing method for the building foundation ground in Japan. *Proc. the Deep Mixing Workshop 2002* (pp. 139-149). Tokyo: Port and Airport Research Institute and Coastal Development Institute of Technology.

Gallavresi, F. (1992). Proc.,Grouting improvement of foundation soils. *Grouting,soil improvement and geosynthetics* (pp. vol.1, 1-13). New York: ASCE.

Garth, A. (2008). *Analysing data using SPSS* . Sheffield Hallam University.

Harr, M. E. (1977). *Mechanics of Particulate Media: A Probabilistic Approach.* West Lafayette, Indiana,USA: McGraw-Hill,Inc.

Honjo, Y. (1982). A Probabilistic Approach to Evaluate Shear Strength of Heterogeneous Stabilized Ground by Deep Mixing Method. *Soil and Foundations, 22*(1), 23-38.

Houlsby, N. M., & Houlsby, G. T. (2013). Statistical fitting of undrained strength data. *Geotechnique, 63(14)*, 1253–1263.

Johnson, C. E., Johnson, A. H., & Huntington, T. G. (1990). SAMPLE SIZE REQUIREMENTS FOR THE DETERMINATION OF CHANGES IN SOIL NUTRIENT POOLS. *Soil Science, 150(3)*, 637-644.

Johnson, N. L., & Kotz, S. (1970). *Continuous univariate distributions.* New York: Hougton Mifflin.

Kasama, K., Whittle, A. J., & Zen, K. (2012). Effect of spatia lvariability on the bearing capacity of cement-treated ground. *Soils andFoundations , 52*(4), 600-619.

Kawasaki, T., Saitoh, S., Suzuki, Y., & Babasaki, R. (1984). Deep mixing method using cement slurry as hardening agent. *Seminar on Soil Improvement and Construction Techniques in Soft Ground, Singapore*.

Kingsley, H. W. (1986). Probability distribution of strength parameters in uniform soils. *Journal of Engineering Mechanics, 112*(3), 345-350.

Lafarge. (n.d.). Retrieved from Lafarge: http://www.lafarge.com.my/wps/portal/my/2_3_B_2-Detail?WCM_GLOBAL_CONTEXT=/wps/wcm/connectlib_my/Site_my/AllProductDataSheet/ProductDatasheet+Exemple_1271136044673/ProductDatasheet+EN

Lamb, P. (1970). Safety factors and the probability distribution of soil strength. *Canadian Geotechnical Journal , 7*(3), 225-242.

Larsson, S. (2001). Binder distribution in lime-cement columns. *Ground Improvement, 5*(3), 111-122.

Larsson, S., Dahlstrom, M., & Nilsson, M. (2005). Uniformity of lime-cement columns for deep mixing: a field study. *Ground Improvement , 9*(1), 1-15.

Lee , F. H., Chew, S. H., & Lee, Y. (1997). Jet grouting in Singapore Marine CLay. *Proceeding of 3YGEC, Singapore*.

Lee , F. H., Chin, K. G., Xiao, H., & Chen, J. (2013). Cement-soil treatment in underground construction. *Indian Geotechnical Conference* (pp. 576-584). Roorkee, India: Indian Geotechnical Society(IGS),.

Lee, F. H., Lee, C. H., & Dasari, G. R. (2006). Centrifuge modeling of wet deep mixing processes in soft clays. *Géotechnique, 56*(10), 677-691.

Lee, F. H., Lee, C. H., Dasari, G. R., & Zheng, J. (2008). Centrifuge study on uniformity of wet deep mixing. *International Journal of Physical Modelling in Geotechnics*, 1-20.

Lee, F. H., Lee, Y., Chew, S. H., & Young, K. Y. (2005). Strength and modulus of marine clay-cement mixes. *Journal of Geotechnical and Geoenvironmental Engineering , 131*, 178-186.

Li , J., Tian, Y., & Cassidy , M. J. (2005). Failure Mechanism and Bearing Capacity of Footings Buried at Various Depth in Spatially Random Soil. *Journal of Geotechnocal and Geoenvironmental Engineering*, 141(2).

Lim, S., & Zollinger, D. G. (2003). Estimation of the Compressive Strength and Modulus of Elasticity of Cement Treated Aggregate Base Materials. *Meeting of the Transportation Research Board.* Washington .D.C.

Liu, Y., Lee, F. H., Quek, S. T., Chen, J., & Yi, J. T. (2015). Effect of spatial variation of strength and modulus on the lateral compression response of cement-admixed clay slab. *Géotechnique, Volume 65 Issue 10*, pp. 851-865.

Liu, Y., Zheng, J. J., & Guo, J. (2008). Statistical evaluation for strength of pile by deep mixing method. *proceedings of 2nd Internetional conference on geotechnical engineering for disaster mitigation & rehabilitation*.

LTA. (2010). *Engineering Group Materials & Workmanship Specification for Civil & Structural Works.* Singapore: Land Transport Authority.

Lu, Y. (2014). *Early Strength Development of Cement Mixed Singapore Marine Clay-Doctoral Thesis.* Singapore: National University of Singapore.

Matsuo, O. (2002). Determination of design parameters for deep mixing. *Proc., Tokyo Workshop 2002 on Deep Mixing* (pp. 77-79). Tokyo: Port and Airport Research Institute and Coastal Development Institute of Technology.

Mitchell, J. K. (1976). The properties of cement-stabilized soils. In *Proceeding of Residential Workshop on Materials and Methods For Low Cost Road, Rail, and Reclamation Works,Australia* (pp. 365–404).

Miura, N., Horpibulsuk, S., & Nagaraj, T. S. (2001). Engineering behaviour of cement stabilized clay at high water content. *Soil Foundation, 41(5)*, 33-45.

Namikawa, T., & Koseki, J. (2013). Effects of spatial correlation on the compression behaviorof a cement-treated column. *Journal of Geotechnical and Geoenvironmental Engineering, 139*(8), 1346-1359.

Phoon, K. K. (2006). Bootstrap Estimation of Sample Autocorrelation Functions. *GeoCongress* , (pp. 1-6).

Phoon, K. K., & kulhawy, F. H. (1999). Characterization of geotechnical variability. *Can.Geotech.J.36*, 612-624.

Pitts, J. (1992). Landforms and Geomorphic Evolution of the Islands During the Quaternary. In A. Gupta, & J. Pitts, *Physical Adjustment in a Changing Landscape: The Singapore Story* (pp. 83-143). Singapore: Singapore University Press.

Popescu, R., Deodatis, G., & Nobahar, A. (2005). Effects of random heterogeneity of soil properties on bearing capacity. *Probablistic Engineering Mechanics , 20*(4), 324-341.

Rackwirz, R. (2000). Reviewing probabilistic soils modelling. *Computers and Geotechnics, 26*, 199-223.

Robson, D. S., & Whitlock, J. H. (1964). Estimation of a Truncation Point. *Biometrika, 51(1-2)*, 33-39.

Santoso, A. M., Phoon, K. K., & Tan, T. S. (2013). Estimating strength of stabilized dredged fill using multivariate normal model. *Journal of Geotechnical and Geoenvirinmental Enginnering, 139*(11), 1944-1953.

Schneider, H. R. (1999). Determination of characterisic soil properties . *Geotechmical Engineering for Transportation Infrastructure Vol 1*, 273-281.

Schultze, E. (1972). Frequency distributions and correlations of soil properties. In *Statistics and probability in civil engineering.* Hong Kong University Press.

Sivakumar Babu, G. L., Srivastava, A., & Sivapulliah, P. V. (2011). Reliability analysis of strength of cement treated soils. *Georisk: Assessment and Management of Risk for Engineered Systems and Geohazards, 5*(3-4), 157-162.

Srivastava, A., & Sivakumar Babu, G. L. (2009). Effect of soil variability on the bearing capacity of clay and in slope stability problems. *Engineering Geology, 108*, 142-152.

Standardization), C. (. (2002). *BS EN 1990:2002 Eurocode - Basis of structural design.* Brussels.

Tan, S. L. (1983). Geotechnical Properties and Laboratory Testing of Soft Soils in Singapore. *1st International Seminar on Construction Problems in Soft Soils* (pp. 1-47). Singapore: Nanyang Technological Institute.

Tanaka, H., Locat, J., Shibuya, S., Tan, T. S., & Shiwakoti, D. R. (2001). Characterization of Singapore, Bangkok, and Ariake clays. *Canadian Geotechnical Journal, 38*, 378-400.

Trustrum, K., & Jayatilaka, A. D. (1983). Applicability of Weibull analysis for brittle material. *Journal of Materials Science, 18(9),* 2765-2770.

Usui, H. (2005). Quality control of cement deep mixing method. *Proc., Int. Conf. on Deep Mixing* (pp. 635–638). Stockholm, Sweden: Swedish Deep Stabilization Research Centre.

Vahdatirad, M. J., Griffiths, D. V., Sorensen, J. D., & Fenton, G. A. (2014). Reliability analysis of a gravity-based foundation for wind turbines: a code-based design assessment. *Géotechnique, 64(8),* 635-645.

Vanmarck, E. (1983). *Random Field: Analysis and Synthesis.* THE M.I.T. PRESS.

Vanmarcke, E. H. (1983). *Random Fields: Analysis and Synthesis.* Cambridge: MIT Press.

Verastegui Flores, R. D., & Di Emidio, G. (2011). Hardening of kaolin clay mixed with different binders. *Deformation Characteristics if Geomaterials Proc. 5th Int.Symposium on Deformation Characteristics of Geomaterials* (pp. Vol 1, 669-676). Seoul: OPS Press.

Vlad, A., & Badea, B. (2008). Analysing the dependence between variance and mean estimated values: a theoretical and experimental approach. In *Computational Science and Its Applications – ICCSA 2008* (pp. 753 - 767). Berlin: Springer Berlin Heidelberg.

Wikipedia. (8 August, 2015). *https://en.wikipedia.org/wiki/Sample_maximum_and_minimum*. Retrieved from Wikipedia: https://en.wikipedia.org/wiki/Sample_maximum_and_minimum

Xiao, H. W., Lee, F. H., & Chin, K. G. (2014). Yielding of cement-treated marine clay. *Soils and Foundations, 6,* 488 - 501.

Yong, K. Y., & Karunaratne, G. P. (1990). Recent developments in soft clay engineering in Singapore. *Proc., Kansai Int. Geotech. Forum '90: Comparative Geotechnical Engineering,* (pp. 1-8). Osaka, Japan.

Zureick, A. H., Bennett, R. M., & Ellingwood, B. R. (2006). Statistical Characterization of Fiber-Reinforced Polymer Composite Material Properties for Structural Design. *Journal of Structural Engineering, 132*(8), 1320-1327.

Appendix A Procedure for Discrete Integration in Probability Density Function Prediction

Firstly, range of r is estimated according to Eq.5.3. The lower bound of *r*, $r_{\min}$, is estimated with upper limit of in-situ water content and lower limit of cement slurry concentration; whereas the upper bound of *r*, $r_{\max}$, can be reached when both in-situ water content and cement slurry concentration are minimized.

Secondly, the whole range of *r*, *c* and *w* can be approximated by a set of n discrete value with constant interval Δr, Δc and Δw respectively:

$$r_{\min}, r_2, r_3, ...r_i, ..r_{n-1}, r_{\max}$$

$$c_{\min}, c_2, c_3, ...c_i, ..c_{n-1}, c_{\max}$$

And

$$w_{\min}, w_2, w_3, ...w_i, ..w_{n-1}, w_{\max}$$

In order to improve the accuracy of calculation, Δr is set to 0.01, whereas Δc and Δw are equal to 0.0001.

Each r_i corresponds several sets of approximated *c* and *w* in sets:

$[(c_{i1}, w_{i1}), (c_{i2}, w_{i2})...(c_{ik}, w_{ik})....(c_{in}, w_{in})]$. For each set r_i satisfies:

$$r_i = R(x_{ik}, w_{ik}) = \frac{1 + mx_{ik} + (mx_{ik})^2}{(w_{ik} x_{ik} + a)^n} \quad \text{(A.1)}$$

Where $$x_{ik} = X(c_{ik}, w_{ik}) = \frac{(1+a)}{(1+w_{ik})}\left(\frac{1}{c_{ik}} - 1\right) \quad \text{(A.2)}$$

In reverse, c_{ik} could be written as:

$$c_{ik} = X^{-1}(x_{ik}, w_{ik}) \quad \text{(A.3)}$$

Where: $x_{ik} = R^{-1}(r_i, w_{ik})$ (A.4)

In condition that: 1). $g(r, w)$ is a one to one mapping and continuous on r; and 2). $g(r, w)$ is differentiable and $\frac{dg(r,w)}{dr}$ is not equal to zero at *r*. We have:

$$\frac{dg(r_i, w_{ik})}{dr_i} = \frac{1}{\frac{dr(c_{ik}, w_{ik})}{dc_{ik}}} \quad \text{(A.5)}$$

Hence, derivation of *r* can be expressed as:

$$\frac{dr(c_{ik}, w_{ik})}{dc}_{|c_{ik}} = \frac{dR(x_{ik}, w_{ik})}{dx}_{|x_{ik}} \cdot \frac{dX(c_{ik}, w_{ik})}{dc}_{|c_{ik}} \quad \text{(A.6)}$$

$$f_C\left[g(r_i, w_{ik})\right] = f_C\left[X^{-1}(x_{ik}, w_{ik})\right] \quad \text{(A.7)}$$

To conclude, for each r_i,

$$f_R(r_i) = \sum_{k=1}^{n} \frac{1}{\frac{dR(x_{ik}, w_{ik})}{dx}_{|x_{ik}} \cdot \frac{dX(c_{ik}, w_{ik})}{dc}_{|c_{ik}}} \cdot f_C(c_{ik}) \cdot f_W(w_{ik})\Delta w \quad \text{(A.8)}$$

Appendix B Non-parametric bootstrapping

Perhaps the most important merit of non-parameter Bootstrapping method is its simplicity: provided that the data sets are representative of the population, the data set can be input directly without any fitting operation (Bourdeau and Amundaray, 2005).

There two keywords in principle of non-parametric Bootstrapping: Sample and Re-sample. Sample is a collection of n measurements regardless of order: $A=\{y_1, y_2 ... y_n\}$. Re-sample refers to an unordered collection of *n* items drawn randomly from A with replacement: $A^*=\{y_1^*, y_2^* ... y_n^*\}$. Each y_i^* follows the uniform distribution to be equal to any y_j in the measurement (Davison and Hinkley, 1997):

$$P(y_i^* = y_j \mid A) = 1/n, 1 \le i, j \le n \tag{B.1}$$

The quality of input data may affect the accuracy of bootstrap estimation. Firstly, the original input data shall be representative of its real population. If input data are biased, then the output is probably biased as well (Bourdeau and Amundaray, 2005). Secondly, it was highlighted by Phoon (2006) that the components in input dataset shall be independently and identically distributed (*i.i.d*), in such a way that every resample dataset A^* is a collection of *i.i.d.* data. Previous study shows that horizontal autocorrelation of UCS in cement-treated soil from sites are negligible compared to horizontal distance lag between core samples, while vertical scale of fluctuation is around 3 m, which is shorter than most intervals between UCS core- samples. Hence, it is reasonable to consider the 28-day normalized UCS data sets from two sites as independent and identically distributed.

Besides the quality of input data, the reliability of bootstrap resampling depends on number of simulations: higher the amount of repetitions, more accurate the result is. Bourdeau and Amundaray (2005) found that the bootstrap estimation on expectation and standard deviation get converged after approximately 600 simulations with sample size more than

200. Efron and Tibshirani (1986) suggested that a reasonable confidence interval can be achieved with a number of simulations in the range of 1000 to 2000. Nowadays, with the help of fast-developing computer technology, it is not difficult to repeat bootstrap simulation for thousands even ten thousand times. In this study, number of simulations, *m* is equal to 3000 for a conservative estimation.

One challenge in geotechnical variability estimation is the evaluation of soil properties using small sample statistics. In this study, number of available field datasets of 28-day UCS in Marina One and MBFC sites are 1145 and 232, respectively, which is significantly abundant comparing to the small sites. Hence, the two input datasets can be considered to be representative of real soil properties. In order to examining the reliability of three criteria in different sample size, a resampling schedule can be adopted with number of resampling set smaller than number of input dataset (e.g: Johnson *et al.*, 1990; Bourdeau and Amundaray, 2005). A schematic example of Johnson et al (1990)'s proposal is illustrated in **Figure B.1**:

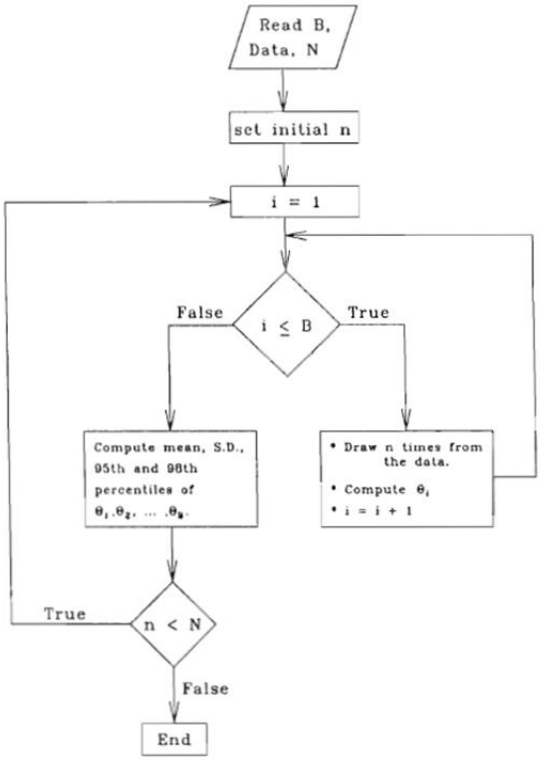

Figure B. 1 Schematic flow diagram illustrating the resampling procedure with number of resampled measures smaller than number of input data, *m*. The number of repetition, *B* herein is 500 (after Johnson *et al.*, 1990)

In this study, *n* data points were randomly re-sampled with replacement from each of the two field data sets. In each resampled dataset A^*, the design values corresponding to three robust criteria can be obtained. The procedure of resampling can be repeated for 3000 times, so that 3000 design values can be obtained for each criterion, from which the COVs of design values can be calculated.

Appendix C Estimation of variation in modified criteria 2-3

The variance of variable *z* in Eq.6.4 can be respectively estimated as:

$$Var(z) = Var(\mu - h \cdot S) \tag{C1}$$

Assuming the sample mean and sample standard deviation are uncorrelated, which is usually the case (Vlad and Badea, 2008), yields:

$$Var(z) = \frac{\sigma_u^2}{n} + h^2 \cdot Var(S) \tag{C2}$$

in which σ_u is the population standard deviation. On the other hand, the variance of S^2 is (Ang and Tang, 1975):

$$Var(S^2) = \frac{\sigma_u^4}{n}\left(\kappa - \frac{n-3}{n-1}\right) \tag{C3}$$

in which κ is the kurtosis of the probability distribution of UCS (e.g. the kurtosis for the normal distribution is 3). Thus, the variance of *S* can be evaluated from that of S^2 by the Taylor expansion. The second-order approximation of the variance of *S* is:

$$Var(S) = \frac{\sigma_u^2}{4n}\left(\kappa - \frac{n-3}{n-1}\right) \tag{C4}$$

Eq.C2 can be rewritten as

$$Var(z) = \frac{\sigma_u^2}{n} + h^2 \cdot \frac{\sigma_u^2}{4n}\left(\kappa - \frac{n-3}{n-1}\right) \tag{C5}$$

Then, the standard deviation of z (denoted as σ_z) is

$$\sigma_z = \sigma_u \sqrt{\frac{1}{n} + \frac{h^2}{4n}\left(\kappa - \frac{n-3}{n-1}\right)} \tag{C6}$$

If the PDF of UCS is chosen as the Beta distribution, then its kurtosis κ merely depends on the shape parameters of the Beta distribution (Johnson and Kotz, 1970); for a given pair of shape parameters, σ_z depends on the sample size n, reduction coefficient h and standard deviation of sample.

To assess the PDF of z, 100 data points (i.e. n = 100) were randomly sampled with replacement from the 1149 data pool of the Marina One project, and the procedure was repeated for 1000 times so that a histogram of z can be obtained by bootstrap method. As illustrated in **Figure C.1**, the histogram from bootstrap results can be well fitted by the normal distribution and pass the KS test at a 5% confidence level, and thus the PDF of z can be reasonably assumed to follow the normal distribution.

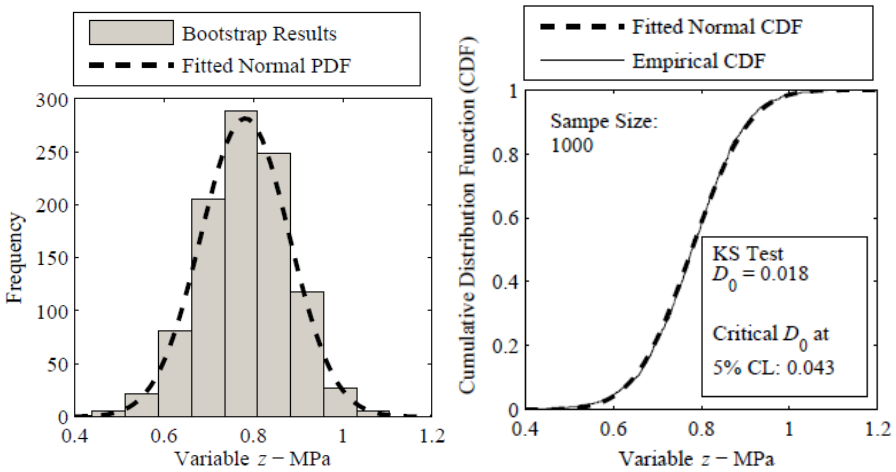

Figure C. 1 Illustration of normality of random variable *z*. (left) probability density function (PDF), (right) cumulative distribution function (CDF).